THÈSE

UNIVERSITE DE PAU ET DES PAYS DE L'ADOUR

École doctorale des sciences exactes et leurs applications (ED211)

Soutenance prévue le 4 Octobre 2019

par **Arley NOVA RINCÓN**

pour obtenir le grade de docteur
de l'Université de Pau et des Pays de l'Adour
Spécialité : Énergétique

Optimisation dynamique d'un système de distribution de froid à l'échelle urbaine

-Dynamic optimization of a district cooling distribution network-

MEMBRES DU JURY

RAPPORTEURS

• Galo Antonio CARRILLO LE ROUX	Professeur / Université de São Paulo(USP) – Brésil
• Jorge Mario GÓMEZ RAMÍREZ	Professeur Associé / Université des Andes – Colombie

EXAMINATEURS

• Pascal FLOQUET	Professeur des Universités / ENSIACET Toulouse
• Sabine SOCHARD	Maître de Conférences / Université de Pau et des Pays de l'Adour

DIRECTEURS

• Jean-Michel RENEAUME	Professeur des Universités / Université de Pau et des Pays de l'Adour
• Sylvain SERRA	Maître de Conférences / Université de Pau et des Pays de l'Adour

UNIVERSITÉ DE PAU ET DES PAYS DE L'ADOUR

Acknowledgements

Firstly, I would like to express my sincere gratitude to my advisors Dr Sabine Sochard (M.C), Dr Sylvain Serra (M.C) and Prof. Jean Michel Reneaume for the continuous support during these three years of research work, also for their patience, and motivation. I would like to extend a special acknowledgement to Sabine, for her close guidance in the development of this manuscript as well as for her interest in my full understanding of the implemented methods.

Besides my advisors, I would like to thank the rest of my thesis committee: Prof. Galo Carrillo Leroux, Prof. Jorge Mario Gómez Ramírez and Dr Pascal Floquet, for their insightful comments and questions which allowed me to widen the scope my research work. Particularly, I am grateful to Pr. Gómez for enlightening me the first glance of the world of research in process optimization at Universidad de Los Andes.

I thank my colleagues (PhD candidates) and professors at the LaTEP, as well as all the staff at the ENSGTI, for their always welcoming attitude and their important role in the improvement of my linguistic skills in the French language.

Moving to more personal expressions of gratitude, I thank the families Bedoya-Velez and Martinez-Lopez, for becoming my family of adoption here in France. Thanks for all the good moments, mainly for all the mountain bike journeys with Daniel, Pablo and Angel. The “escape plans” you proposed were an authentical relief in the stressful moments.

Here, I would like to thank my family: my parents and my sister for supporting me spiritually from the distance throughout these three years. This thesis is the result not only my effort but also of all the values I learned at home, the discipline, the persistence and the conscientious work.

Finally, and with the most intense feelings of admiration and love, I express all my gratitude to my wife Natalia, for accepting the challenge of taking this road by my side, three years ago. Thank you for being my confidant, and my counsellor in the most complicated and stressful moments during this process. Most of my motivations came from her incomparable support.

More valuable than the work I present in this manuscript, are all the things that I have learned, both intellectually and personally, in this remarkable life experience of doing a PhD.

Abstract

Dynamic optimization of a district cooling distribution network

Arley NOVA-RINCÓN

Supervisors: Jean-Michel RENEAUME, Sylvain SERRA
Laboratoire de Thermique, Energétique et Procédés (LaTEP)

Due to the increasing demand for cooling worldwide and the need for reliable and energy-efficient alternatives to provide it, the analysis of district cooling (DC) networks has become a focus of interest in recent years. Currently, most of the developments in the field of numerical simulation and optimization of these systems have been done by implementing steady-state models. Considering this, in the present work we proposed a methodology based on mathematical programming for the dynamic simulation and optimization of the distribution system in district cooling networks.

The dynamic model includes a partial differential equation to describe the variation of the temperature in the pipes, and heat and mass balances in the users and in the interconnecting nodes of the network. This arrangement is known as a partial differential algebraic equation (PDAE) problem. We detail the implementation of 2D- Orthogonal Collocation on Finite Elements (OCFE) for the discretization of the dynamic problem. Then the previously discretized model is added to the optimization constraint set, according to the simultaneous (equation-oriented) solution strategy. The optimization variables (decision variables) include the spatial and temporal profiles of the temperatures and temporal profiles of the mass flows of the system. Additional optimization variables (pipe diameters…) are progressively introduced. We apply this methodology for the analysis of an operational and a cost objective function in a medium size cooling system, serving 20 consumers grouped in five different categories with fluctuating cooling demands subject to variable external conditions. The first objective function considers that in DC networks, the temperature of the cooling utility returning to the production site must be close to the design temperature of the installed technology to ensure proper efficiency and avoid the technical issue known as low ΔT syndrome. Then, still ensuring this condition, the second objective function aims to minimize a cost function (production and pumping costs) including the diameter of the pipes as decision variables. The methodology allowed the computation of the optimal mass flow profiles to operate the system under the desired conditions and the estimation of the pipe diameters of the distribution network for two different costs of production. For the two objective functions, the dynamic simulation and optimization were performed using insulated and non-insulated piping.

The proposed methodology exhibits low CPU cost that demonstrates its potential use for the development of applications for the operation and forecasting of distributed systems.

Keywords: District cooling systems, dynamic optimization, 2D-OCFE

Résumé

Optimisation dynamique d'un système de distribution de froid à l'échelle urbaine

Arley NOVA-RINCÓN

Directeurs: Jean-Michel RENEAUME, Sylvain SERRA
UNIV PAU & PAYS ADOUR / E2S UPPA, Laboratoire de Thermique, Énergétique et Procédés-IPRA

L'utilisation de froid (industriel et climatisation) dans le monde ne cesse d'augmenter et les prévisions annoncent un accroissement continu de la demande de froid dans les années à venir. De ce fait, la recherche d'un moyen fiable et performant permettant la fourniture de froid est plus que jamais d'actualité. Dans ce contexte, les réseaux de froid urbains sont de plus en plus étudiés. Actuellement, la plupart des études portant sur la simulation numérique ou l'optimisation de ces systèmes ont été mises en œuvre en régime stationnaire. Compte tenu de cela, le présent manuscrit propose une méthodologie de résolution mathématique pour la simulation et l'optimisation dynamiques d'un réseau de froid urbain.

Le modèle dynamique inclut les équations différentielles permettant de représenter les variations de température dans les canalisations, ainsi que les bilans de masse et d'énergie aux nœuds du réseau et dans les échangeurs thermiques alimentant les consommateurs. Le modèle ainsi construit est un système d'équations aux dérivées partielles et algébriques. Nous détaillons la méthode de double collocation orthogonale sur éléments finis permettant de discrétiser ces équations afin d'obtenir un système comprenant uniquement des équations algébriques. Le modèle ainsi discrétisé est alors ajouté aux contraintes du problème d'optimisation à résoudre, conformément à la stratégie de résolution orientée équations. Les variables d'optimisation (de décision) sont les profils spatiaux et temporels de température et les profils temporels de débit dans tout le système. D'autres variables d'optimisation, tels que les diamètres des canalisations, sont ajoutées par la suite. Cette méthodologie d'optimisation dynamique est résolue pour deux fonctions objectif différentes (exploitation et économique) appliquées à un cas test, inspiré de la littérature, comprenant 20 consommateurs représentant 5 catégories de bâtiments différents ayant des demandes temporelles de froid variables. Tout ceci est soumis aux variations de température extérieure pour différentes localisations.

La première fonction objective a pour but de maintenir la température de retour dans l'unité de production de froid proche de la température considérée pour le dimensionnement de cette unité afin d'assurer un fonctionnement efficace et d'éviter un problème bien connu dans les réseaux de froid appelé « low ΔT syndrome ».

Ensuite, en garantissant toujours un tel fonctionnement, la seconde fonction objective a pour but de minimiser une fonction coût incluant les coûts de production de froid et de pompage dans le réseau

en considérant les diamètres comme variables d'optimisation. Une procédure particulière, enchainement de simulations stationnaires puis dynamiques, est proposée afin d'obtenir une initialisation permettant la convergence vers un optimum de confiance du problème d'optimisation dynamique. Cette méthodologie a permis d'obtenir les profils temporels optimaux des variables de contrôle du système dans les conditions d'utilisation désirées ainsi que les diamètres de l'ensemble du réseau pour deux coûts représentant différents types de technologies de production de froid.
Les simulations et optimisations dynamiques (pour les deux fonctions objectif) ont été réalisées pour des tuyaux isolés et pour des tuyaux non isolés.
La méthodologie mise en place présente un temps de résolution faible sur un ordinateur portable classique ce qui démontre son potentiel d'utilisation pour le développement d'application de contrôle et de prédiction de ce type de système.

Keywords: Réseau de froid, optimisation dynamique, Double collocation orthogonale sur éléments finis

Contents

List of figures

List of Tables

NOMENCLATURE

Symbols

C_{cold}	Cost of producing cold utility	€/kWh
C_{elec}	Cost of electricity	€/kWh
Cp	Specific Heat Capacity,	J/(kg.K)
D_i	Internal diameter of pipes	m
L	Pipe length	m
L_f	Length of spatial finite element	
$\dot{m}$	Mass flow rate	kg/s
N_x	Spatial collocation matrix	
N_x	Temporal collocation matrix	
Pw	Power in the production site	kW
Pw_{pump}	Electrical energy demanded by the pump	kWh
Q	Cooling Demand	kW
r_a	Internal radius of the pipe	m
r_b	External radius of the pipe	m
r_c	Radius including insulation layer	m
r_d	Radius including casing layer	m
R'	Total thermal resistance	m.K/W
t	Time	s
T	Temperature	K
v	velocity	m/s
W_{pump}	Mechanical work of the pump	kJ

Greek symbols

ΔP	Pressure drops	kPa
ΔT	Temperature difference	K
Δt_e	Size of temporal finite element	
η_{pump}	Total efficiency of the pump	
λ	Coefficient of friction	
ρ	Density	Kg/m^3
ξ	Normalized spatial variable	
τ	Normalized time variable	
θ	Steady-state temperature	

Sets and index

C_p	Set of consumers
D_{t_i}	Linear transformation for time derivative
D_{x_j}	Linear transformation for space derivative
e	Index for time elements
f	Index for distance elements
i	Index for time collocation points in time
j	Index for distance collocation points
k	Index of pipes
p	Sub-index for main pipes
in_{Cp}	Sub-index for pipes entering to clients
out_{Cp}	Sub-index for pipes leaving clients
r	Return pipe
s	Soil
w	Water

INTRODUCTION (ENG)

Cooling is used for diverse purposes in different sectors, from industrial refrigeration to guarantee safe food storage, transport, commercial to domestic refrigeration and air-conditioning. It is also important for the supply of medicines, cooling data centres, production of chemicals, plastics, metallurgic processes, and many other sectors and usages. This diversity of applications and the growing demand for cooling services**,** that only in the building sector has doubled since 2000, due to the combination of warmer temperatures and increased activity caused by population and economic growth**,** demand efficient and affordable solutions. Here, district cooling systems (DCS) arise as a potential technology to supply these needs with both lower cost and environmental benefits. District cooling networks together with district heating networks represent a category of distribution of utilities known as district energy systems. Particularly, DCS supply chilled water produced in a central (or multiple) plant(s) to buildings and industrial sites through a network of underground pipes. The chilled water can be produced using the same technologies than in air conditioning systems (compression refrigeration cycles), but generally at a much larger scale. More sustainable technologies include the use of natural sources of cold (sea, rivers, deep lakes and groundwater) or heat (residual heat from industry, geothermal or even solar thermal sources) to as utility for refrigeration cycles.

Considering the advantages of DCS in terms of energy efficiency and reduction of emissions, the European Union has been supporting the development of many projects led by industrial-academic consortiums aiming to improve system planning, control and management of district cooling systems, as well as their development and implementation using low and zero carbon-emitting sources. Mathematical programming has supported these advances, implementing complex models and innovative methods, including optimization techniques to obtain more accurate and representative results. The literature reports numerous works at the design stage, concerning the optimization of the cost of investment. These include the network topology, optimizing the sizing (pipe diameter, heat exchanger area) and operation (temperature, mass flow rates) parameters in order to minimize the investment cost while respecting a set of constraints (demands of consumers, temperature level). These works have led to optimum results corresponding to the nominal working conditions of the network assuming a steady-state operation. Nevertheless, the incursion of renewables to produce energy and the diversity of demands of the potential new consumers to be interconnected require the development of tools based on fully dynamic models. These dynamic-based tools will allow improving the operation, design, control and forecasting of the current and future systems, considering variations in the levels of demand of the consumers, in the environmental conditions of the location where the systems are installed, and in the production when renewable sources are used, leading to the use and

management of storage systems. Today, the development of applications for the analysis and optimization of district cooling systems based on dynamic models is scarce. Then, this is an important area that needs to be studied for the development of tools that respond to the current challenges in the operation and design of these systems.

Considering this, the objective of this thesis is to develop a methodology for the dynamic optimization of the distribution system of a district cooling network. This will allow computing the optimal temporal profiles of the operation parameters of the distribution system, considering also variations in the ambient temperature. The implemented methodology is illustrated thanks to a medium size distribution system serving 20 users with specific variations and levels of demand. The work of research for the development of this methodology is presented in the present manuscript that is divided into four chapters.

Chapter one presents a literature review that includes the generalities of district cooling systems and their development in Europe and in France. Then, the chapter introduces the challenges that the development of these systems imposes, including the importance of developing optimization tools based on dynamic modelling. The review also details previous works on the optimization of distributed energy systems. Then we introduce the generalities of dynamic optimization, including the methods that can be implemented for the solution of this kind of problems. Based on the literature findings, we introduce the method we chose for the discretization of the dynamic problems (orthogonal collocation on finite elements) to finish with the objectives of this thesis.

Chapter two details the topology, consumers' cooling demands and the external conditions for the proposed case study. Using this illustrative example, the chapter details the mathematical model of the system, including an analysis of the degrees of freedom that will be considered for the optimizations. To conclude, we present the implementation of the discretization strategy for the solution of the dynamic problem.

Considering the discretized model, Chapter three introduces the methodology for the proper initialization of the dynamic optimization problems. The methodology is based on the successive solutions of steady-state simulations to initialize a dynamic simulation problem, whose results will be used as initialization for the dynamic optimization analyses. The chapter details the results of the intermediate simulations that include the definition of diameters and thermal resistances in the pipes, the distribution of temperatures along with the distribution network, and the response of the network

to the variations in demand and external conditions for a constant flow policy. The analysis is made for insulated and non-insulated pipes.

Finally, Chapter four presents the two proposed objective functions and their corresponding results. The first one aims to compute the optimal mass flow profiles that guarantee a constant temperature on the pipes leaving the consumers to avoid a common technical issue in district cooling known as “low ΔT syndrome”. The second objective aims to find the optimal pipe diameters that minimize the value of an operational cost that considers the cost of producing the cold utility and the electrical power demanded by a pump sending the chilled water to the network. The two objective functions are evaluated using both insulated and non-insulated pipes. The consistency of the results presented in Chapters three and four and the reported computational times highlight the robustness of both, the chosen discretization strategy and the proposed methodology of solution.

INTRODUCTION (FR)

De nombreux secteurs, allant de la réfrigération industrielle, pour garantir la conservation des aliments, à la climatisation des commerces, transports et habitations, nécessitent du froid. Les besoins en refroidissement sont également importants dans le secteur médical, dans les centres de données, dans certains procédés des industries chimiques, plastiques ou métallurgiques, et dans bien d'autres secteurs. Cette diversité d'applications et la demande croissante en froid, qui, rien que dans le secteur du bâtiment, a doublé depuis 2000 à cause du réchauffement climatique et de la croissance économique, implique la mise au point de solutions réalistes et efficaces. Dans ce contexte, les réseaux de froid apparaissent comme une solution capable de fournir ces besoins à des coûts relativement faibles avec, qui plus est, un bénéfice environnemental. Les réseaux de froid ainsi que les réseaux de chaleur constituent des systèmes énergétiques centralisés (de quartier). En particulier, les réseaux de froid fournissent de l'eau réfrigérée, produite dans une ou plusieurs unités de production, à différents bâtiments ou sites industriels par le biais d'un réseau de canalisations enterrées. L'eau réfrigérée peut être produite par le même type de technologie que pour les systèmes de climatisation (cycles frigorifiques à compression), mais à plus grande échelle. Cependant, on peut utiliser des technologies économiquement et écologiquement plus durables, telles que l'utilisation de sources froides naturelles (mer, eaux fluviales ou souterraines ou lacs profonds) ou de sources chaudes (chaleur fatale industrielle, géothermie ou chaleur solaire) alimentant des cycles frigorifiques à absorption par exemple.

Consciente des avantages des réseaux de froid tant sur le plan de l'efficacité énergétique que de la réduction d'émissions de gaz à effet de serre, l'Union Européenne soutient depuis plusieurs années le développement de projets portés par des consortiums constitués d'académiques et d'industriels, dont le but est d'améliorer la gestion (planification), la conduite et le contrôle des réseaux de froid, ainsi que leur développement et leur mise en œuvre avec des sources bas carbone. Dans le but d'obtenir des résultats précis et représentatifs, la programmation mathématique a permis la mise en œuvre de modèles complexes et de méthodes innovantes incluant des techniques d'optimisation. De nombreux articles présents dans la littérature font état de travaux concernant l'optimisation des coûts d'investissement à l'étape de conception. Il s'agit de calculer la topologie du réseau, le dimensionnement (diamètre des conduites, aires d'échange) et les variables de fonctionnement du réseau (températures, débits) qui minimisent le coût d'investissement tout en respectant un ensemble de contraintes (niveau de température, satisfaction des besoins des consommateurs). Ces travaux ont généralement fourni les points de fonctionnement nominaux des réseaux considérés, en faisant l'hypothèse d'un régime permanent. Cependant l'utilisation d'énergie renouvelable pour produire le

froid ainsi que la diversité des besoins des clients rendent nécessaires le développement d'outils basés sur des modèles dynamiques. Ces derniers permettront en effet d'améliorer la conduite, le dimensionnement, le contrôle et la gestion (planification) des systèmes, nouveaux ou déjà installés, en prenant en compte les variations de demande des différents consommateurs, les variations des conditions climatiques extérieures à la localisation où ces systèmes sont installées et les variations dans la production (cas de sources renouvelables – Solaire…) conduisant à l'utilisation et à la gestion de moyens de stockage. Actuellement le développement d'applications basées sur des modèles dynamiques pour l'analyse et l'optimisation de réseaux de froid est rare. Il y a donc un besoin urgent d'études portant sur le développement d'outils capables de répondre aux défis actuels que constituent la conception et la conduite de ces systèmes.

Dans cette optique, l'objectif de cette thèse est de développer une méthodologie pour l'optimisation dynamique du système de distribution d'un réseau de froid, qui permettra d'obtenir les profils temporels des paramètres de fonctionnement de ce système en prenant en compte les variations de la température ambiante. Cette méthodologie sera illustrée par un exemple de taille moyenne avec 20 consommateurs connectés, chacun avec son profil temporel de demande. Le travail de recherche mené pour le développement de cette méthodologie est présenté dans ce manuscrit de thèse divisé en quatre chapitres.

Le chapitre un présente une revue bibliographique commençant par les généralités sur les réseaux de froid et leurs implantations en Europe et en France. Ensuite, ce chapitre introduit les défis que le développement de tels systèmes impose, parmi lesquels le développement d'outil d'optimisation basés sur des modèles dynamiques. La revue bibliographique détaille alors les travaux ayant porté sur l'optimisation de ces systèmes énergétiques de distribution puis introduit les généralités concernant l'optimisation dynamique ainsi que les méthodes mises en œuvre pour résoudre ce type de problème. Sur la base des résultats de la littérature, nous introduisons la méthode que nous avons choisie pour la discrétisation des problèmes dynamiques (collocation orthogonale sur éléments finis) puis ce chapitre se termine avec la présentation des objectifs de la thèse.

Le chapitre deux détaille, pour le cas étudié, la topologie, les profils de demande des consommateurs et des profils de température extérieure suivant la localisation du réseau. A travers cet exemple, ce chapitre présente le modèle mathématique représentant la physique du réseau et une analyse de degré de liberté qui sera utile pour les optimisations. Ce chapitre se termine par la présentation de la mise en œuvre de la technique de discrétisation utilisée pour résoudre le système.

Le chapitre trois introduit la méthodologie pour initialiser correctement les problèmes d'optimisation dynamiques mettant en œuvre le modèle précédemment discrétisé. La méthode utilisée est basée sur

des résolutions successives de simulations quasi-statiques pour initialiser le problème de simulation dynamique dont les résultats seront utilisés pour initialiser les optimisations dynamiques. Ce chapitre détaille les résultats de ces simulations intermédiaires incluant, pour une politique de débit constant, la définition des diamètres et des résistances thermiques des canalisations, la distribution des températures le long des canalisations du réseau, et la réponse du réseau aux profils de demande et de température extérieure. Cette analyse est faite pour des tuyaux isolés et non-isolés.

Le chapitre quatre présente les résultats d'optimisations dynamiques considérant deux types de fonctions objectif. La première permet de calculer les profils optimaux des débits permettant de respecter une température constante dans les canalisations quittant chaque consommateur, ceci afin d'éviter un problème technique classique dans les réseaux de froid appelé syndrome du faible ΔT (low ΔT syndrom). La seconde fonction objective cherche, en plus, à obtenir les diamètres optimaux des canalisations qui minimisent, cette fois, un coût opérationnel calculé sur la base d'un coût de production de l'utilité froide et du coût de l'énergie électrique nécessaire au pompage de l'eau froide à travers le réseau. Les deux fonctions objectives sont calculées pour des canalisations isolées et non-isolées.

Finalement, la cohérence des résultats présentés dans les chapitres trois et quatre et les temps calcul annoncés mettent en évidence la robustesse de la stratégie de discrétisation choisie et de la méthode de résolution proposée.

Chapter 1. District Cooling Systems

As presented in the introduction of this work, the first chapter details the generalities and challenges in the development of district cooling systems. Based on these challenges, we introduce the objectives of this work and the tools and methods we propose to accomplish them.

Section 1 introduces the concept of district energy systems. From this, section 2 presents the generalities of district cooling systems and their development in the European and French markets. This section finishes presenting the current challenges in the research and development in this system with a focus on numerical applications. Following this, Section 3 presents a literature review of some approximations for the dynamic modelling of the district system. Then section 4 presents and categorize the applications in the optimization of district systems highlighting the lack of contributions based on dynamic models. Considering this, section 5 presents the generalities of dynamic optimization, including the formulation and the diversity of methods for their solution pointing out the advantages of the formulation based on collocation methods introduced then in section 6. Finally, section7 presents the objectives of the present work.

Chapter contents

1.1 District Energy Systems

According to 2017 data, heating and cooling account for half of the energy consumption in the European Union [1], [2]. From which, 45% is used in the residential sector, 36% in industry and 18% in services [3]. Furthermore, most of the fuel used by for heating and cooling still comes from non-renewables (75% as estimated by the European Commission [4] and detailed in Figure 1-1), representing a major source of CO_2 emissions that need to be urgently mitigated [3], [5], [6].

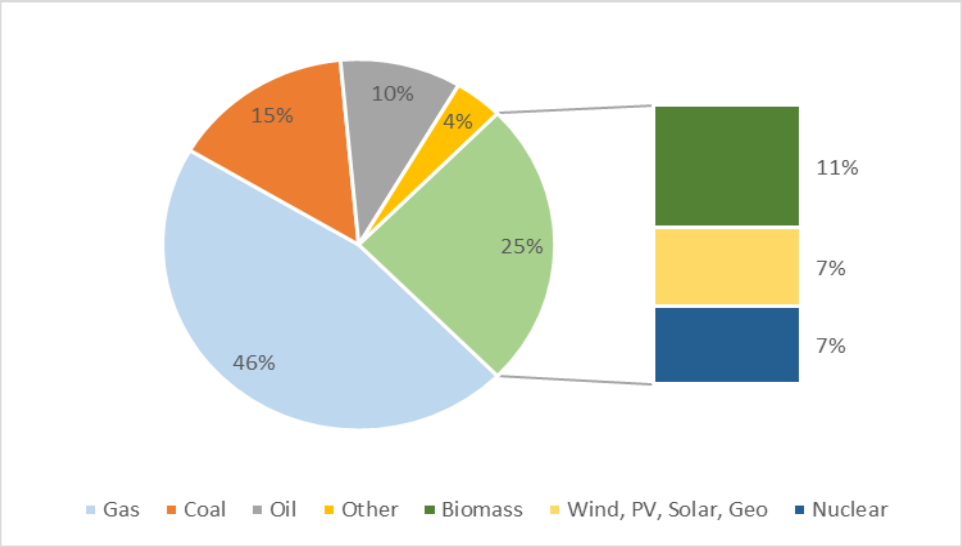

Figure 1-1. Energy sources for heating and cooling, based on data in [4]

Being aware of this, district energy systems arise as an interesting alternative to mitigate the environmental impact caused by these emissions [1], [2], [7]. Indeed district energy systems, known also as District Heating and Cooling systems (DHC) [8], consist of a network of underground insulated pipes that pump hot or cold utility from a central energy plant and route it to multiple buildings in a district, neighbourhood or city [9]. The utility gives or takes heat from the user, according to the case, and then recirculates back to the central plant through a close-loop return line as shown in Figure 1-2. As stated by Lake *et al.* [10] and Rezaie and Rosen [11] in their reviews, these systems compared with individual heating and cooling equipment, have higher efficiency, are more economically attractive for high demand buildings, reduce fuel consumption, improve community energy management and allow a better control of emissions.

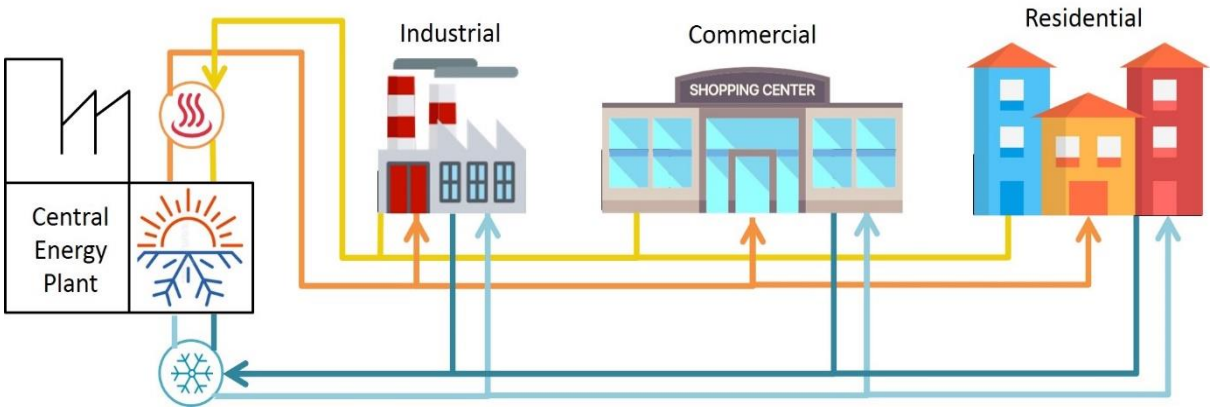

Figure 1-2. General scheme for a DHC system

1.2 District Cooling Systems

The access to cooling services has an important impact in different sectors including healthcare, education, and sustainability [12]. It can be evidenced by its wide applications in different sectors including industrial refrigeration (to guarantee safe food storage), transport, commercial and domestic refrigeration, air-conditioning (AC), supply of medicines, cooling data centres, production of chemicals, plastics, metallurgic processes and many other sectors and usages [13]. Considering this, district cooling networks can represent an attractive solution to cover the demand in these sectors.

Compared to heat, cooling systems have long been under-represented in energy policy as well as in research [14]. Evidence of this, is the total current installed heating capacity in the 45 called "champion cities for district energy use" in 2015, which reach more than 36 GW while the total cooling installed capacity was 6 GW [7]. This is linked with the fact that cooling demand nowadays is considerably lower than the heating demand as detailed in Figure 1-3 (2% (space and process cooling) vs 48% (space, process and other heating and hot water) of the total energy use in the European market in 2015).

Furthermore, as already said in the previous section, heating and cooling account for half of the energy consumption in the European Union. Among these 50%, space heating accounts for 54% and space cooling for 2% according to the Heat Roadmap Europe 4th project data[15], as detailed in Figure 1-3.

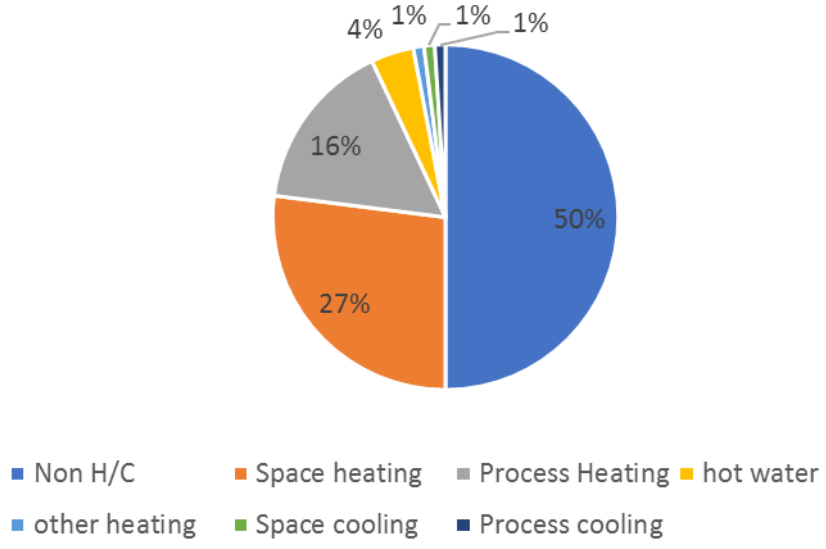

Figure 1-3 Energy use in the European market in 2015, Based on ref [15]

However, space heating is expected to decrease in the future because of the well-insulated building envelopes whereas space cooling is expected to increase because of climate change and urbanization. Hence, in their modelling of global residential sector energy demand Isaac and van Vuuren predicted

that heating energy demand decreased by 34% worldwide by 2100 while air-conditioning energy demand increased by 72%, with considerable impact at regional scale[16]. According to the International Energy Agency's report "The Future of Cooling" [17], we will pass from 1.6 billion buildings with air conditioning worldwide in 2018 to 5.6 billion by 2050. The power required to supply this increased demand is equivalent to the current combined electricity capacity of the United States, the European Union and Japan. In this scenario, district cooling represents one of the most interesting options to cover the increasing demand in space cooling with a lower dependence on the electric grid which allows also the implementation of more sustainable technologies to cover the demand of many users in a city at the same time. Furthermore, Dominković *et al.*[18] state that there is a big potential for the spread development of these systems in hot and humid climate zones (*e.g* Southeast Asian and South America), where the demand for space cooling is more important than in the European market, where district cooling has been historically more developed as reported by Eveloy and Ayou[19].

These facts have encouraged many shareholders from a broad variety of sectors providing cooling technologies or demanding chilling, cooling or refrigeration, to raise awareness of this undervalued element of energy systems [13]. Following this direction, the European Union has also been supporting the development of many projects leading by industrial-academic consortiums like INDIGO [20] which aims to- improve system planning, control and management of district cooling systems (DCS); RESCUE [21] which pursues for the development and implementation District Cooling Systems using low and zero carbon-emitting sources; among others [22].

1.2.1 Generalities of district cooling

The configuration of a DCS includes a central plant, a distribution network, and several customer site connections (energy transfer stations). Furthermore, when using renewable sources to produce cold, these systems include thermal storage systems.

The benefits of district cooling include (I) low energy requirements, (II) energy efficiency and (III) peak period saving potential[23].

I. District cooling consumes up to 50% less energy than conventional individual technologies, thanks to the highly efficient chiller technology and the ability to maintain a steady-state level of efficiency over time.

II. This technology needs 15% less capacity for the same cooling loads compared with isolated units. In addition, district cooling is flexible in capacity design and installation.

District cooling can serve different kind of clients (industrial, residential, commercial), with very different demand requirements and is able to aggregate the peak demand. On the

other hand, individual systems have to be designed to meet the demand of each isolated user (with an excess capacity between 30-50%). The aggregation offered by DCS results in a reduction of up to 25% of the peak load compared with the individual sum of peak loads.

III. Cooling networks have the capability of thermal storage, which smooths out power requirements reducing the stress on the power system at peak hours. It is possible to store up to 30% of potential outputs. By contrasts, individual systems enforce their full load on power systems at peak hours.

District cooling has also benefited from various advances in technologies that have to increase its interest as an important way to supply the growing cooling demand. Some of these advances include [24]:

- New chiller technologies, with upgraded efficiencies.
- Enhanced efficiency of piping and distribution systems
- Cheaper and more efficient insulation technologies
- Significant increment of cogeneration systems, which improve thermal efficiency (70%-85%)
- Advances in cooling storage technologies.

These advances and the flexibility of these systems offer the opportunity to integrate different technologies for the production and storage of cold utilities to serve the most diverse kind of clients. The production of chilled water can be achieved by different methods, which includes the use of Absorption refrigeration machines, compression equipment and combinations of mechanic and thermal driven absorption systems [25], or via "free cooling" which refers to cold water from deep lakes, rivers, aquifers or the ocean [26]. Moreover, these systems can be powered with renewable energy options like wind, solar energy, biomass, and geothermal [27]. For thermal storage, it is possible to use, chilled water tanks, ice and phase change materials (PCM). Figure 1-4 details the relationship between the production of the cold utility, and the storage technologies with different kinds of users connected to a DCS as presented by Gang *et al*. [27]. Cooling networks can also be integrated with Combined Heat and Power (CHP) systems to develop three-generation systems, known as Combined Cold Heat and Power systems (CCHP), which supplies electricity, hot and cold services to the users [28].

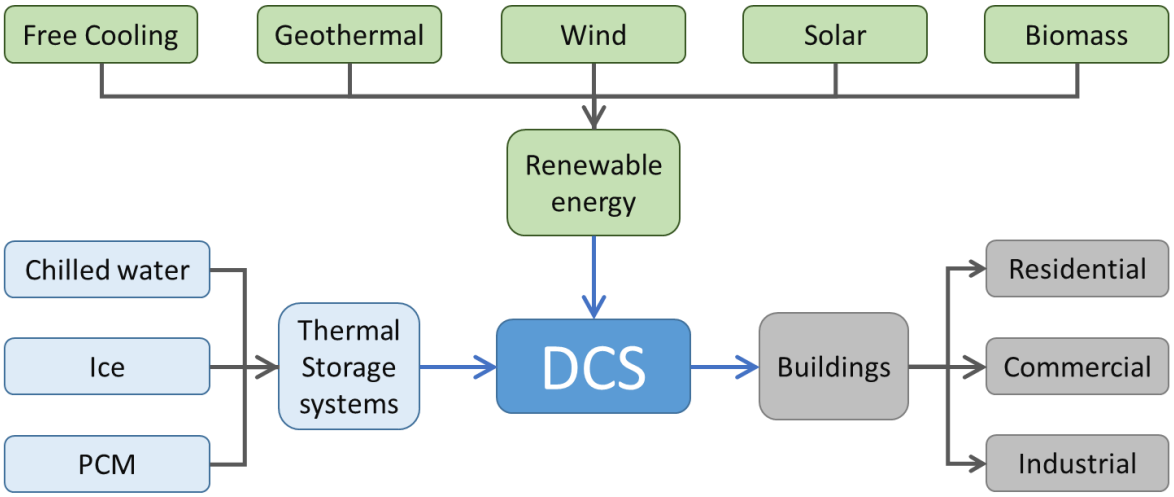

Figure 1-4. Flexibility and integration of technologies in DCS

District cooling interest and expansion is currently increasing around the world. In the Middle East, this growing is notorious in the Gulf region, where its evolution is exponential since the 1990s, with plans to triplicate their capacity by 2030. In the United States, some local legislation has changed to favour the implementation of these technologies, including subsidies aiming to a demand increment of district cooling. In China, DCS is still a growing industry. India is aiming to implement district cooling in five of its major cities with the support of the United Nations Environmental Program (UNEP) [29].

Additionally, district cooling can bring important benefits to society including the reduction of CO_2 and environmental hazardous refrigerants (HCFC), improvement of building environments (space and reduction of noise), reduction of peak electrical consumption in summer (guarantying local reliability of electricity supply). More benefits of the implementation of district cooling are detailed in the European report [30]. However, district cooling presents also some drawbacks including the fact that some isolated areas could not be efficiently connected to these networks and the high capital cost that might be required for their implementation [7].

1.2.1.1 District Cooling in Europe

District cooling has been developing around the most populated cities in Europe, to supply mainly the service sector, and in some cases the residential and industrial sectors [31]. By 2006, the continent reported 115 cooling systems, as detailed in Figure 1-5. In some of the European countries, the development of district cooling might depend on the previous experiences they have with district cooling like in Paris, Helsinki and Stockholm. In other cases, the development is more recent and rooted to innovate local urban projects like in Barcelona and Lisbon [30].

Figure 1-5. Mapping of district cooling in Europe in 2006 (biggest per country have a star) as presented in ref.[30]

As reported in 2015 by the European Commission, the total installed capacity of district cooling is 2.4 GW, which represents less than 1% of the installed district heating capacity of 301.5 GW in the region, due to the difference of demand between these two services. The largest district cooling capacities are in France (669 MW), Sweden (650 MW), Spain (317 MW), Finland (247 MW), Italy (172 MW) and Germany (168 MW). Austria (55 MW), Poland (35 MW), Denmark (34 MW) and Hungary (7 MW) also have district cooling systems. Moreover by 2011 two thirds of the energy delivered by these systems took place in France and Sweden.

Considering these facts and the cooling demands for 2015 reported by Persson and Werner for residential and service sectors (Figure 1-6) [32], we can evidence that there is a big need for the development of district cooling in all the region. France and Sweden as leaders in the implementation of district cooling, are in contrast 14th and 23rd in the rank of cooling demand, while countries with major demands present a poor development of these systems.

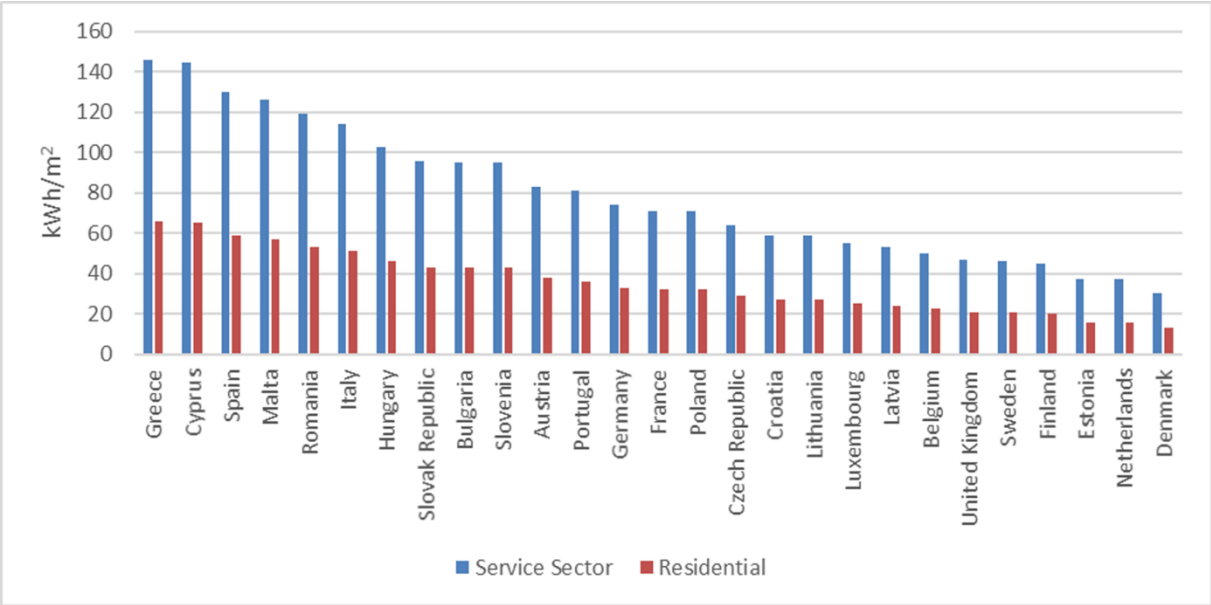

Figure 1-6. Specific cooling demands by country, based on data in ref[32]

Due to increment and trends of useful floor areas that are cooled, and/or air-conditioned in the continent over the last few years, a sharp increment in the cooling demand is expected by 2020. The Global CCS Institute reports an increase of 82% in the cooling demand of the residential sector and 60% in the service sector for the period 2007-2020. For 2020, the saturation rates of these sectors will be of 40% and 60% respectively. Additional expansion might be caused by an increment in overall occupied floor space, climate changes and additional technical installations. Variations in building standards and social behaviour might also affect this increment. Taking this into account, a substantial increment in cooling demand is expected from 2020 to 2030 (6%).

The eventual implementation of district cooling to cover 25% of the European Cooling market, would lead to a reduction between 50 to 60TWh in the annual electricity consumption [13], resulting also in a reduction of investments in electricity capacity by 30 million €. In addition, the reduction of annual CO_2 savings would be up 60 million tons, which represent 15% of the European Union's Kyoto commitment [30].

1.2.1.2 Penetration of district cooling in France

According to the 2018 survey of FEDENE (Fédération des Services Energie Environnement) [33], France has a total installed capacity of district cooling systems (DCS) of 1 TWh, becoming one of the most extensive systems in Europe. Nevertheless, the implementation of these systems along the country is not as widespread as for district heating systems (DHS) as detailed in Figure 1-7 and Table 1-1

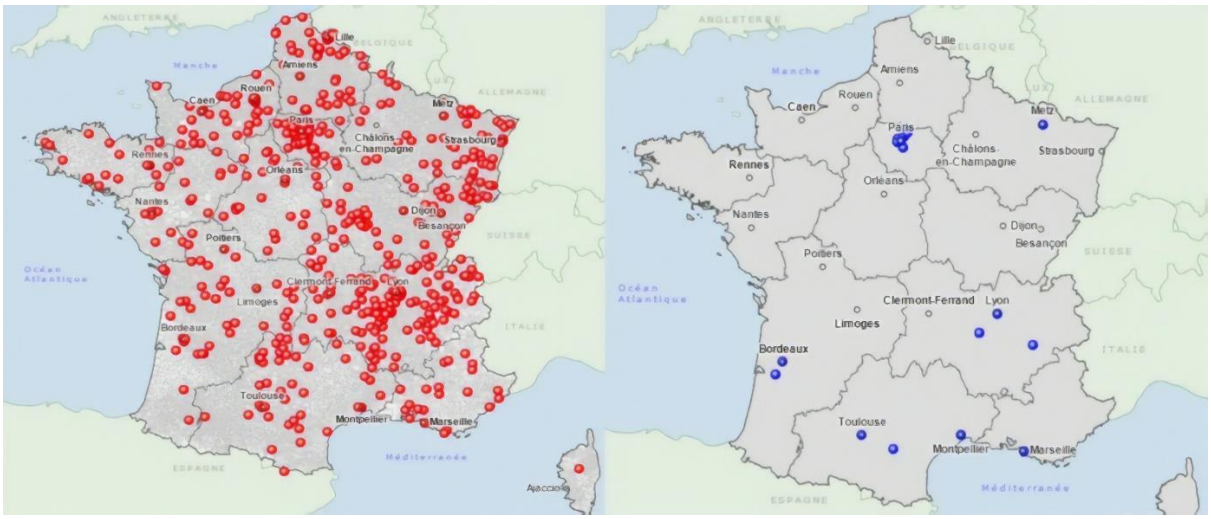

Figure 1-7. Indicative mapping of DHS (left) and DCS (right) in France[33]

Table 1-1 details the distribution of heating and cooling networks in the country according to the survey.

Table 1-1. Distribution of heating and cooling networks in France

	Heating networks	Cooling networks
Number of networks	761	23
Total length of networks	5397 km	198 km
Delivered power	25 TWh	1 TWh
Buildings connected	38212	1234

This shows that although the development of district cooling networks in the systems in the country is one of the highest of the continent, there is still opportunity to increase its implementation mainly in the regions away from the big cities.

As seen in the map of Figure 1-7, Paris concentrates much of the cooling potential of the country, but it should be added that Paris also represents one of the leaders on district cooling in the world [34]. The development of district cooling in this city dates from 1968 when a centralized heating and cooling system was built as part of the renovation of the area where the shopping centre of Forum Les Halles is located today. To achieve economic feasibility, the system had to supply other buildings, and they decided to connect the Louvre museum. In this early stage of development, the system produced the cold from centrifugal chillers with cooling towers installed on the top of the building, coupled with ice energy storage. As the system expanded, with more clients, connections and production sites, its economic feasibility raised up [35]. In 1991 Climespace [36], became a shareholder with the intention of expanding the District cooling system of Paris.

Today, this city has developed the largest cooling network of Europe, part of which uses the Seine river for cooling [7]. The 10 production sites and the 3 storage centres meet the cooling requirements of hotels, department stores, offices, state-building and museums. The 75 km long network serves more than 650 customers with an equivalent area of 6 million m^2 [37].

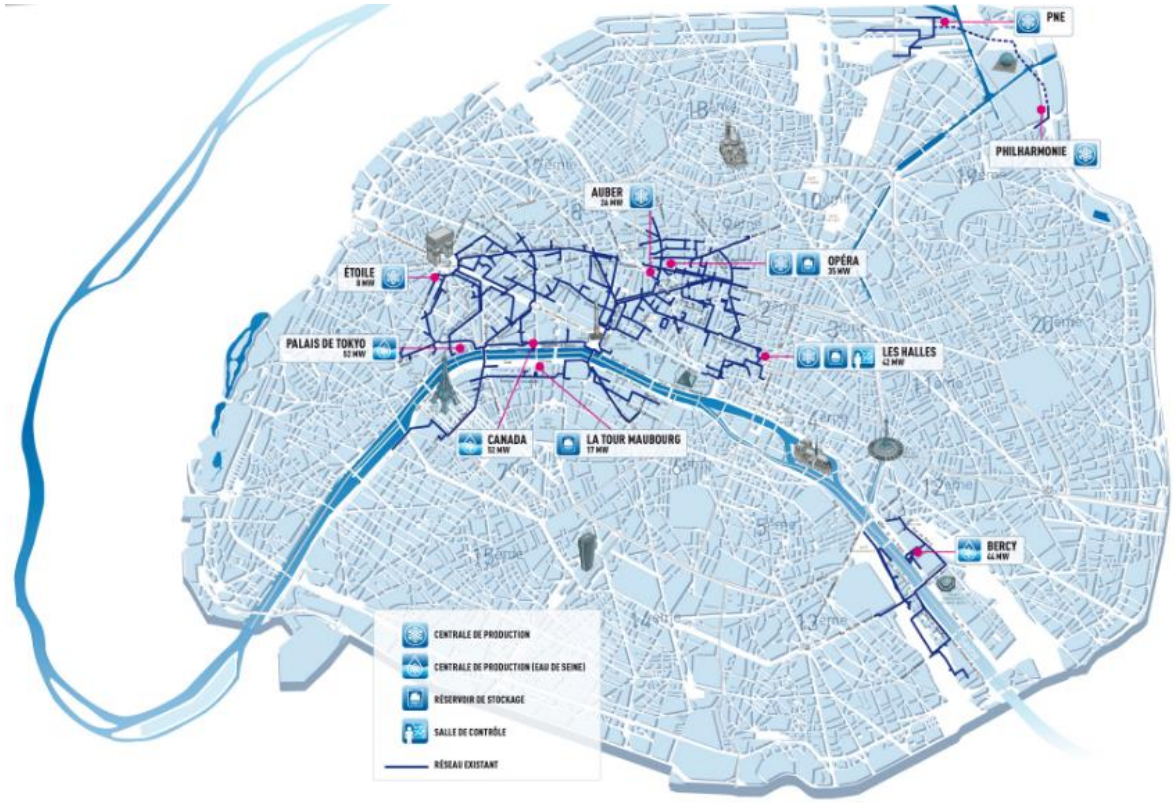

Figure 1-8. Map of the Parisian Cooling Network[35]

1.2.2 Challenges on research in District Cooling

Due to its growing importance, demand and market, in the last 20 years the studies on district cooling have considerably increased [14]. The topics of growing interests include the integration of these systems with sustainable energy technologies and the optimization of its planning design and operation [27].

Literature states the use of thermal storage systems in DCS, but few studies addressed the design and control optimization of the integrated system. Problems including the optimal size of the storage system and the amount of energy to be stored need to be further investigated. The performance in different climate areas needs more studies as well as the comparison with traditional cooling systems. Rational design and planning of energy systems have an essential role to achieve energy saving/efficiency and maximum economic benefits of its implementation. Nevertheless, to accomplish these goals it is necessary to deal with [38]:

1. Spatial and temporal aspects, related to the location and consumption (power demand, temperature level), production and price profiles respectively.
2. High variety and number of network layouts and size of energy systems as possible candidates.

One of the reported drawbacks for the implementation of district cooling relies on the limited knowledge of Know-how and technical skills [11], and some authors have highlighted the need to focus research on technologies and policies necessary to economic transition from single user systems to district [10].

Moreover, in the field of modelling and simulation of this systems, there are still improvements to be made regarding the coupling building-level models with system models of components (pumps, pipes), as well as a shift to fully dynamic models [39]. Finally, studies on control optimization of the entire chilled water system including DCS and users, considering dynamic character and interactions [27] and minimization of costs could improve the development of this technology.

1.3 Dynamic modelling and simulation in DHC

Most of the available literature on dynamic modelling and optimization of district energy systems centre their interest in the analysis of district heating systems. Nevertheless, these models can be applied to district cooling, but the following differences should be considered [40]:

- The smaller temperature difference in the case of DC between supply and return pipes compared with DH.
- Even slight changes in network temperatures (e.g. 0.1K) can have an influence on the efficiency of cooling generation.
- The direction of heat fluxes through the walls of buried pipes can change during the year (heat gains or losses) as the network temperature is in the range of the soil temperature

Studies on equation-based methods for the analysis of energy networks [41]–[45], use a one-dimensional heat transfer equation to describe the temperature transients in the pipes [46] that is defined as:

$$\overbrace{\rho_{cf} \cdot Cp_{cf} \cdot A_p \cdot \frac{\partial T}{\partial t}}^{1} + \overbrace{\dot{m}_{cf} \cdot Cp_{cf} \cdot \frac{\partial T}{\partial x}}^{2} = \overbrace{k_{cf} \cdot A_p \cdot \frac{\partial^2 T}{\partial x^2}}^{3} + \overbrace{\frac{T_s - T}{R'}}^{4} \quad (1\text{-}1)$$

Where ρ_{cf}, Cp_{cf}, A_p, and $\dot{m}_{cf}$ are the density, specific heat capacity, cross-section area, and mass flow rate of cooling fluid in the pipe, respectively. k_{cf} and R' are the thermal conductivity of the cooling fluid and the total thermal resistance per unit length of pipe; T stands for temperature in the pipe, T_s for the temperature of the soil surface, and t and x for time and distance variables. The groups 1 to 4 in equation (1-1) represent the gains, the enthalpy flux, conductive and convective heat transfer of the fluid.

This heat equation is subject to the following assumptions:

- ✓ Plug flow
- ✓ The heat transfer is considered only in the radial direction
- ✓ Conduction heat transfer is considered through the pipe, the insulation, the casing and the soil
- ✓ Material properties are constant and independent of temperature.
- ✓ It does not include thermal interactions between supply and return pipes
- ✓ Thermal inertia of the pipes, the casing and the insulation is neglected

The term of conductive heat transfer in the fluid (3) is negligible compared to the other components of the equation and can be neglected [44]

The computation of the total thermal resistance R' is a function of the thermal conductivities of the pipe, the insulation, the casing and the soil respectively as well as the flow regimen of the pipe (through the internal convection heat transfer coefficient) and is given by [42]:

$$R' = \frac{1}{2\pi r_a \bar{h}} + \frac{\ln\left(\frac{r_b}{r_a}\right)}{2\pi k_{ab}} + \frac{\ln\left(\frac{r_c}{r_b}\right)}{2\pi k_{bc}} + \frac{\ln\left(\frac{r_d}{r_c}\right)}{2\pi k_{cd}} + \frac{1}{Sk_s} \tag{1-2}$$

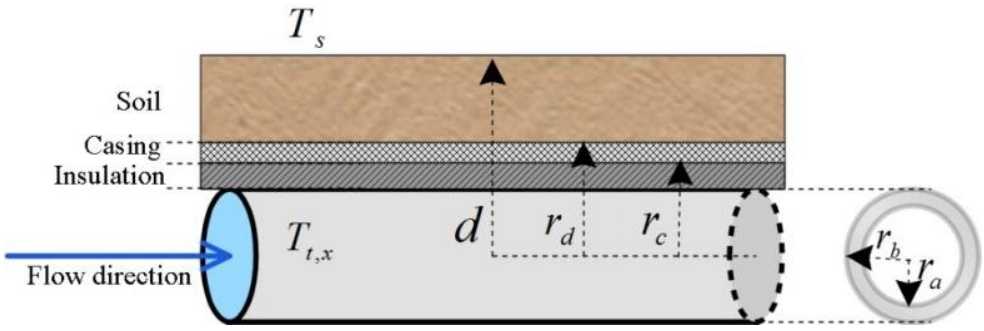

Figure 1-9. Representation of a buried pipe

Where $\bar{h}$ is the average convection heat transfer coefficient in the pipe; k_{ab}, k_{bc}, k_{cd}, and k_s are the thermal conductivities of the pipe, insulation, casing, and soil, respectively and S is the conduction shape factor, that can be approximated as [46]:

$$S = \frac{2\pi L}{\ln\left(\frac{4d}{2r_d}\right)} \tag{1-3}$$

For $d > 3r_d$

The average convective heat transfer coefficient is computed as:

$$\bar{h} = \frac{\overline{Nu} k_{cf}}{2r_a} \tag{1-4}$$

Where $\overline{Nu}$ is the local Nusselt number assuming turbulent flow in a smooth circular tube and can be computed from the Dittus-Boelter equation as[47]:

$$Nu = 0.023 Re^{4/5} Pr^{0.4} \tag{1-5}$$

Finally, Reynolds and Prandtl's numbers are represented by:

$$Re = \frac{\rho_{cf} v \cdot 2r_a}{\mu_{cf}} \tag{1-6}$$

$$Pr = \frac{\left(Cp_{cf} \mu_{cf}\right)}{k_{cf}} \tag{1-7}$$

Where v is the flow velocity, μ_{cf} is the dynamic viscosity of the cooling fluid. The presented partial differential equation has been used for the dynamic of district heating systems, but as stated at the beginning of the section it can be applied to study district cooling systems.

The solution of the Partial Differential Equation (PDE) (1-1) can be addressed using discretization strategies (e.g. Finite elements, finite volumes, finite differences) or 1D analytical solutions coupled with physical approximations.

Using partial discretization, the PDE becomes a system of ordinary differential equations (ODE) that can be solved using a numerical integrator implementing a method such as Runge-Kutta. While using total discretization, the PDE becomes a set of algebraic equations. Among the approximations using discretization strategies, Ben Hassine *et al.* [41] implemented explicit finite differences of 1st order $\left(\frac{\partial T(x,t)}{\partial x} = \frac{T(x,t)-T(x-\Delta x,t)}{\Delta x}, \frac{\partial T(x,t)}{\partial t} = \frac{T(x,t)-T(x,t-\Delta t)}{\Delta t}\right)$ to fully discretize the PDE resulting into a system of nonlinear equations that can be solved explicitly. They present a quasi-dynamic approach, implemented in Matlab®, where the flow and pressure in the network are calculated using a static flow model, and the temperature is calculated dynamically

On the other hand, there are estimations based on a succession of steady states, as proposed by Duquette *et al.* [42], or the Lagrangian approach of other authors [43]. The first ones solve the equation (1-1) analytically in steady-state, finding an expression that computes the outlet temperature. In this case, the integration of the temperature is performed along the length of the pipe. Then, a transport delay is computed to simulate the fluid flow in the pipe using a numerical time series model, implemented in Simulink®. At each time step, a new estimate of the transport delay is computed (since the mass flow is time-dependent) and stored. Hence, the fluid temperature at the pipe outlet considering the transport delay is calculated, enabling to model the propagation of the temperature in the pipe. This implementation is attractive in terms of computational time, nevertheless, due to the storage of data and the growing of the model during the simulations it is not suitable for optimization applications. Besides, the implementation focused only on the distribution network and no indication was given on how to extend the methodology to model the users or the heat/cold producer. Other authors use an equivalent approach, which analytically solves the Lagrangian (material) derivative over time (also known as the method of characteristics). In this case, the integration of the temperature is made from the initial time to the value of the final time that includes the transport delay. The latter is computed using the velocity in the pipe which is linked to the mass flow that can be constant or variable as stated by Velut and Tummescheit. Van der Heijde *et al.* [44] and Schweiger *et al.* [45] perform this implementation in Modelica®, where the calculation of the fluid and temperature propagation are separated from the heat loss calculation, combining a plug flow approach with an ideal mixed volume model.

1.4 Optimization approaches

The optimization of district energy systems is strongly motivated by minimizing the cost of infrastructure and the emissions maximizing the production of the hot or cold utility, or its efficiency. Such optimization is particularly challenging because of technical characteristics and the size of real-world applications [38]. In general, mathematical optimization of these systems is strongly unbalanced in favour of the analysis of district heating systems, as stayed by Werner [14] and evidenced in the number of publications registered in the Elsevier's abstract and citation database Scopus between January 2000 and March 2019 for each kind of system. Figure 1-10 compares the number of publications in the mentioned period registered in the Scopus database when searching for "district heating optimization" (1062 documents) and "district cooling optimization" (271 documents).

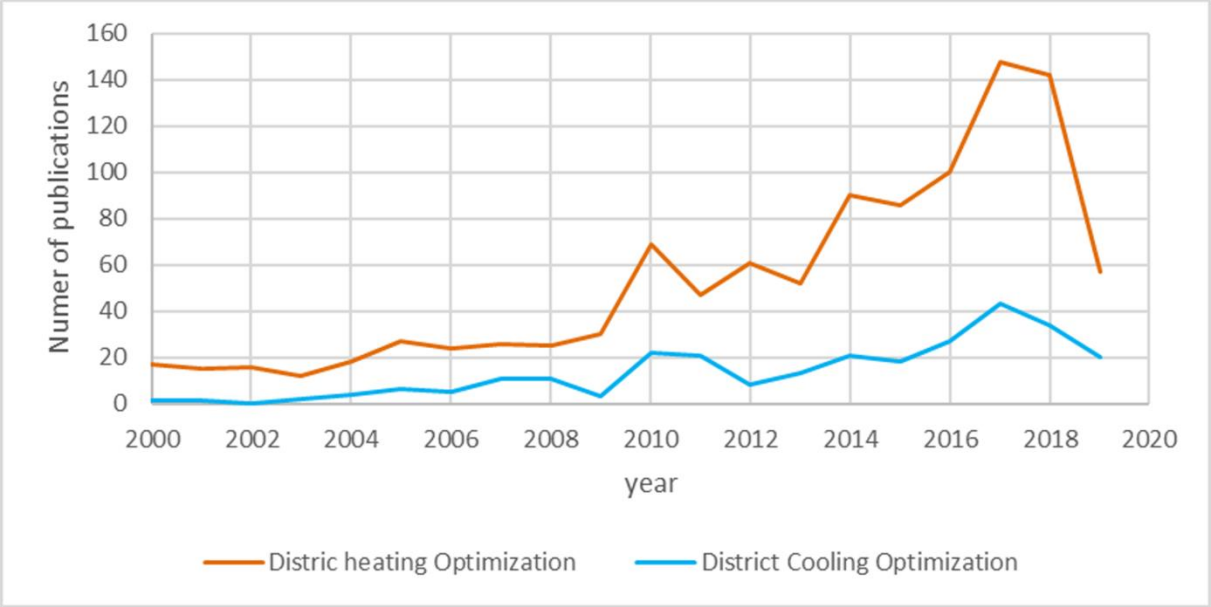

Figure 1-10. Comparison of research in Optimization of district heating and district cooling systems

It is important to point out that each kind of systems presents its own issues, related not only with the kind of utility produced (hot or cold) but also with its operation for improving the system efficiency, as it will be detailed in the objectives of this work.

These facts highlight the importance of studies focused on district cooling networks. But despite the lack of analysis of district cooling systems, it is important to highlight that most of the methodologies implemented for the different analysis in DHS can be used to study DCS as well.

Before introducing the applications of optimization in district energy systems, it is important to present a general classification of the type of problems we find in mathematical optimization. An optimization problem consists of one (or sometimes more) objective function to be minimized (e.g.

Operational cost, CO_2 emissions) or maximized (efficiency, production), subject to the fulfilment of physical or operational constraints of the system, represented as equality or inequality constraints, by manipulating a set of decision variables. Depending on the nature of the decision variables (continuous or discrete), it is possible to establish a general categorization of optimization problems, that is independent of the methods implemented to solve the problem as stated by Biegler and Grossmann [48]. If the problem is described only by continuous variables, considering the nature of the constraints and the objective function that describes the system (linear or non-linear) we have linear programming (LP) and non-linear programming (NLP) problems. When discrete variables are involved, they are classified as mixed-integer linear programming (MILP) and mixed-integer non-linear programming (MINLP) problems. Finally, when dealing with dynamic models, two approaches are possible. Either we represent the dynamic problem as a succession of steady-state problems known as multi-period optimization, or we actually deal with the dynamic of the system. In this latter, we can do this either via the Pontryagin's principle (optimal control) or via discretization, formulating the dynamic problem as an algebraic problem (NLP, MILP or MINLP) known as dynamic optimization.

Following the presented classification, we can organise the studies on the optimization of district heating and cooling as presented in Table 1-2. The table details selected contributions in terms of the kind of problem that is solved and their main applications. More extensive reviews on the applications of optimization in District energy systems are presented by Talebi *et al.* [49] Sameti *et al.* [38], Gang *et al.* [27]. Eveloy and Ayou[19] also present optimization applications specifically for DC, highlighting that most of the studies have focused on the optimization of the distribution network infrastructure (MILP and MINLP formulations) considering steady-state models.

Table 1-2. Classification of works on Optimization of DHC

Continuous Variables	**Integer variables**	
NLP	**MILP**	**MINLP**
	Data based Chow *et al.*[50] - Diversity factor	**Data based** Deng *et al.*[51] -Scheduling
	Steady-state Söderman[52] - Topology - Operation (flow rates)	**Steady State** Mertz *et al.*[53] Marty *et al.*[54] - Topology - Sizing - Operation
	Multiperiod Khir *et al.* [55] - Sizing - Topology	

Continuous Variables	Integer variables	
NLP	**MILP**	**MINLP**
	- Operation	
Dynamic Schweiger et al.[45] - Operation Powel and Edgar[56] - Temperature control Powel et al[57] - Operation **This contribution** - Operation - Pipe diameters		**Dynamic data based MIQCP** Schweiger et al.[45] - Scheduling

Due to the complexity involved in the models to describe these systems, the applications of LP in district heating and cooling are scarce.

Most of the applications are focused on the optimization of the distribution network infrastructure that includes the selection of technologies, the number and kinds of users connected to the network, existence of network elements (pumps, chillers, storage tanks, pipes), that results in implementations with integer variables (MILP and MINLP).

Among the application in district cooling, Chow *et al.* [50] presented a MILP formulation that optimized the diversity factor, which is the proportion of diverse types of buildings (Office, Residential, shops, hotels and mass transit railway stations) leading to a uniform cooling load to ensure a high stability to the cold production system to be installed. They first calculate 24 hourly typical profiles of demands for five types of buildings using a freeware building energy analysis program that can predict the energy use and cost for all types of buildings, for 36 typical days (three typical days per month). Then, with these data, they implemented a genetic algorithm to solve a MILP problem that aims to minimize a fluctuation index with respect to the maximum cooling demand. Here the optimization variables are the number of buildings for each of the five categories. In order to try to avoid local optima, they used a genetic algorithm. However, their study does not consider the topology of the network, which might have an important impact on the delay and in the formulation of the fluctuation index.

Moving to MINLP applications, Deng *et al.* [51] presented an approach for the optimal scheduling of an actual DHC system that minimized its daily operation cost. The system was composed of an electric chiller system, a ground source heat pump, a thermal storage system and a combined cooling, heating and power system. The nonlinearities of the continuous variables corresponded to the operational conditions of each of the components of the system, while the discrete variables corresponded to the use (on/off) of the chillers in different periods of energy demand. This contribution optimized the energy mixing of the system, aiming to cover a given total demand, but assumed that the equipment always operated at nominal levels. However, they did not consider the interactions of the clients with the distribution system nor their location respect to the production site.

Continuing with steady-state studies, Söderman [52] presented an optimization of the structure and operation of an existing cooling network, based on a steady-state model for the maximum cooling demand of the users. He also presented a project in which the capacity of the network would be increased to serve almost the double of customers. For the expansion of the network, he computed the location of new energy storage and production sites, as well as pipe connections of the new interconnected system. This work included the linearization of the mathematical model of the network. The problems were solved using the MILP solver CPLEX. Although this contribution, contrary to the previous one, presented a detailed analysis of the network, some parameters (pipe diameters) are not reported in the contribution. Also, the steady-state assumption might prevent the use of renewables for the expansion of the network. Finally, the assumption of constant cooling demands might result in overestimation of the production of cold.

MINLP steady-state applications in heating networks include the works of Mertz *et al.* [53] and Marty *et al.* [54]. The first performed a combinatory non-linear optimization to find the topology and substation's exchangers size that minimized the global cost of a district heating network. The resulting MINLP problem was solved using DICOPT within GAMS®. Marty *et al.* [54] implemented a strategy to simultaneously optimize the district heating network topology, the Organic Rankine Cycle (ORC) sizing of a geothermal plant as well as the distribution of the geothermal fluid between the ORC and the DHN. For the solution of the proposed MINLP problem, they used the MINLP solver DICOPT in the environment of GAMS®. Since the main critical point in solving an MINLP problem is the initialization, Mertz *et al.* [53] and Marty *et al.* [54] also presented their strategy to overcome this point. However, all of these studies were performed for steady-state conditions although the variable demand of the customers, the thermal storage or, sometimes, the use of intermittency renewable energy become the DHN and DCN into dynamic systems.

The multiperiod application presented by Khir and Haouari [55] developed an approximation for the optimal design of a DCS whose results comprised the chiller plant size, a storage tank size, layout of the network and the quantities of energy produced and stored during each period. The implementation was made in the software package ILOG CPLEX, and the results aimed to minimize the sum of investment and the operational cost of the system. District planning included studies on the influence of the number and kind of buildings served by the cooling network. Their model considers the demand of the user at each period, but it does not consider the dynamics of the temperature in the pipes of the system.

As stated by Gang *et al.* [27] and Allegrini *et al.* [39], one of the most unexplored subjects of study in the field of energy systems is the dynamic optimization and control of these systems. Recent advances in this field include the optimal production planning in district heating systems [45], control of a solar thermal plant with thermal energy storage [56] and dynamic optimization of hybrid Solar thermal and fossil Fuel system[57].

Schweiger *et al.* [45] presented a framework to represent on-grid energy systems and to perform dynamic thermo-hydraulic simulation of energy systems. The framework was based on the modelling language of Modelica®, performing the continuous optimization tasks with the OPTIMICA compiler toolkit, and the discrete optimization in the environment of the open-source Phyton module Pyomo. They decomposed the resulting mixed-integer-optimal control problem into a Mixed Integer Quadratic Constrained Programming (MIQCP) problem and a continuous problem. The results of the first one provided the status and heat production of each unit. Then the discrete variables representing the status of each unit were fixed by this solution of the MIQCP, although the real heat production was calculated in the continuous problem. This latter was transformed into a Nonlinear Programming (NLP) problem using a method of direct collocation that was then solved using the interior point algorithm IPOPT. The objective function proposed in this work (and which had to be minimized) was the supply temperature of the producer all along the considered time span. Although this implementation is based on physical models, it is fully tool-oriented to Modelica users, offering few details on the mathematical modelling and treatment of the dynamic optimization problem. This fact makes difficult to replicate their methodology on other available tools for modelling and optimization.

Powell and Edgar [56] presented the control of a solar thermal power plant with energy storage. The system was composed by solar collectors, thermal energy storage tanks and a boiler. The energy balances in the collectors resulted into a system of 3 partial differential equations, that were reduced into a system of ordinary differential equations (ODE) by representing the spatial differential terms

using backwards finite differences. The resulting system was solved in time using Runge-Kutta numerical integration for each segment over time. Continuing with the study of this system, Powel *et al.* [57] presented the dynamic optimization of a more complex system that included a bypass line in the storage system to prevent mixing of fluids at different temperatures, that led to exergy destruction. The addition of this bypass gave additional options of operation to use in the optimization of the system. The model included a set of PDEs to describe the thermal phenomena on each of the components of the system, and a set of algebraic expressions to represent the heat and mass balances in the valves, and the bypass creating a system of Partial Differential Algebraic Equations (PDAEs). The objective function to be minimized was the total supplemental and pupping energy needed while maintaining constant the total heat output. A simultaneous strategy based on Orthogonal Collocation on Finite Elements (OCFE) was used to transform the PDAE into a set of algebraic equations that can be solved with any standard NLP solver. The problem was formulated and solved using the python-based software APMonitor [58] specialized in the solution DAE systems using OCFE.

To our knowledge, the studies on the dynamic optimization of district energy systems are limited to the presented works. It is important to highlight that even though we can model the physical and thermal phenomena of district heating and district cooling using the same transfer equations, there is a need to deep study the dynamic behaviour and optimization of the latter systems. Aiming to contribute in this field, this work presents a methodology based on mathematical programming for the dynamic optimization of cooling networks. The model considers the dynamics of the temperature in the pipes, and the dynamic interactions of the network with the users, subject to a variable ambient temperature during a 24h period.

1.5 Basics on Dynamic optimization

Optimization is a major subject of research in many different fields, from economics, passing through social sciences up to engineering applications. For this reason, the classical calculus and computer sciences have joined their effort in developing methods and applications to implement different and innovating mathematical programming techniques for the solution. Nevertheless, much of the developments are applicable only to steady-state optimization problems [59]. The solution of these problems usually consists in the choice of a single value for the decision variables of the problem to maximize or minimize an objective function at a point.

On the other hand, a dynamic optimization aims to find a time path for the decision variables so that a function is maximized or minimised over a given interval of time. In dynamic optimization, the aim is to find optimal curves $y^*(t)$ that will maximize or minimize the integral of a function F which is a function of the independent variable t (time), the functions $y(t)$, and their derivatives $y'(t)$. Hence, assuming a time period from $t_0 = 0$ to t_1, the dynamic optimization problem is to maximize or minimize the integral function I [60]:

$$I = \int_{t_0}^{t_1} F[t, y(t), y'(t)]\, dt \tag{1-8}$$

$F[t, y(t), y'(t)]$ is assumed to be continuous for t, $y(t)$, and $y'(t)$, and differentiable. The integral I in equation (1-8) is referred as a functional because it is a function composed by the functions $y(t)$, and $y'(t)$. Sometimes, the boundary conditions ($y(t_0)$ and $y(t_1)$) are known, but often just $y(t_0)$ is known. Nevertheless, the optimization can include also computing the best values for these conditions. The key concept that allows solving dynamic optimization problems is the principle of optimality, which indicates that an optimal policy regarding an initial state has the property that after the first decision, the remaining decisions also constitute an optimal policy regarding the state reached after this first decision, and so on [61].

1.5.1 Basic Example

The following example aims to explain the dynamic optimization problem. It is a trajectory optimization problem, where we need to move a block of mass m between 2 points (one dimension), starting and finishing at rest, during a fixed time horizon [62].

- There is no friction with the surface
- The decision (control) variable is the force u applied to the block.
- For a position x, the block will have a speed v, the system dynamics are expressed as:

$$x' = v$$
$$m \cdot v' = u \tag{1-9}$$

- The boundary conditions of the problem are defined as:

$$x(0) = 0\,;\;\; x(1) = 1$$
$$v(0) = 0\,;\;\; v(1) = 0 \tag{1-10}$$

Figure 1-11. Illustrative example of dynamic optimization

A solution to this problem is feasible when it satisfies all the problem requirements, represented by the constraints in (1-9) and the boundary conditions in (1-10). Some feasible trajectories are presented in Figure 1-12 (a) and together they form what is known as admissible controls.

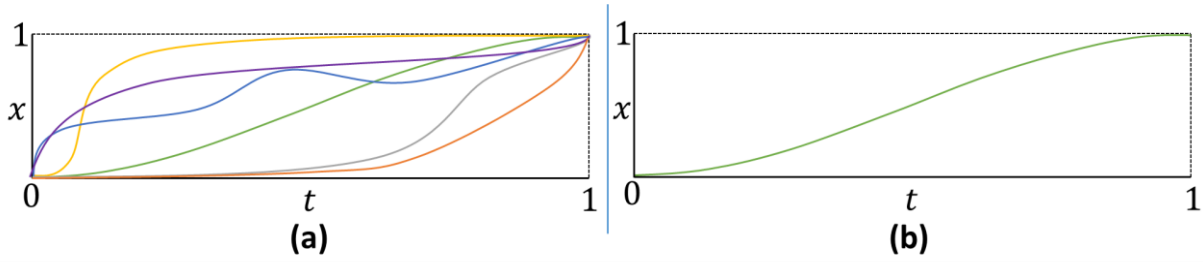

Figure 1-12. Feasible trajectories (a) and Optimal trajectory for the moving block problem

One interesting objective for this problem is to minimize the absolute work to move the block from $x = 0$ to $x = 1$, represented as:

$$\min_{u(t),x(t),v(t)} \int_0^1 |u(t) \cdot v(t)|\, dt \tag{1-11}$$

After the solution of this problem, the optimal trajectory that minimizes the absolute work will follow the form of the curve presented in Figure 1-12 (b). The optimal trajectory the force should follow is presented in Figure 1-13 and corresponds to an instantaneous impact in $t = 0$ and instantaneous braking force (same magnitude in the opposite direction) to stop the block at $t = 1$.

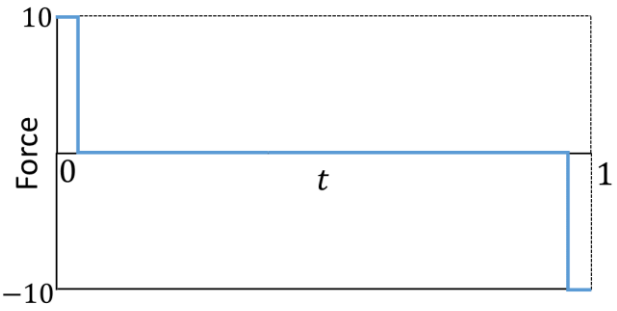

Figure 1-13. Optimal force trajectory for minimum absolute work

Interest in dynamic simulation and optimization of processes has increased significantly over the last 3 decades [63]. The latter has been used for different kinds of *off-line* tasks, like transitions between operating regimes, operation of batch processes, parameter estimation, and design of control systems. Likewise, online tasks like control and identification for model predictive control applications [64].

1.5.2 Formulation of a dynamic optimization problem

A dynamic system is represented, in general, by an arrangement of differential equations describing the dynamic behaviour of the system, and a set of algebraic equations that describe the constraints (conservation laws, position constraints, size parameters, etc) of the studied problem. When the model includes partial differential equations, the problem is known as Partial Differential Algebraic Equation (PDAE) system. On the other hand, if the problem only includes ordinary differential equations, we will have a differential-algebraic equation (DAE) system[48]. A PDAE system can be transformed into a DAE one, keeping only the differential terms of one integration variable and discretizing the others. For a system described only by continuous variables considering just temporal variations, the dynamic optimization problem can be represented as [64]:

$$\min_{z,y,u,par} J = \phi\left(t_f, z\left(t_f\right)\right) + \int_{t_0}^{t_f} \mathcal{L}(t,z,y,u)dt \tag{1-12}$$

Subject to

$$\frac{dz(t)}{dt} = f(t,z(t),y(t),u(t),par),\ \ z(t_0) = z_0, \tag{1-13}$$

$$g(x(t),y(t),u(t),p) = 0, \tag{1-14}$$

$$g_f\left(z\left(t_f\right)\right) = 0, \tag{1-15}$$

$$u_L \le u(t) \le u_U, \qquad y_L \le y(t) \le z_y, \qquad z_L \le z(t) \le z_U \tag{1-16}$$

Where $z(t)$ are the differential state variables, $y(t)$ the algebraic state variables, $u(t)$ the control variables, all the previous being functions of the time $t \in [t_0, t_f]$, and par represents the time-independent parameters. The constraints of this optimization problem ((1-13) to (1-15)) are the DAEs representing the system. This formulation is known as the problem of Bolza [65], where J is a scalar to be minimized. The first term corresponds to the term of Mayer and the integral term corresponds to the term of Lagrange. Thus, depending on the application, in dynamic optimization, it is possible to formulate objective functions of the form of Bolza, Mayer or Lagrange.

Biegler [66], [67] reported different ways for the solution of dynamic optimization problems as shown in Figure 1-14. The problem can be solved by applying a variational approach, which is based on Pontryagin's Maximum Principle [68]. However, this approach could not handle efficiently inequality constraints [68].

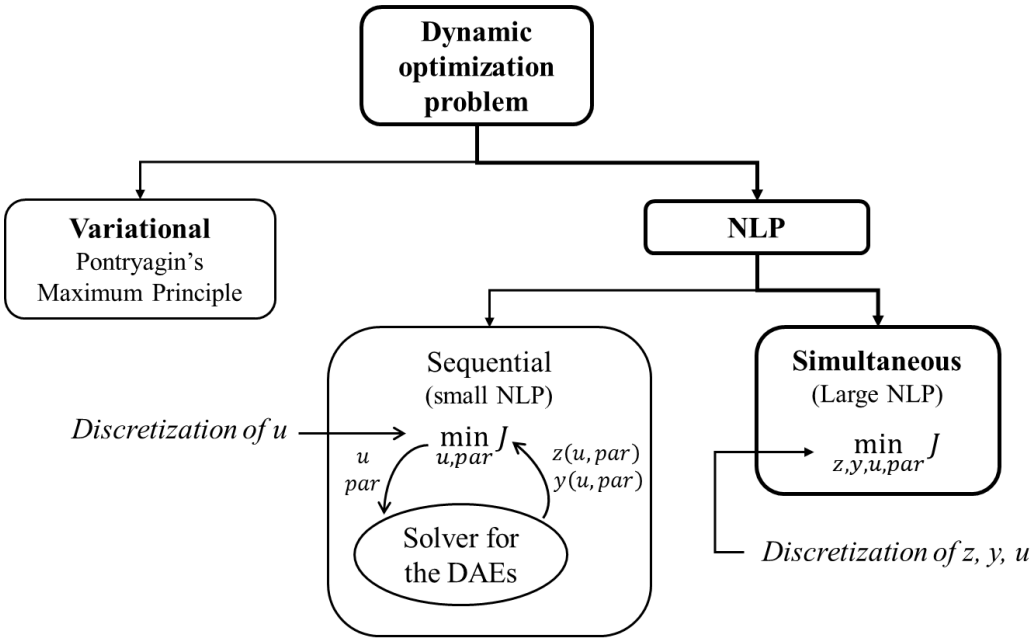

Figure 1-14: Solution strategies for dynamic optimization problems

Other strategies applying NLP solver can be used. It involves the discretization of the time-dependent variables, that enables to formulate an NLP problem, which is solved with respect to these new discretized variables. Depending on the variables that are discretized, two approaches are possible. The first strategy is the sequential approach: in this case, only the control variables are discretized. For a set of control variables and parameters, a DAE solver in a loop solves the state variables of the DAE system and returns the state and algebraic variables to the NLP optimization level. The control variables (in fact the discretized variables that represent them) and the parameters are updated by the

NLP solver. This strategy can be time-consuming. On the other hand, in the simultaneous approach, both state and control variables are discretized in time. Hence, the DAE system is solved only once, at the optimal point, and therefore this can avoid computational effort to obtain intermediate solutions of the DAE system. The author proposes the use of orthogonal collocation on finite elements (OCFE) [69] for the implementation of the simultaneous approach. OCFE is an extension of the method of orthogonal collocation, which is based on the use of orthogonal polynomials to represent the solution of the dynamic variables. The generalities of the method are presented in the next section, while their implementation will be introduced in the next chapter.

1.6 Collocation Methods

Among the discretization strategies that can be implemented for the solution of differential problems like the heat transfer equation (1-1), we have the collocation-based methods. The principle of these methods consists in approximating the state variable involved in a differential equation as a sum of some selected trial functions of the integration variable. Then, ensuring that the differential equation is satisfied at a set of collocation points enables to transform the differential equation into a set of algebraic equations whose unknown variables are the coefficients of the trial functions in the sum that approximates the state variable [70]. The choice of appropriate collocation point is crucial to achieving more convenient and accurate results. If the trial functions are chosen as orthogonal or Lagrange basis polynomials, the state variable is approximated by a polynomial. Then, when the roots of orthogonal polynomials are used as collocation points, we will have the specific case of orthogonal collocation [71]; the state variable is then approximated by a polynomial interpolating the values of the state variable at the collocation points. The method has been used by some authors for solving initial-value and boundary value problems, such as Finlayson[69], Ebrahimzadeh *et al.*[72] and Binous *et al*. [73].

One of the advantages of the method, as stayed by Finlayson [74], is that compared with finite differences, the polynomial interpolation used in orthogonal collocation gives a continuous representation of the state variable over the whole domain. While in the finite difference methods the solution is obtained by interpolation of neighbouring grid points. This fact has important advantages because as we increase the number of collocation points, the rate of convergence to the exact solution will do so.

When the nature of the phenomenon demands a more detailed discretization for a better description of its dynamics, the domain of integration can be divided into subdomains or finite elements, where the orthogonal collocation method is implemented allowing the use of a large number of grid points. Carey and Finlayson[69] presented this implementation as orthogonal collocation on finite elements (OCFE), for the analysis of a catalytic pellet that includes heat and mass transfer with chemical reaction. They compare the results obtained with OCFE with the analysis made with orthogonal collocation and finite differences, reporting better convergence, and a lower requirement of grid points for the collocation methods. Biegler [75], also reports better convergence and lower computational requirements for the OCFE method compared with other discretization methods.

OCFE has been used to handle with DAE problems with diverse applications, including batch process optimization, crystallization, dynamic data reconciliation and parameter estimation, nonlinear model

predictive control, and reactor design and synthesis[64]. Other implementations include the work of Biegler [66], who presents off-line parameter estimation and online tasks like state estimations, nonlinear model predictive control and dynamic real-time optimization for a low-density polyethene reactor. Also, Hedengren *et al.* [76] performed parameter estimation and dynamic optimization in a quadruple tanks process. In a more recent contribution [67], Biegler presents an optimal control strategy for the multi-stage grade transition optimization of the polymerization process for the production of linear low-density polyethene and the determination of optimal recipes for a semi-batch polyol process.

Among all the literature revision made for this work, we found only three authors who have implemented OCFE to fully discretize PDAE formulations. Jacobsen *et al.* [77] for the model predictive control of a solid oxide fuel cell, Mittal *et al.* [78] to solve diffusion-dispersion models and Esche *et al.* [79] for the optimal operation of a membrane reactor. Moreover, in these contributions, the authors did not detail the implementation of the method. Considering this, in the present work we propose the use of 2D-OCFE to fully discretize the resulting PDAE that describes the dynamics of district cooling networks.

1.7 Thesis objectives

The energy transition supposes new challenges in terms of the use, accessibility and efficiency of the energy the world requires, to guarantee wellness to more members of a fast-growing society. Considering this, many cities in the world have been implementing the use of distributed energy system, to cover the needs of heat and cold for building comfort with a lower impact than the use of individual systems.

The development of distributed networks has been supported by numerical studies, as an important tool to define the configuration, size and capacity of these systems (and their corresponding subsystems). Here, the assumption of steady-state operation was an adequate approximation for the development of these applications. Nevertheless, the incursion of renewables as a potential source of energy, the growing and diverse cooling demands in the cities and the fast development of these systems represent new challenges for their planning, design and operation. Here, the development of dynamic models appears as a more reliable tool for the assessment of these new problematics than the steady-state approximations that have been used until now. Specifically, the development of dynamic optimization allows predicting the operation profiles of the control variables that minimize (or maximize) the value of a given objective function. Then, we can use dynamic optimization to predict the proper operation of cooling networks and extend these results to develop more exhaustive design methodologies, that consider the dynamics of the system.

Bearing this in mind, the objective of this thesis is to develop a methodology for the dynamic optimization of the distribution system of a district cooling network, based on the analysis of a case study, that considers perturbations in the levels of demand of the users and in the external temperature. For this, we develop first the dynamic model that describes the variation of the temperature in the pipes, and its interactions at the consumers' sites that results in a PDAE formulation. Then, we implement 2D-orthogonal collocation on finite elements to discretize the problem resulting in an algebraic formulation, that will be used to perform an operational and an operation cost optimization.

The formulation of the first objective function considers the importance of guaranteeing an appropriate temperature of the utility returning to the production site, in order to avoid an issue that affects the thermal efficiency of the system, known as low ΔT Syndrome[24], [25]. Then, keeping this optimal operation the second objective function aims to minimize a cost function including the

diameter of the pipes as decision variables. Considering that, contrary to heat networks, the use of insulation in district cooling networks is not mandatory but is related to the heat gains that the distribution system presents depending on the characteristics (soil and ambient temperatures) of the location of the network as well as the cost for the production of cold[25], [80], the analyses of the two objective functions were performed for distribution pipes with and without insulation.

Chapter 2. Case study and mathematical model

Chapter 1 described the generalities, current development and the importance of district cooling networks. This chapter also presented a review on the different optimization applications for their design and operation, highlighting the importance of developing dynamic studies, aiming to respond to the new challenges that the development of district cooling networks is facing.

Bearing this in mind, in Chapter 2 we propose the dynamic analysis of a study case, including its mathematical model and the corresponding discretization for simulation and optimization purposes. Section 2.1 specifies the configuration of the system, including topology, kinds and number of consumers. Finally, it presents the characteristics of different climate zones, where the behaviour of the system will be compared. Then, Section 2.2 details the mathematical model that includes heat and mass balances, as well as the hydraulic constraints in the pipes. To finish this chapter, Section 2.3 introduces the generalities of OCFE and its implementation in 2-D for the total discretization of the problem.

Chapter contents

2.1 Case Study System

We develop a dynamic analysis over an academic case study, whose conditions are based on real data. The system consists of 20 users distributed over an urban area with known locations. Based on this distribution, we propose a set of nodes and pipes that connect the production site and the users. Then, we build the cooling demand profile for each user based on typical performances for diverse kinds of buildings reported by an industrial supplier of cooling services. Finally, we present the external conditions to which the system will be subject.

2.1.1 System's configuration

The topology of the system is based on the illustrative example presented by Söderman [52]. From the coordinates the author presented for the location of the users, and assuming that the pipes follow a straight path, it is possible to compute the lengths of the pipes, detailed in Table 2-1.

Table 2-1. Lengths of main and lateral pipes of the system

Main pipes			Lateral pipes		
Pipe		Length[m]	Pipe		Length[m]
0	0_r	50	in_{C_1}	out_{C_1}	40
1	1_r	279.93	in_{C_2}	out_{C_2}	0.1
2	2_r	720.07	in_{C_3}	out_{C_3}	242.99
3	3_r	176.46	in_{C_4}	out_{C_4}	95.21
4	4_r	124.69	in_{C_5}	out_{C_5}	110.64
5	5_r	397.32	in_{C_6}	out_{C_6}	227.56
6	6_r	124.97	in_{C_7}	out_{C_7}	102.58
7	7_r	338.27	in_{C_8}	out_{C_8}	0.43
8	8_r	198.19	in_{C_9}	out_{C_9}	147.38
9	9_r	478.17	$in_{C_{10}}$	$out_{C_{10}}$	330.51
10	10_r	147.01	$in_{C_{11}}$	$out_{C_{11}}$	110.62
11	11_r	73.54	$in_{C_{12}}$	$out_{C_{12}}$	154.73
12	12_r	279.38	$in_{C_{13}}$	$out_{C_{13}}$	0.32
13	13_r	382.3	$in_{C_{14}}$	$out_{C_{14}}$	404.71
14	14_r	190.01	$in_{C_{15}}$	$out_{C_{15}}$	95.14
15	15_r	12.13	$in_{C_{16}}$	$out_{C_{16}}$	371.66
16	16_r	268.79	$in_{C_{17}}$	$out_{C_{17}}$	363.38
17	17_r	1280.6	$in_{C_{18}}$	$out_{C_{18}}$	371.94
18	18_r	198.28	$in_{C_{19}}$	$out_{C_{19}}$	91.03
19	19_r	32.89	$in_{C_{20}}$	$out_{C_{20}}$	0.1
20	20_r	438.04			

Using the presented information, and considering that there are no connections in cascade between the clients, Figure 2-1 presents a scheme of the cold network, main pipes (0-20), lateral

pipes $\left(in_{C_1} - in_{C_{20}}\right)$, the nodes and the users in a simplified way that is useful for modelling purposes. The complete system includes also a return network from the users to the production site (PS), that is represented by the return pipes (0_r - 20_r and $out_{C_1} - out_{C_{20}}$) with the same lengths as those of the outward path pipes. Then, the whole network is an arrangement of 82 pipes with a total length close to 19 km (18904.11 m).

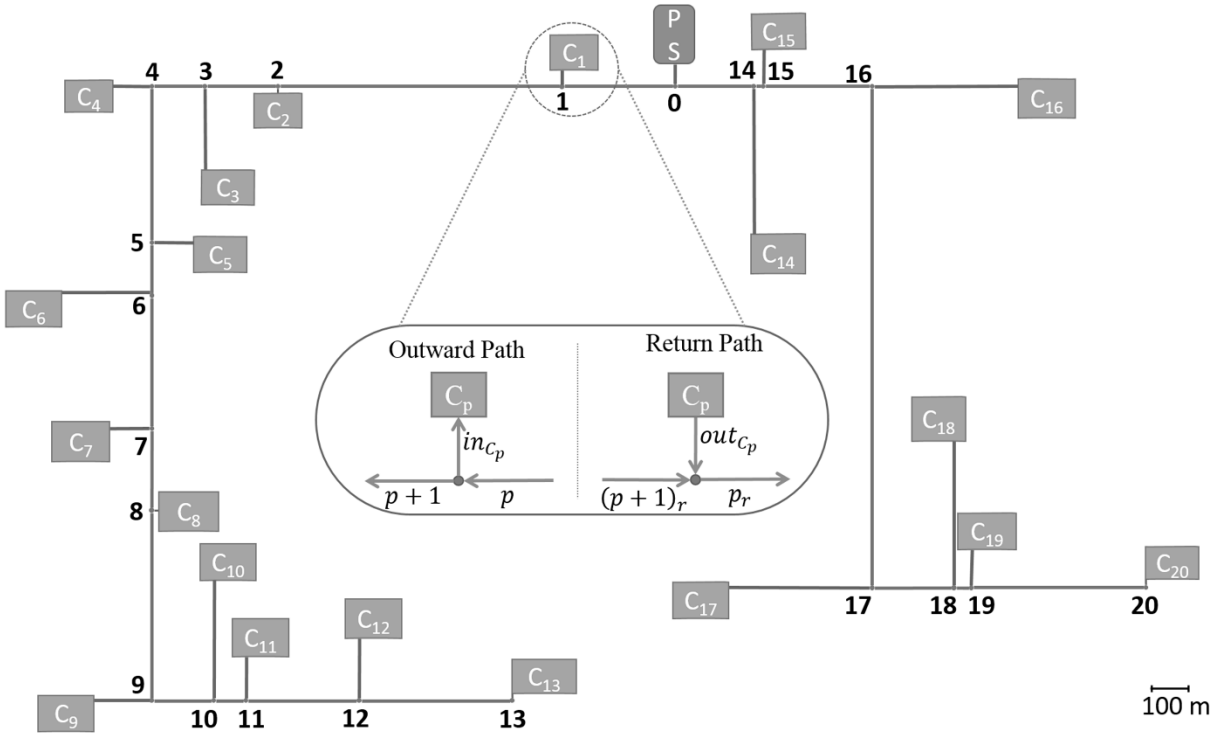

Figure 2-1. Representation of the cooling network

2.1.2 Consumers and their cooling demands

For this work, we built cooling demand profiles based on the daily cooling demand curves presented by Olama [24] for different kinds of buildings including, office, residential, hotel or service apartments, shopping and leisure. These profiles were developed by the refrigeration energy company ARANER [81], and represent the variation of the demand as a percentage of the cooling peak load of the buildings as seen in Figure 2-2.

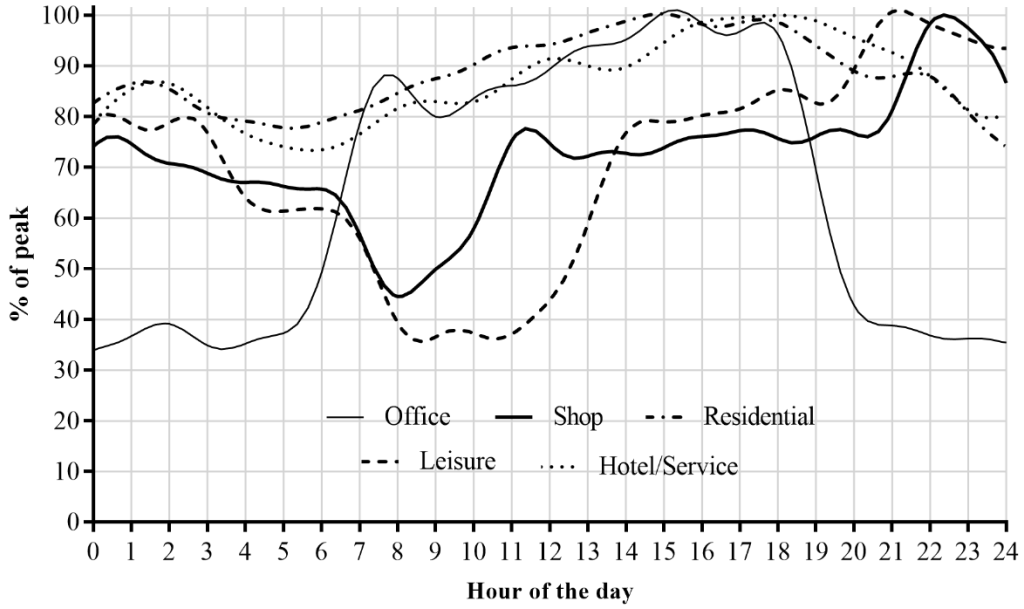

Figure 2-2. Demand for different kind of buildings

Using the peak cooling demands (maximum load) presented by Söderman for this system [52], which are based on real data (Table 2-2), and the aforementioned profiles (Figure 8-2) we can compute the demand profiles of the 20 consumers.

Table 2-2. Consumer's peak cooling demands

Consumer	Type	Max Load [kW]	Consumer	Type	Max Load [kW]
C_1	Shop	1640	C_{11}	Residential	800
C_2	Office	700	C_{12}	Office	100
C_3	Leisure	200	C_{13}	Shop	180
C_4	Office	780	C_{14}	Office	1500
C_5	Shop	100	C_{15}	Hotel/Services	650
C_6	Office	900	C_{16}	Hotel/Services	380
C_7	Office	100	C_{17}	Leisure	455
C_8	Residential	250	C_{18}	Hotel/Services	900
C_9	Hotel/Services	400	C_{19}	Leisure	360
C_{10}	Office	170	C_{20}	Leisure	1220

Considering these data, Figure 2-3 details the cooling demand profiles of the major consumers per building category on each branch of the network.

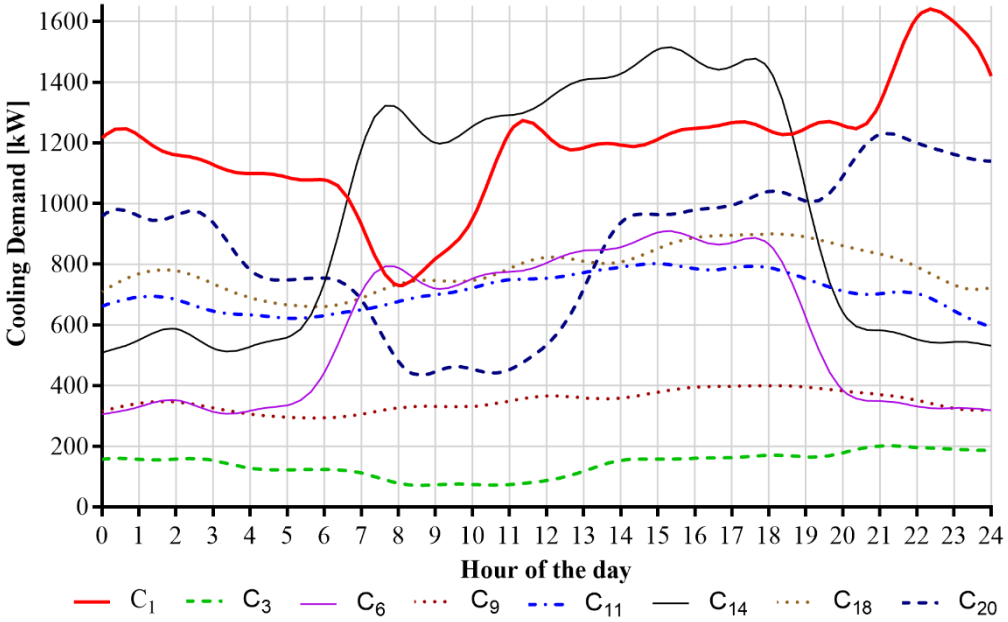

Figure 2-3. Cooling demands of major consumers per building category

We will study the described system under different external conditions, including diverse kinds and characteristics of the soil as well as differentiated ambient temperatures corresponding to different climate zones.

2.1.3 Soils and climate zones

The kind of soil and its moisture affect its thermal conductivity as reported by the ASHRAE's district cooling guide [25], and evidenced in the expression to compute the total thermal resistance (equation (1-2)).

Table 2-3. Soil thermal conductivities

Soil Moisture (By mass)	Thermal conductivity, [W/m.K]		
	Sand	Silt	Clay
Low, <4%	0.29	0.14	0.14
Medium, 4%-20%	1.87	1.30	1
High, >20%	2.16	2.16	2.16

In order to analyse the implementation of a district cooling network in different climate areas and its impact on the total thermal resistance and on the thermal distribution in the pipes, we chose three cases (cities) with different daily ambient temperature profiles and soil characteristics detailed below:

- Ras Al Khaimah (UAE): Low moisture; sandy soil.
- Paris: Medium moisture; clay soil
- Kuala Lumpur (KL): High moisture; clay soil

Figure 2-4 details the profile temperature in the hottest day in 2018 for each of the selected cities. These profiles were built using real data from the global community Weather Underground, which collects data from more than 250 000 weather stations around the world [82].

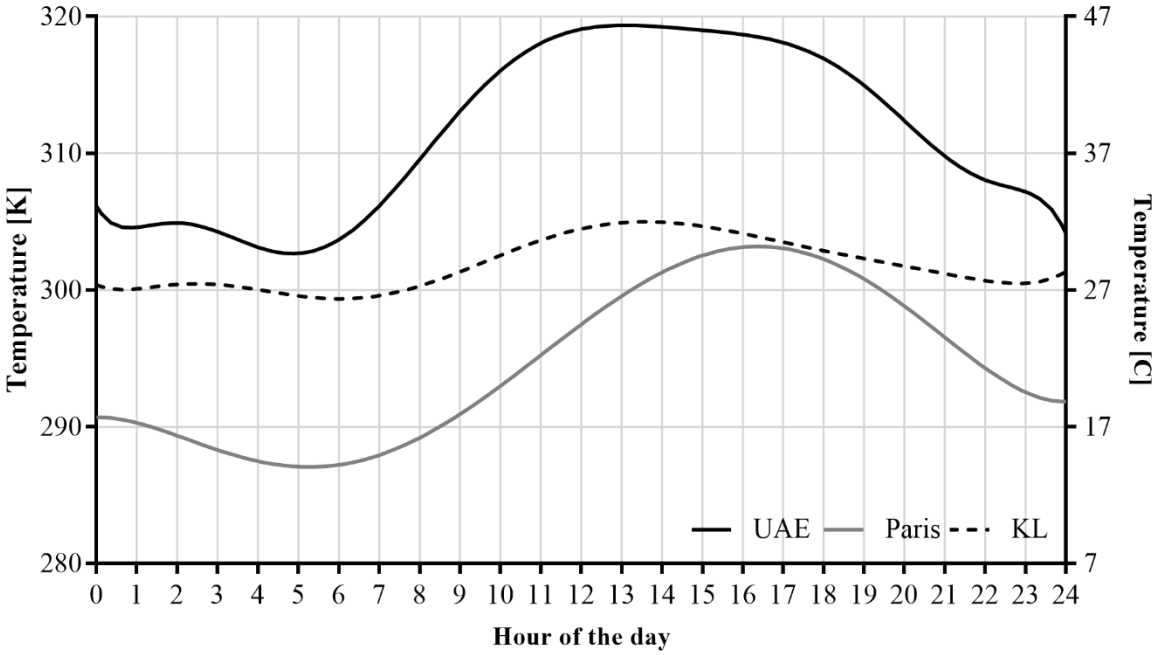

Figure 2-4. Summer Temperature profiles in the studied climate zones

With the configuration of the system already defined, the next section details the mathematical model that describes the dynamic operation of the network, the generalities of the discretization strategy and its implementation.

2.2 Mathematical model

The model of the DCS is constituted by the heat transfer equation in each pipe, together with mass and energy balances at each node of the system, under the following assumptions:

- The system uses water as cooling fluid (w).
- The mass flow in each pipe is time-dependent and uniform.
- The physical properties of the fluid are assumed constant.

2.2.1 Heat balance in the pipes

Considering this and the assumptions for the one-dimensional heat transfer equation presented in Section 3 of chapter 1, the heat transfer in each pipe is described by:

$$\rho_w \cdot Cp_w \cdot A \cdot \frac{\partial T(t,x)}{\partial t} + \dot{m}(t) \cdot Cp_w \cdot \frac{\partial T(t,x)}{\partial x} = \frac{T_s - T(t,x)}{R'} \tag{2-1}$$

2.2.2 Heat balances in the nodes

Initial condition

For each pipe k, the initial spatial profile of temperature is known from a steady-state simulation:

$$T_k(0,x) = \theta_k(x) \tag{2-2}$$

Here, $\theta_k(x)$ represents the spatial distribution of temperature along the pipe k at $t = 0$. The way to achieve this steady-state simulation will be discussed later.

Boundary conditions

We assume that chilled water is produced at a constant temperature (277K). Then, for the pipe leaving the production site ($p = 0$), we have:

$$T_0(t,0) = 277 \text{ K} \tag{2-3}$$

The nodes in the outward path are splitters, where the outlet temperature of the pipe entering the node is equivalent to the inlet temperature of the pipe leaving it,

$$\begin{gathered} T_p(t,L_p) = T_{p+1}(t,0) = T_{in_{C_p}}(t,0) \quad , p = 1 \dots 12,14, \dots 19 \\ T_0(t,L_0) = T_1(t,0) = T_{14}(t,0) \\ T_p(t,L_p) = T_{in_{C_p}}(t,0) \quad , \quad p = 13\,, 20 \end{gathered} \tag{2-4}$$

Where L_k is the length of pipe k. k may be $p, p_r, in_{C_p}, out_{C_p}$.

On the other hand, heat balances for the return path and the consumers ($C_p = (C_1, C_2, \dots, C_{20})$) will define the boundary condition of the pipes leaving these elements of the system. As we consider constant properties, they will be:

$$\begin{gathered}\dot{m}_{p_r}(t)\cdot T_{p_r}(t,0) = \dot{m}_{(p+1)_r}(t)\cdot T_{(p+1)_r}\left(t, L_{(p+1)_r}\right) + \dot{m}_{out_{C_p}}(t)\cdot T_{out_{C_p}}\left(t, L_{out_{C_p}}\right), \\ p = 1 \dots 12{,}14, \dots 19 \\ \dot{m}_{0_r}(t)\cdot T_{0_r}(t,0) = \dot{m}_{1_r}(t)\cdot T_{1_r}\left(t, L_{1_r}\right) + \dot{m}_{14_r}(t)\cdot T_{14_r}\left(t, L_{14_r}\right) \\ \dot{m}_{p_r}(t)\cdot T_{p_r}(t,0) = \dot{m}_{out_{C_p}}(t)\cdot T_{out_{C_p}}\left(t, L_{out_{C_p}}\right) \quad , \quad p = 13\,, 20\end{gathered} \tag{2-5}$$

$$Q_{C_p}(t) = \dot{m}_{in_{C_p}}(t)\cdot \mathrm{C}p_w \cdot \left(T_{out_{C_p}}(t,0) - T_{in_{C_p}}\left(t, L_{in_{C_p}}\right)\right) \tag{2-6}$$

Where $T_{in_{C_p}}\left(t, L_p\right)$ and $T_{out_{C_p}}(t,0)$ are the inlet and outlet temperatures of the exchanger.

2.2.3 Mass Balances in the nodes

For the nodes and consumers, the mass balances are given by:

Outward path

$$\begin{gathered}\dot{m}_p(t) = \dot{m}_{p+1}(t) + \dot{m}_{in_{C_p}}(t) \quad p = 1 \dots 12{,}14 \dots 19 \\ \dot{m}_p(t) = \dot{m}_{in_{C_p}}(t) \quad p = 13\,, 20 \\ \dot{m}_0(t) = \dot{m}_1(t) + \ \dot{m}_{14}(t)\end{gathered} \tag{2-7}$$

Return path

$$\begin{gathered}\dot{m}_{p_r}(t) = \dot{m}_{(p+1)_r}(t) + \dot{m}_{out_{C_p}}(t) \quad p = 1 \dots 12{,}14 \dots 19 \\ \dot{m}_{p_r}(t) = \dot{m}_{out_{C_p}}(t) \quad p = 13\,, 20 \\ \dot{m}_{0_r}(t) = \dot{m}_{1_r} + \ \dot{m}_{14_r}\end{gathered} \tag{2-8}$$

Consumers

$$\dot{m}_{in_{C_p}}(t) = \dot{m}_{out_{C_p}}(t) \ \ p = 1 \dots 20 \tag{2-9}$$

With the heat and energy balances of the system already formulated, the next section presents the analysis of degrees of freedom of the system and the supplementary relationships that we included to have zero degrees of freedom for simulation purposes.

2.2.4 Degrees of freedom and flow policy

From the set of equations ((2-1) to (2-9)), it is possible to make the analysis of degrees of freedom of the system for the 82 pipes at each instant t, as detailed in Table 2-4.

Table 2-4. Analysis of degrees of freedom of the system

Variables		Equations	
Variable	# of variables	Equation	# of equations
$T_k(x,t)$	82	(2-1)	**82**
		1st order in t and x PDE, which requires **1** Initial Condition and **1** Boundary Condition per pipe, given by:	
		IC: (2-2)	**82**
		BC: (2-3)	1
		(2-4)	40
		(2-5)	21
		(2-6)	20
$\dot{m}_k(t)$	82	(2-7)	21
		(2-8)	21
		(2-9)	20

82

62

The number of degrees of freedom of the system is 20 at each instant t, representing the profiles to be given for dynamic simulation or computed via dynamic optimization.

Considering this, for dynamic simulation purposes we have to complete the degrees of freedom of the system. We can do this by defining the flow policy we will use to accomplish the cooling demand of each consumer. Some systems operate under constant production conditions as shown in Figure 2-5, where the production of cold ($\dot{m}_0$) and the mass flow in the main network ($\dot{m}_p$ and $\dot{m}_{in_{C_p}}$) are constant at the level necessary to cover the peak of the total demand of the system. In this way, the producer guarantees enough cold to the system during the studied period but it results in cost overruns for production and pumping of the chilled water. At each consumer's substation, there is a common

pipe $Cm(t)$, which connects the main and return network, to regulate the flow to the consumer ($vin_{C_p}(t)$) over time, sending important quantities of cold water directly to the return network in the periods of low demand, and the total flow of $\dot{m}_{in_{C_p}}$ to the consumer when its demand corresponds to the peak. The literature reports this policy as constant-primary secondary-variable flow [24], [25].

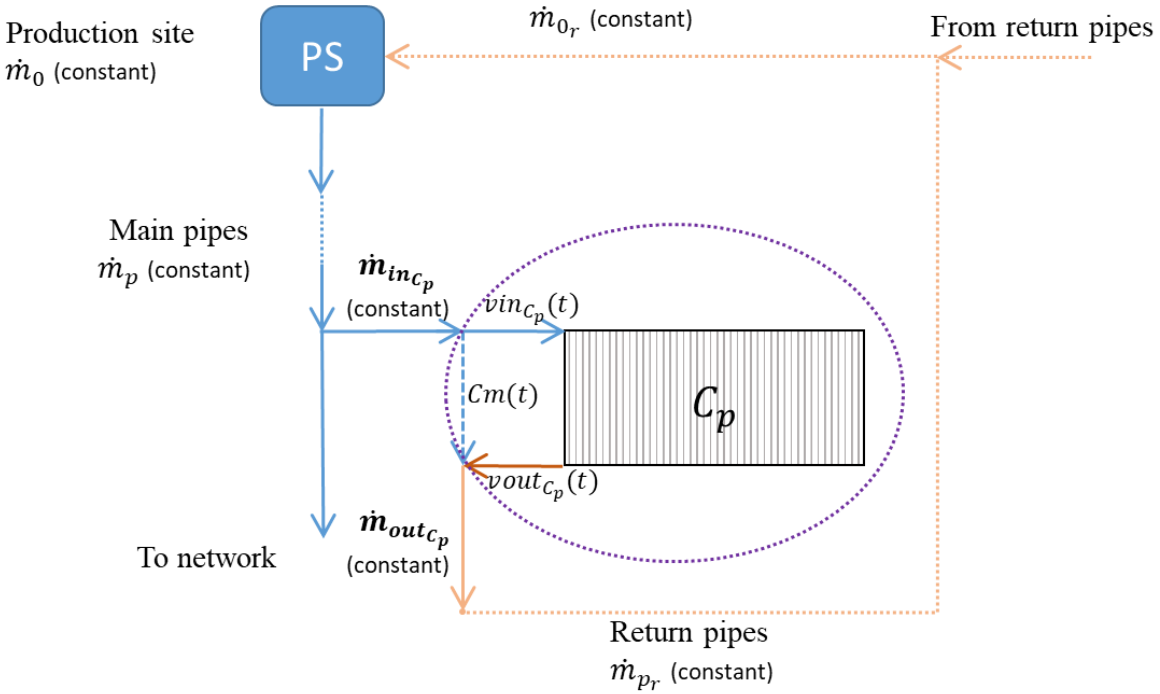

Figure 2-5. Constant flow policy diagram

Then, to represent the constant flow in the main network we first define a constant mass flow leaving the production site by:

$$\dot{m}_0(t) = \dot{m}_{0\mathrm{Cte}} \tag{2-10}$$

Furthermore, in the splitters, we assume that the mass flows entering to the consumers at each time ($\dot{m}_{in_{C_p}}(t)$) are proportional to their corresponding maximum peak demand ($Peak(C_p)$ from Table 2-2). We can do this by fixing the ratio between these variables for all the consumers over time as:

$$\frac{Peak(1)}{\dot{m}_{in_{C_1}}} = \frac{Peak(p)}{\dot{m}_{in_{C_p}}}, \quad \forall\, p \in \{2, \dots, 20\} \tag{2-11}$$

The mass and energy balances presented in section 2.2.3 are the balances at each consumer for the boundaries defined by the dotted borderline presented in Figure 2-5. Hence only the mass flows $\dot{m}_{in_{C_1}}$ and $\dot{m}_{in_{C_p}}$, that will be constant when implementing the flow policy represented by equations

(2-10) and (2-11), are computed. The pipes $Cm(t)$, $vin_{C_p}(t)$ and $vout_{C_p}(t)$ belong to the user's substation and their flows are not considered in this analysis.

The dynamic response of the system will be initially analysed under constant production mass flow $\dot{m}_{0\mathrm{Cte}}$ as expressed in (2-10). This value corresponds to the value of the producer mass flow in steady-state, which is computed using the relations (2-11) and imposing a return temperature (2-12) to complete the 20 degrees of freedom.

$$T_{0_r}(L_{0_r}) = 287 \tag{2-12}$$

Then, to simulate the constant flow policy in the dynamic simulation the 20 degrees of freedom are completed using (2-10) and (2-11).

The optimization analyses include the study of the constant flow policy and the optimization of the operation of the system using a dynamic flow policy. In the first case, (2-10) and (2-11) will be constraints and the value $m_{0\mathrm{Cte}}$ will be the only optimization variable. In the second case, these constraints are not considered, giving as optimization variables the profiles $\dot{m}_0(t)$ and $\dot{m}_{inC_p}(t), p = 1 \dots 20$.

2.2.5 Flow velocities

In order to simulate properly the dynamics of the system, it is necessary to define the hydraulics of the chilled water in the network's pipes. For this we consider the recommended flow velocities for sizing cooling water pipes reported by Branan [83], detailed in Table 2-5. The reported pipe sizes correspond to nominal diameters. Annex A reports data for PVC schedule 40 pipes, including nominal and internal diameters, wall thicknesses and maximum pressures. The system must respect the velocity bounds during the simulation and optimization analysis.

Table 2-5. Maximum allowable speeds in pipes

	Mains	**Laterals**
Nominal pipe size [in]	max vel. [m/s]	max vel. [m/s]
2	--	1.31
3	0.94	1.32
4	1.08	1.54
6	1.29	1.69
8	1.27	1.76
10	1.37	1.86

	Mains	Laterals
Nominal pipe size [in]	max vel. [m/s]	max vel. [m/s]
12	1.56	2.08
14	1.56	2.19
16	1.80	2.41
18	1.90	2.53
20	2.03	--

Considering this, the velocity $v_k(t)$ inside a pipe k, is bounded as:

$$v_k(t) \leq v_{max,k} \tag{2-13}$$

Here, $v_{max,k}$ corresponds to the values reported in Table 2-5. This criterion will be used to compute the diameter of the pipes.

With this inequality, we complete the mathematical model that we will use to describe the dynamics of the proposed district cooling distribution system. In the next section, we detail the implementation of double orthogonal collocation on finite elements to discretize the presented dynamic mathematical model, which is a PDAE system.

2.3 Discretization strategy and mathematical model

In the present work, we use 2D-OCFE to transform equation (2-1) into a set of algebraic equations, which results highly advantageous and efficient for simultaneous optimization applications [67]. To our knowledge, there are no studies related to the dynamic operation of DCS that use 2D-OCFE to handle the resulting PDAE problem.

In this section, we present the generalities of the numerical method and its implementation to discretize equation (2-1). Then, based on this implementation, we present the discretized mathematical model of the system that includes the energy and mass balance in the connection nodes and users' sites.

2.3.1 Generalities and implementation of 1D-OCFE

A collocation method approximates the unknown solution (the state variable) of an ordinary differential equation as a finite sum of known trial functions of the integration variable and enforces the ordinary differential equation to be satisfied at some collocation points. An equidistant spacing of the collocation points is not generally appropriate and Villadsen and Stewart have suggested that positioning of the collocation points at the zeros of orthogonal polynomial leads to a rapidly convergent interpolation scheme even for functions that are poorly represented by polynomials[84]. Therefore, considering that the trial functions are Lagrange basis polynomials, the integration variable is normalized, and the collocation points are chosen as roots of orthogonal polynomials, then the method is called orthogonal collocation. When using OCFE method the state variable is approximated by an interpolating polynomial different on each finite element, and the state variable continuity must be ensured at the boundaries.

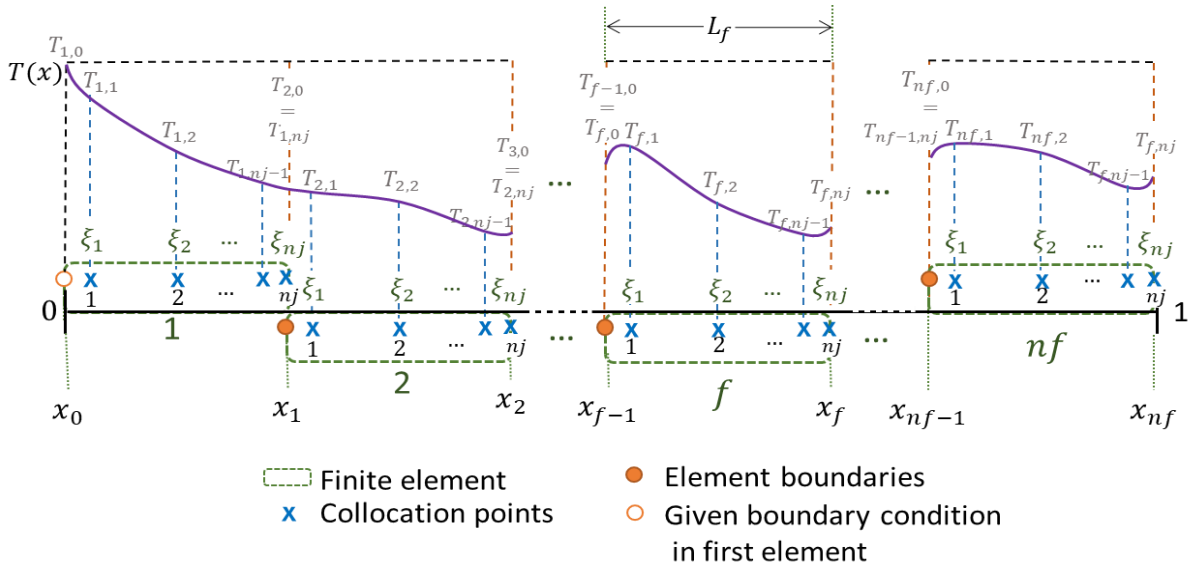

Figure 2-6. Spatial representation of 1D-OCFE

Let us consider an example where the spatial variable is the only integration variable (1D case) as represented in Figure 2-6. It could be the model of our DCS in steady-state conditions. Then, by dividing the whole domain into nf elements (x_{f-1} and x_f being the boundaries of the f^{th} element and L_f its length) and considering that the state variable is approximated by a polynomial of order nj (e.g. $nj+1$ collocation points are used on each element), then the state variable (temperature for example) can be expressed on the f^{th} element as the following Lagrange interpolation polynomial:

$$T(\xi) = \sum_{j=0}^{nj} T_{f,j}\, \ell_j(\xi) \tag{2-14}$$

With

$$\xi = \frac{x - x_{f-1}}{x_f - x_{f-1}} = \frac{x - x_{f-1}}{L_f} \quad , \xi \epsilon [0,1] \tag{2-15}$$

As the normalized spatial variable, and

$$\ell_j(\xi) = \prod_{\substack{k=0 \\ k \neq j}}^{nj} \frac{\xi - \xi_k}{\xi_j - \xi_k} \tag{2-16}$$

the j^{th} Lagrange basis polynomial of degree nj. When using Lagrange polynomials as trial functions, the coefficient of the j^{th} trial function on the f^{th} element represents the variable at the collocation point ξ_j (i.e. $T(\xi_j) = T_{f,j}$).

Then, the implementation of the collocation method consists in writing that the differential equation is satisfied on each collocation point ξ_j. In each element f, the state variable is replaced by $T_{f,j}$ and the derivative can be calculated by deriving the Lagrange interpolation polynomial leading to a linear combination of the $nj+1$ coefficients $T_{f,k}$ $(k = 0, \dots nj)$. Then the differential equation satisfied at this collocation point ξ_j leads to an algebraic equation involving the $nj+1$ coefficients $T_{f,k}$ $(k = 0, \dots nj)$. Finally, solving the system of all the $nf \times (nj+1)$ algebraic equations we will obtain the $nf \times (nj+1)$ values $T_{f,j}$ of the temperature at these collocation points.

2.3.2 The collocation matrix

In order to estimate the derivative terms, Hedengren *et al.* [76] have proposed a convenient way which includes the boundary condition. We have adapted it to collocation on finite elements and we detail it below. It begins writing a classical formulation of the Lagrange interpolation polynomial on the f^{th} element as:

$$T(\xi) = \alpha_0 + \alpha_1\xi + \alpha_2\xi^2 + \alpha_3\xi^3 + \cdots + \alpha_{nj}\xi^{nj} \tag{2-17}$$

From this approximation, we can represent also the derivative as:

$$\frac{dT}{d\xi} = \alpha_1 + 2\alpha_2\xi^1 + 3\alpha_3\xi^2 + \cdots + nj\alpha_{nj}\xi^{nj-1} \tag{2-18}$$

With the general forms of the state variable and its derivative, it is possible to express them on each of the selected collocation points. Then, we can formulate the system presented in equation (2-19), that aims to find a matrix M that relates the values of the derivative at the collocation points and the coefficients as:

$$\begin{bmatrix} \left(\frac{dT}{d\xi}\right)_{f,1} \\ \left(\frac{dT}{d\xi}\right)_{f,2} \\ \vdots \\ \left(\frac{dT}{d\xi}\right)_{f,nj} \end{bmatrix} = \begin{bmatrix} \frac{dT}{d\xi}(\xi_1) \\ \frac{dT}{d\xi}(\xi_2) \\ \vdots \\ \frac{dT}{d\xi}(\xi_{nj}) \end{bmatrix} = M_x \left(\begin{bmatrix} T_{f,1} \\ T_{f,2} \\ \vdots \\ T_{f,nj} \end{bmatrix} - \begin{bmatrix} T_{f,0} \\ T_{f,0} \\ \vdots \\ T_{f,0} \end{bmatrix} \right) \tag{2-19}$$

In the polynomial representation (2-17), the coefficient α_0 corresponds to the boundary condition of the f^{th} element, $T_{f,0}$, when the initial position is defined as zero. For the first element, this value ($T_{1,0}$, the temperature at the pipe inlet) must be given, whereas for the following elements it corresponds to the final value of the previous one. Then, substituting the approximation of the state variable (equation(2-17)) and its derivative (equation(2-18)) in the previous expression $T_{f,0}$ will be cancelled giving:

$$\begin{bmatrix} 1 & 2\xi_1 & 3\xi_1^2 & \cdots & nj\xi_1^{nj-1} \\ 1 & 2\xi_2 & 3\xi_2^2 & \cdots & nj\xi_2^{nj-1} \\ & & \vdots & & \\ 1 & 2\xi_{nj} & 3\xi_{nj}^2 & \cdots & nj\xi_{nj}^{nj-1} \end{bmatrix} \begin{bmatrix} \alpha_1 \\ \alpha_2 \\ \vdots \\ \alpha_{nj} \end{bmatrix} = M_x \begin{bmatrix} \xi_1 & \xi_1^2 & \cdots & \xi_1^{nj} \\ \xi_2 & \xi_2^2 & \cdots & \xi_2^{nj} \\ & & \vdots & \\ \xi_{nj} & \xi_{nj}^2 & \cdots & \xi_{nj}^{nj} \end{bmatrix} \begin{bmatrix} \alpha_1 \\ \alpha_2 \\ \vdots \\ \alpha_{nj} \end{bmatrix} \tag{2-20}$$

Since all the values ξ_j are different, the determinant of the matrix on the right-hand side of the equation will be non-null and therefore it will be invertible. Then, rearranging and solving for M_x, it will get:

$$M_x = \begin{bmatrix} 1 & 2\xi_1 & 3\xi_1^2 & \cdots & nj\xi_1^{nj-1} \\ 1 & 2\xi_2 & 3\xi_2^2 & \cdots & nj\xi_2^{nj-1} \\ & & \vdots & & \\ 1 & 2\xi_{nj} & 3\xi_{nj}^2 & \cdots & nj\xi_{nj}^{nj-1} \end{bmatrix} \begin{bmatrix} \xi_1 & \xi_1^2 & \cdots & \xi_1^{nj} \\ \xi_2 & \xi_2^2 & \cdots & \xi_2^{nj} \\ & & \vdots & \\ \xi_{nj} & \xi_{nj}^2 & \cdots & \xi_{nj}^{nj} \end{bmatrix}^{-1} \quad (2\text{-}21)$$

From (2-15), we can note that:

$$\frac{dT}{dx} = \frac{1}{L_f}\frac{dT}{d\xi} \quad (2\text{-}22)$$

Then, replacing in (2-19) and rearranging we will have:

$$\begin{bmatrix} \left(\frac{dT}{dx}\right)_{f,1} \\ \left(\frac{dT}{dx}\right)_{f,2} \\ \vdots \\ \left(\frac{dT}{dx}\right)_{f,nj} \end{bmatrix} = \frac{1}{L_f} \cdot M_x \left(\begin{bmatrix} T_{f,1} \\ T_{f,2} \\ \vdots \\ T_{f,nj} \end{bmatrix} - \begin{bmatrix} T_{f,0} \\ T_{f,0} \\ \vdots \\ T_{f,0} \end{bmatrix} \right) \quad (2\text{-}23)$$

The derivative term $\frac{dT}{dx}\left(L_f\xi_j + x_{f-1}\right)$ is noted as $\left(\frac{dT}{dx}\right)_{f,j}$. Here, M_x is the collocation matrix that correlates the value of the derivatives of the state variable at each collocation points of an element with the parameters that represent the variable on this element. Once the collocation points are defined, we use equation (2-21) to obtain the collocation matrices M_x which enables to discretize the derivative terms using equation (2-23). For the present application, we use the nodes of the shifted Legendre Gauss Lobatto quadrature as collocation points [85]. Thus, 0 and 1 are nodes and there are $nj - 1$ internal nodes. Then the continuity of the state variable in the elements bounds is defined as:

$$T_{f,0} = T_{f-1,nj} \qquad f = 2, \dots nf \quad (2\text{-}24)$$

Then, on each element, the ODE has to be written only on nj points ($\xi_j, j = 1 \dots nj$) since the boundary condition $\left(\text{e.g. } T_{f,0} = T\left(L_f\xi_0 + x_{f-1}\right) = T\left(x_{f-1}\right)\right)$ of each element is known.

When dealing with steady-state simulation, the above methodology has been applied to our DCS and the temperature, which depends only on x has been noted $T(t\ fixed, x) = \theta(x)$.

In the following subsection, we present the implementation of the method for both time (t) and space domains (x).

2.3.3 Implementation of 2D OCFE

The method of orthogonal collocation on finite elements for 2 dimensions can be formulated as an extension of the presented 1D derivation, as stated by Surjanhata [86], Finlayson [74] and Esche *et al.* [79], using the corresponding variables for each direction as well as a different polynomial or number of roots. First, the time horizon is divided into ne intervals (finite elements), and inside each interval, $ni+1$ collocation points are chosen. Similarly, each pipe has nf segments with $nj+1$ collocation points. Therefore, we define the sets $e \in (1,2,\dots,ne), i \in (0,1,\dots,ni), f \in (1,2,\dots,nf), j \in (0,1,\dots,nj)$. As we made for the spatial domain, we introduce the normalize time on each element e as:

$$\tau = \frac{t - t_{e-1}}{t_e - t_{e-1}} = \frac{t - t_{e-1}}{\Delta t_e} \quad , \tau \epsilon [0,1] \tag{2-25}$$

Then let us consider the temperature of the spatial-time domain corresponding to element e in time and element f in space. It is now approximated by the following function of ξ and τ (degree ni in τ and nj in ξ):

$$T(\tau,\xi) = \sum_{i=0}^{ni}\sum_{j=0}^{nj} T_{e,i,f,j}\,\ell_i(\tau)\ell_j(\xi) \tag{2-26}$$

The properties of the Lagrange basis polynomials lead to $T(\tau_i,\xi_j) = T_{e,i,f,j}$ and therefore:

$$T(\tau,\xi_j) = \sum_{i=0}^{ni} T_{e,i,f,j}\,\ell_i(\tau) \tag{2-27}$$

and

$$T(\tau_i,\xi) = \sum_{j=0}^{nj} T_{e,i,f,j}\,\ell_j(\xi) \tag{2-28}$$

To compute $\frac{\partial T}{\partial \tau}(\tau_i,\xi_j)$ we will derivate the Lagrange interpolation polynomial described by equation(2-27). This latter represents the evolution in time of the temperature in the present element (e) for the given position (f,j) and involves coefficients $T_{e,l,f,j}$ with e,f,j fixed, and l varying from 0 to ni (and passing through the particular value i) which are represented by '▧' in Figure 2-7. The same logic applies to compute $\frac{\partial T}{\partial \xi}(\tau_i,\xi_j)$: we will derivate the Lagrange interpolation polynomial described by equation (2-28) that represents the evolution in space of the temperature in the present element (f) for the given time (e,i). It involves the coefficients $T_{e,i,f,l}$ with e,i,f fixed, and l varying from 0 to nj (passing through the particular point j) which are represented by '▨' in Figure 2-7.

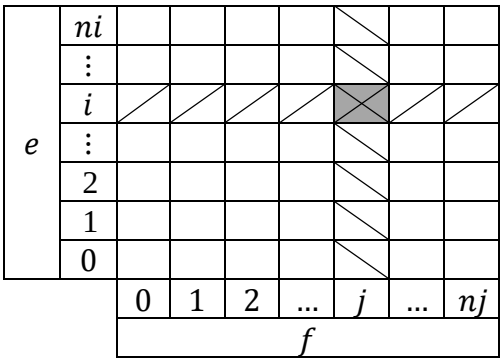

Figure 2-7. Representation of the temperature discretization (one element per domain)

Considering this, and applying the same methodology presented in the previous section for 1D-OCFE, we can approximate $\frac{\partial T}{\partial t}$ and $\frac{\partial T}{\partial x}$ as:

$$\begin{bmatrix} \left(\frac{\partial T}{\partial t}\right)_{e,1,f,j} \\ \left(\frac{\partial T}{\partial t}\right)_{e,2,f,j} \\ \vdots \\ \left(\frac{\partial T}{\partial t}\right)_{e,ni,f,j} \end{bmatrix} = \frac{1}{\Delta t_e} \cdot M_t \left(\begin{bmatrix} T_{e,1,f,j} \\ T_{e,2,f,j} \\ \vdots \\ T_{e,ni,f,j} \end{bmatrix} - \begin{bmatrix} T_{e,0,f,j} \\ T_{e,0,f,j} \\ \vdots \\ T_{e,0,f,j} \end{bmatrix} \right) \tag{2-29}$$

$$\begin{bmatrix} \left(\frac{\partial T}{\partial x}\right)_{e,i,f,1} \\ \left(\frac{\partial T}{\partial x}\right)_{e,i,f,2} \\ \vdots \\ \left(\frac{\partial T}{\partial x}\right)_{e,i,f,nj} \end{bmatrix} = \frac{1}{L_f} \cdot M_x \left(\begin{bmatrix} T_{e,i,f,1} \\ T_{e,i,f,2} \\ \vdots \\ T_{e,i,f,nj} \end{bmatrix} - \begin{bmatrix} T_{e,i,f,0} \\ T_{e,i,f,0} \\ \vdots \\ T_{e,i,f,0} \end{bmatrix} \right) \tag{2-30}$$

In equation (2-29) M_t represents the collocation matrix for the normalized domain of t, and Δt_e the size of the time element. The derivative terms $\frac{\partial T}{\partial x}\left(\Delta t_e \tau_i + t_{e-1}, L_f \xi_j + x_{f-1}\right)$ and $\frac{\partial T}{\partial t}\left(\Delta t_e \tau_i + t_{e-1}, L_f \xi_j + x_{f-1}\right)$ are noted as $\left(\frac{\partial T}{\partial x}\right)_{e,i,f,j}$ and $\left(\frac{\partial T}{\partial t}\right)_{e,i,f,j}$.

This representation is extended to all the pipes of the system. Then, the temperature of each pipe k (k may be $p, p_r, in_{C_p}, out_{C_p}$) $T_k(t,x)$ is expressed with the use of the $ne \times (ni+1) \times nf \times (nj+1)$ coefficients $T_{k,e,i,f,j}$.

For the first element on each domain, the values of the boundary conditions, $T_{k,1,0,f,j}$ and $T_{k,e,i,1,0}$, must be known, as will be detailed in the next section. And for the subsequent elements, the values of the boundary conditions, $T_{k,e,0,f,j}$ and $T_{k,e,i,f,0}$, correspond to those of the final point of the prior element ($T_{k,e-1,ni,f,j}$ and $T_{k,e,i,f-1,nj}$). Indeed, for the present application, we use the nodes of the shifted Legendre Gauss Lobatto quadrature as collocation points so that 0 and 1 are both collocation points.

Then for the other spatial-time points (other than $e,0,f,j$ and $e,i,f,0$) (e.g. $(\xi_j,\tau_i), j=1\dots nj, i=1\dots ni$)) we assume that equation (2-1) is satisfied. $T_k(\tau_i,\xi_j)$ is then replaced by $T_{k,e,i,f,j}$ and the derivatives are expressed as follows:

$$\begin{bmatrix} \left(\frac{\partial T}{\partial t}\right)_{e,1,f,j} \\ \left(\frac{\partial T}{\partial t}\right)_{e,2,f,j} \\ \vdots \\ \left(\frac{\partial T}{\partial t}\right)_{e,ni,f,j} \end{bmatrix} = \frac{1}{\Delta t_e}\cdot M_t \left(\begin{bmatrix} T_{k,e,1,f,j} \\ T_{k,e,2,f,j} \\ \vdots \\ T_{k,e,ni,f,j} \end{bmatrix} - \begin{bmatrix} T_{k,e,0,f,j} \\ T_{k,e,0,f,j} \\ \vdots \\ T_{k,e,0,f,j} \end{bmatrix} \right) = \begin{bmatrix} D_{t_1}(k,e,f,j) \\ D_{t_2}(k,e,f,j) \\ \vdots \\ D_{t_{ni-1}}(k,e,f,j) \end{bmatrix} \tag{2-31}$$

$$\begin{bmatrix} \left(\frac{\partial T}{\partial x}\right)_{e,i,f,1} \\ \left(\frac{\partial T}{\partial x}\right)_{e,i,f,2} \\ \vdots \\ \left(\frac{\partial T}{\partial x}\right)_{e,i,f,nj} \end{bmatrix} = \frac{1}{L_f}\cdot M_x \left(\begin{bmatrix} T_{k,e,i,f,1} \\ T_{k,e,i,f,2} \\ \vdots \\ T_{k,e,i,f,nj} \end{bmatrix} - \begin{bmatrix} T_{k,e,i,f,0} \\ T_{k,e,i,f,0} \\ \vdots \\ T_{k,e,i,f,0} \end{bmatrix} \right) = \begin{bmatrix} D_{x_1}(k,e,i,f) \\ D_{x_2}(k,e,i,f) \\ \vdots \\ D_{x_{nj-1}}(k,e,i,f) \end{bmatrix} \tag{2-32}$$

Finally, $D_{t_i}(k,e,f,j)$ and $D_{x_j}(k,e,i,f)$ denote the algebraic combinations to describe the variational terms of the PDE (2-1), allowing us to express the derivate with the coefficients of the discretized model that describes the behaviour of the presented DCS. Considering this, in the next subsection, we describe the implementation of 2D-OCFE to transform the heat equation into a set of algebraic equations, which coupled with the heat and mass balances represent the dynamics of the DCS.

2.3.4 The discretized model

The dynamic analysis of the DCS implies, that also the mass flow on the pipes $\dot{m}_k(t)$ must be discretized. Then, on each element in time, the mass flow can also be represented by a sum of orthogonal polynomials as:

$$\dot{m}_k(\tau) = \sum_{i=0}^{ni} \dot{m}_{k,e,i}\, \ell_i(\tau) \tag{2-33}$$

In section 2.1.2 we presented, for each of the clients connected to the network, its demand profile, $Q_{C_p}(t)$. When the PDE is applied in an element e in time at a collocation point τ_i we use the corresponding value of this profile, which has been noted $Q_{C_p,e,i}$:

$$Q_{C_p,e,i} = Q_{C_p}(\tau_i \Delta t_e + t_{e-1}) \tag{2-34}$$

Similarly, section 2.1.3 details the behaviour of the external temperature for the proposed climate zones $T_s(t)$, that are also input data of the model. When the PDE is applied in an element e in time at a collocation point τ_i we use the corresponding soil temperature which has been noted $T_{s,e,i}$.

$$T_{s,e,i} = T_s(\tau_i \Delta t_e + t_{e-1}) \tag{2-35}$$

Next, we use (2-31) and (2-32) to discretize equation (2-1), on each pipe at each time-spatial point other than the boundary points, $(\tau_i, \xi_j), i = 1 \dots ni, j = 1 \dots nj$, by:

$$\rho_w \cdot Cp_w \cdot A_k \cdot D_{t_i}(k,e,f,j) + \dot{m}_{k,e,i} \cdot Cp_w \cdot D_{x_j}(k,e,i,f) = \frac{T_{s,e,i} - T_{k,e,i,f,j}}{R'_k} \tag{2-36}$$

This formulation represents the PDE (2-1) as a set of $(ne \times ni \times nf \times nj)$ equations per pipe.

The boundary conditions $T_{k,e,0,f,j}$ and $T_{k,e,i,f,0}$ are obtained from the configuration of the problem and from the heat and mass balances as follows:

- As stated before, for the elements $e > 1$ and $f > 1$, on each pipe, the initial conditions correspond to the final point of the prior one.

$$T_{k,e,0,f,j} = T_{k,e-1,ni,f,j}\,, \qquad e = 2 \dots ne\,, \qquad f = 1 \dots nf\,, \qquad j = 1 \dots nj \tag{2-37}$$

$$T_{k,e,i,f,0} = T_{k,e,i,f-1,nj}\,, \qquad f = 2 \dots nf\,, \qquad e = 1 \dots ne, \qquad i = 1, \dots ni \tag{2-38}$$

And

$$T_{k,e,0,f,0} = T_{k,e-1,ni,f-1,nj}\,, \qquad e = 2 \dots ne\,, \qquad f = 2 \dots nf \tag{2-39}$$

- The initial condition of the temperature in the pipes presented in equation (2-2), results in $nf \times (nj + 1)$ equations in terms of discretized variables as:

$$T_{k,1,0,f,j} = \theta_k\left(L_f \xi_j + x_{f-1}\right) = \theta_{k,f,j} \tag{2-40}$$

- For the element $f = 1$, the initial condition depends on the pipe.
  - As stated in (2-3), the production site pumps chilled water at 277K, which in terms of discretized variables is a set of $ne \times (ni + 1) - 1$ equations:

$$T_{0,e,i,1,0} = 277\ \mathrm{K} \tag{2-41}$$

  - The heat balances in the splitters (equation (2-4)), representing the boundary conditions of the pipes leaving them, will be:

$$\begin{gathered} T_{p,e,i,nf,nj} = T_{p+1,e,i,1,0} = T_{in_{C_p},e,i,1,0}\ \ , p = 1 \dots 12{,}14, \dots 19 \\ T_{0,e,i,nf,nj} = T_{1,e,i,1,0} = T_{14,e,i,1,0} \\ T_{p,e,i,nf,nj} = T_{in_{C_p},e,i,1,0}\ \ ,\ \ p = 13\,, 20 \end{gathered} \tag{2-42}$$

  - The boundary conditions in the pipes leaving the mixing nodes (return path) presented in (2-5) will be represented by a set of $ne \times (ni + 1)$ equations in terms of discretized variables as:

$$\begin{gathered} \dot{m}_{p_r,e,i} \cdot T_{p_r,e,i,1,0} = \dot{m}_{p_r+1,e,i} \cdot T_{(p+1)_r,e,i,nf,nj} + \dot{m}_{out_{C_p},e,i} \cdot T_{out_{C_p},e,i,nf,nj}\,, \\ p = 1 \dots 12{,}14, \dots 19 \\ \dot{m}_{(0)_r,e,i} \cdot T_{(0)_r,e,i,1,0} = \dot{m}_{(1)_r,e,i} \cdot T_{(1)_r,e,i,nf,nj} + \dot{m}_{(14)_r,e,i} \cdot T_{(14)_r,e,i,nf,nj} \\ T_{(p)_r,e,i,1,0} = T_{out_{C_p},e,i,nf,nj}\ \ ,\ \ p = 13\,, 20 \end{gathered} \tag{2-43}$$

  - Finally, the boundary conditions of the pipes leaving each consumer is given by the energy balances presented in (2-6), resulting also in a set of $ne \times (ni + 1)$ equations as follows:

$$Q_{C_p,e,i} = \dot{m}_{in_{C_p},e,i} \cdot \mathrm{C}p_w \cdot \left(T_{out_{C_p},e,i,1,0} - T_{in_{C_p},e,i,nf,nj}\right) \tag{2-44}$$

For a better understanding, Figure 2-8 depicts the relationship between the computing of $T_{p,e,i,f,j}$ with the presented equations.

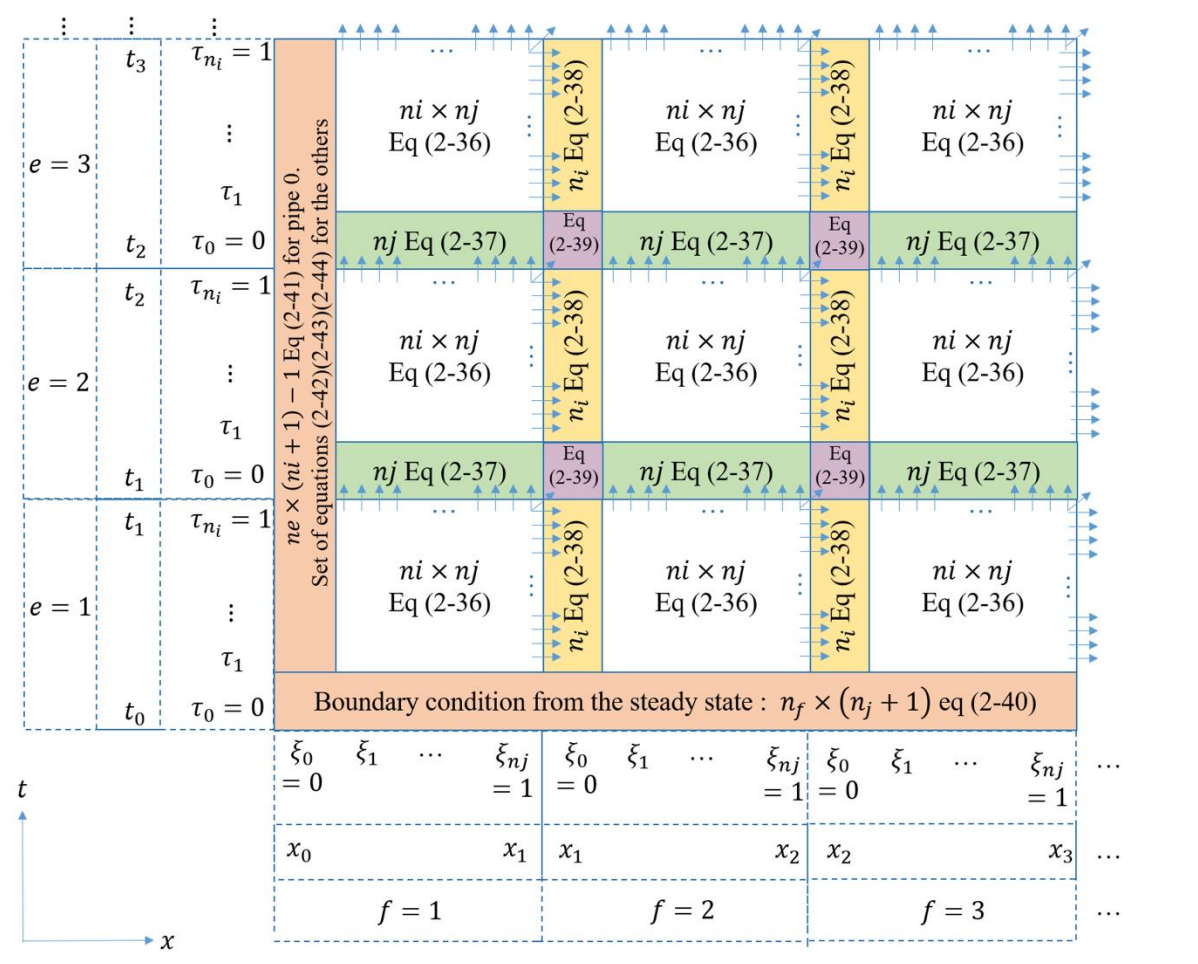

Figure 2-8. Associated equations for the solution of the discretized PDE

Moving to the mass balances, they involve only time-dependent variables as detailed in section 2.2. Then, the mass flow in the production site (2-10), the mass balances in the outward nodes (2-7), return nodes (2-8) and consumers (2-9) in terms of discretized variables will be:

$$\dot{m}_{0,e,i} = \dot{m}_{0Cte} \tag{2-45}$$

$$\begin{aligned} \dot{m}_{p,e,i} &= \dot{m}_{p+1,e,i} + \dot{m}_{in_{C_p},e,i} \quad p = 1 \dots 12,14 \dots 19 \\ \dot{m}_{p,e,i} &= \dot{m}_{in_{C_p},e,i} \quad p = 13\,,20 \\ \dot{m}_{0,e,i} &= \dot{m}_{1,e,i} + \dot{m}_{14,e,i} \end{aligned} \tag{2-46}$$

$$\begin{aligned} \dot{m}_{p_r,e,i} &= \dot{m}_{(p+1)_r,e,i} + \dot{m}_{out_{C_p},e,i} \quad p = 1 \dots 12,14 \dots 19 \\ \dot{m}_{p_r,e,i} &= \dot{m}_{out_{C_p},e,i} \quad p = 13\,,20 \\ \dot{m}_{0_r,e,i} &= \dot{m}_{1_r,e,i} + \dot{m}_{14_r,e,i} \end{aligned} \tag{2-47}$$

$$\dot{m}_{in_{C_p},e,i} = \dot{m}_{out_{C_p},e,i} \quad p = 1 \dots 20 \tag{2-48}$$

Finally, the relationships for constant flow policy (2-11), are represented by:

$$\frac{Peak(1)}{\dot{m}_{in_{C_1},e,i}} = \frac{Peak(p)}{\dot{m}_{in_{C_p},e,i}}, \quad \forall\, p \in \{2, \dots, 20\} \tag{2-49}$$

The discretization of the mathematical model results in a total of $n_{pipes} \times n_e \times (n_i + 1)$ variables $\dot{m}_{k,e,i}$, with $n_{pipes} = 82$, to define the distribution of the chilled water in the presented cooling system. The solution for the variables $\dot{m}_{k,e,i}$, is given by the presented mass balances as:

$1 \times n_e \times (n_i + 1)$ equations (2-45).
$21 \times n_e \times (n_i + 1)$ equations (2-46).
$21 \times n_e \times (n_i + 1)$ equations (2-47).
$20 \times n_e \times (n_i + 1)$ equations (2-48).
$19 \times n_e \times (n_i + 1)$ equations (2-49).

Then, the implementation of 2D-OCFE to the original PDAE problem presented in Section 2.2 results in the set of algebraic equations (2-36) to (2-49). This formulation allows performing the dynamic simulation analysis of the case study, whose main output will be the dynamic response of the system subject to the perturbations, in external temperature and cooling demands. This analysis is presented in the next chapter.

Chapter 3. Dynamic simulation Analysis

Considering the discretized model detailed in the last section of Chapter 2, the present chapter introduces the methodology for the proper initialization of the dynamic optimization problems. This methodology is constituted by a succession of steady-state and dynamic simulations.

First, considering the importance of a good initialization for the proper solution of a simulation, section 3.1 details a strategy based on the solution of less complicated problems for the initialization of a more complicated one. Then section 3.2 presents the main results of these intermediate problems (steady-state simulations) as well as a sensitivity analysis of the discretization strategy in each case. Finally, the dynamic simulation is performed under the conditions of the climatic zone that presented the biggest heat gains in the steady-state analysis.

Chapter Contents

3.1 Initialization and solution strategy

This section details the methodology that allows solving the algebraic problem that resulted from the implementation of 2D-OCFE to discretize the PDAE problem presented in the previous chapter.

In general, the proper solution of optimization problems requires the availability of a good initialization (procedure or data). For the particular case of dynamic optimization problems, Safdarnejad *et al.* [87] present strategies based on warm starts from previous solutions, including techniques of linearization, structural decomposition, and initializations with steady-state or quadratic approximate solutions. The authors also highlighted that a good initialization is crucial for a fast and reliable solution to the dynamic optimization problem.

For this application, we have implemented an initialization procedure based on the previous solution of a steady-state problem, detailed in Figure 3-1.

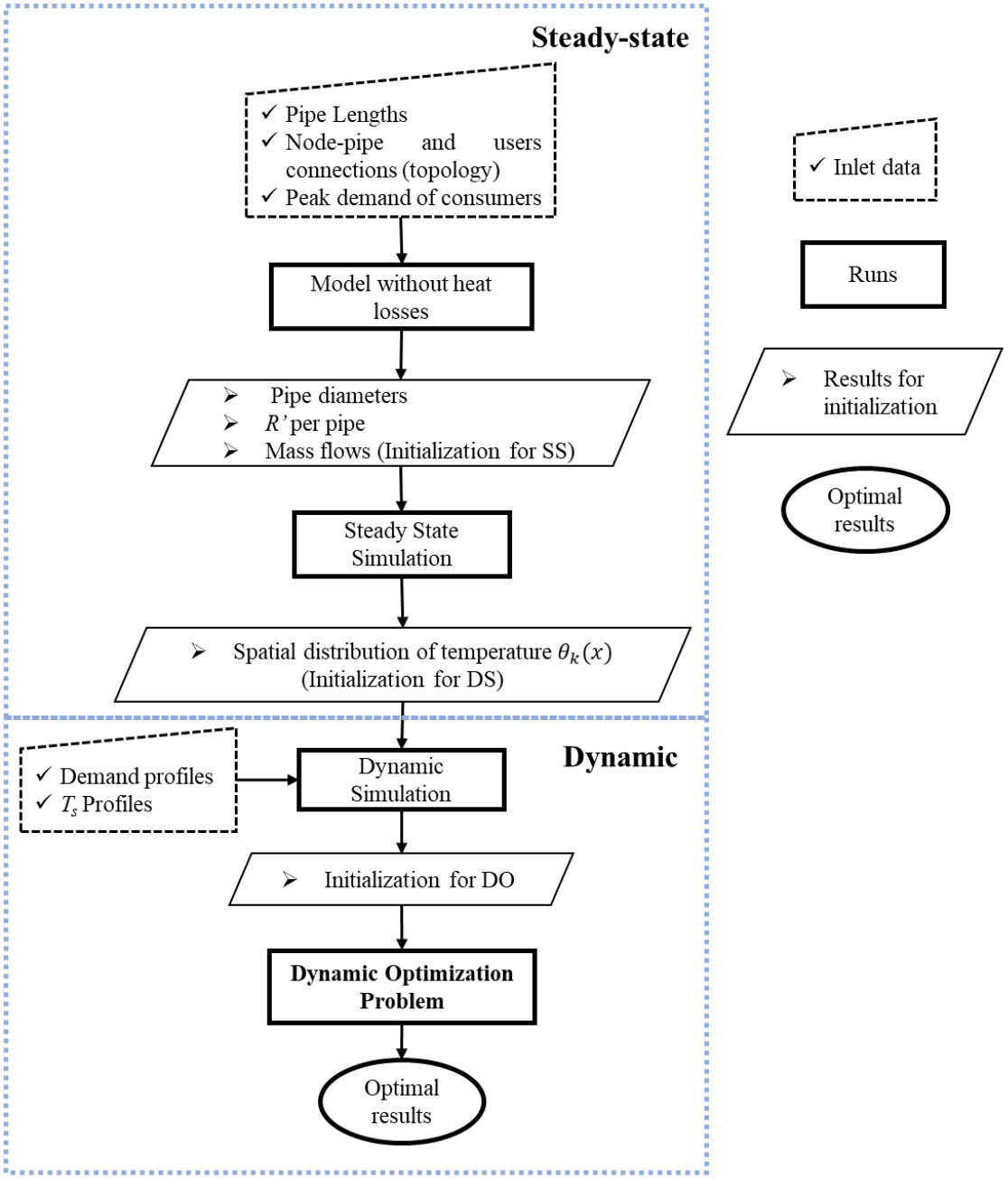

Figure 3-1. Methodology for the initialization and solution of the dynamic optimization problem

Due to the lack of piping data for the selected system [52], we must define the diameters of the pipes throughout the network. For this purpose, we first compute a theoretical maximum mass flow in the main pipes using a model without heat losses. This model includes only the heat and mass balances in the nodes and consumers, for the maximum demand (peak demand) on each consumer and a return temperature of 287 K (which is also the outlet temperature of each consumer exchanger since the heat losses are neglected). Then, for each pipe, for the previously computed flow, we compute the minimum diameter that achieves the maximum known allowable fluid velocity (which is a function of

the diameter, Table 2-5). It is important to mention that the chosen diameters using this iterative step will lead us to a physically achievable operation, but they are not optimal regarding any economic or operational criteria. The computation of the optimal diameter for a cost objective function will be studied in the last section of Chapter 4.

With the diameters already defined, we run the model without heat losses for the maximum total demand of the system (demands $Q_{C_p}(t_{max})$, presented in Figure 3-2 whose result represents the initialization to solve the steady-state (SS) problem. This latter is defined by the equation system (2-36) to (2-49), with $D_{t_i}(k,e,f,j) = 0 \left(\frac{dT(t,x)}{dt} = 0\right)$, external conditions in $t = 0$ and user's demand fixed to $Q_{C_p}(t_{max})$.

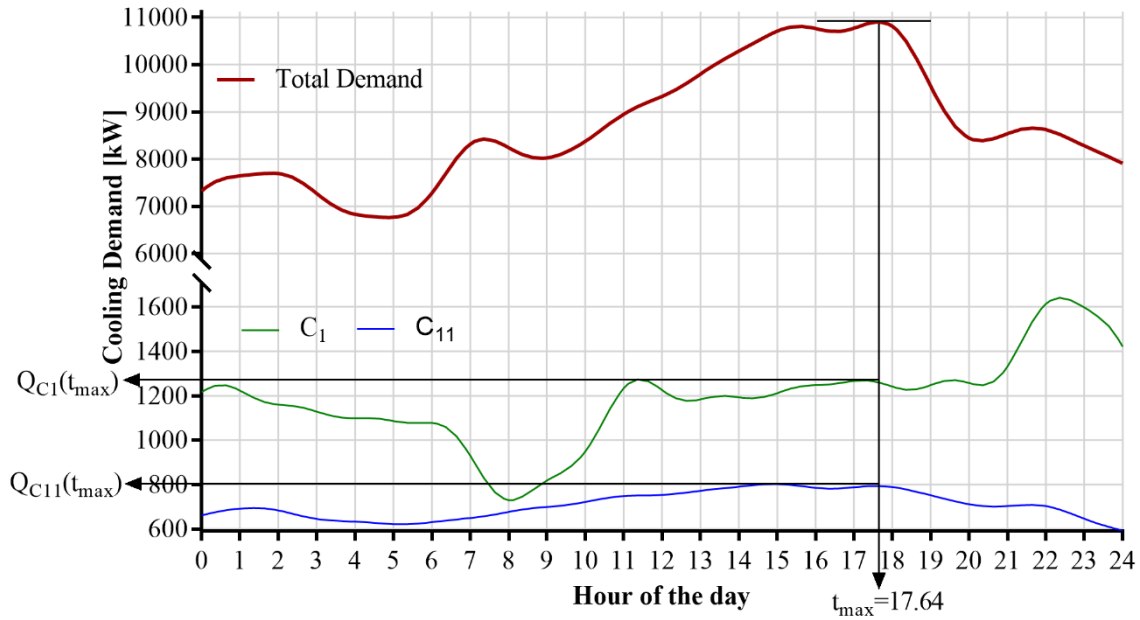

Figure 3-2. Total demand and localization of t_{max} to define demands for steady-state simulation

The main result of the steady-state problem is the spatial distribution of temperature $\theta_k(x)$ for the constant flow policy, which represents the initial condition for the dynamic simulation. This distribution is given by the values of the temperature in the spatial collocation points, $\theta_{k,f,j}$. With this, it is possible to solve the dynamic simulation problem which describes the behaviour of the complete system subject to the environmental and operational perturbations over the selected time horizon. Finally, we use the solution of the dynamic simulation (DS) problem as the initial guess for the dynamic optimization (DO) problem. We implemented all the described stages in the modelling environment of GAMS and solve the different problems involved using the feasible path solver CONOPT, on a quad-core 2.7 GHz CPU with 8 Gb of RAM.

The next section details the results for the model without heat losses, the steady-state and dynamic simulation of the district cooling system.

3.2 Simulation Results

This section details the implementation of the presented solution strategy. First, we present the diameters obtained solving the model without heat losses. Then, using these diameters we compute the spatial distribution of temperature $(\theta_k(x))$ for the conditions of the cities presented in Section 2.1. This steady-state problem is solved for the time that exhibits the maximum total demand. This includes a sensitivity analysis of the number of collocation points (1D) for the solution of this problem. Finally, we detail the dynamic response of the system subject to the perturbations in the demand and the external conditions. This latter includes also a sensitivity analysis (2D) on the number of collocation points on each domain for a reliable solution of the dynamic problems.

3.2.1 Pipe diameters

Using the mentioned iterative procedure with the model without heat losses, we define the distribution of pipe nominal diameters detailed in Table 2-1. These diameters ensure the operation of the system under the proposed demand profiles and will be fixed parameters for the subsequent problems.

Table 3-1. Pipe diameters for the DCS

Pipe		$\dot{m}\left[\frac{kg}{s}\right]$	$v_k\left[\frac{m}{s}\right]$	$v_{max_k}\left[\frac{m}{s}\right]$	nominal diameter [in] (m)
0	0_r	280.46	1.58	2.03	20 (0.508)
1	1_r	150.40	1.33	1.80	16 (0.4064)
2	2_r	111.38	1.29	1.56	14 (0.3556)
14	14_r	130.06	1.50		
3	3_r	94.72	1.32	1.56	12 (0.3048)
4	4_r	89.96	1.26		
5	5_r	71.39	1.00		
6	6_r	69.01	0.96		
15	15_r	94.36	1.32		
16	16_r	78.89	1.10		
17	17_r	69.85	0.98		
7	7_r	47.60	0.94	1.37	10 (0.254)
8	8_r	45.22	0.90		
18	18_r	59.02	1.17		
9	9_r	39.27	1.23	1.27	8 (0.2032)
10	10_r	29.75	0.93		
11	11_r	25.70	0.80		

Pipe		$\dot{m}\left[\frac{kg}{s}\right]$	$v_k\left[\frac{m}{s}\right]$	$v_{max_k}\left[\frac{m}{s}\right]$	nominal diameter [in] (m)
19	19_r	37.60	1.18		
20	20_r	29.03	0.91		
inC_1	$outC_1$	39.03	1.22	1.76	
inC_{14}	$outC_{14}$	35.70	1.12		
inC_2	$outC_2$	16.66	0.90	1.69	6 (0.1524)
inC_4	$outC_4$	18.56	1.01		
inC_6	$outC_6$	21.42	1.16		
inC_{11}	$outC_{11}$	19.04	1.03		
inC_{15}	$outC_{15}$	15.47	0.84		
inC_{18}	$outC_{18}$	21.42	1.16		
inC_{20}	$outC_{20}$	29.03	1.58		
12	12_r	6.66	0.82	1.08	4 (0.1016)
inC_9	$outC_9$	9.52	1.18	1.54	
inC_{16}	$outC_{16}$	9.04	1.12		
inC_{17}	$outC_{17}$	10.83	1.34		
inC_{19}	$outC_{19}$	8.57	1.06		
13	13_r	4.28	0.91	0.94	3 (0.0762)
inC_3	$outC_3$	4.76	1.02	1.32	
inC_8	$outC_8$	5.95	1.27		
inC_{10}	$outC_{10}$	4.05	0.86		
inC_{13}	$outC_{13}$	4.28	0.91		
inC_5	$outC_5$	2.38	1.12	1.31	2 (0.0508)
inC_7	$outC_7$	2.38	1.12		
inC_{12}	$outC_{12}$	2.38	1.12		

Under these conditions, the producer pumps a total flow of 259.66 kg/s of chilled water, to supply the cooling demand corresponding to the maximum demand of the network (t_{max}). The presented distribution of diameters is consistent because the sizes of the pipes decrease as they get away from the production site. Furthermore, the smallest pipes fed users with lower cooling demands. With this data, we define the global thermal resistance per unit length R' of the pipes. To compute the thermal resistances, we assume that all the pipes are buried at the same depth of one meter (d in Figure 1-9). The insulation thermal conductivities and thickness correspond to the values reported by the North American Insulation Manufacturers Association [88]. For the following simulations and the optimizations presented until Section 4.1.2 in Chapter 4, we consider a constant value of thermal

resistance per pipe R'_k. Then, we propose to compute it for a mean flow velocity in each pipe, defined as the mean between the maximum allowed value and the velocity computed in the model without heat losses. Later, the last section of Chapter 4 details a dynamic optimization analysis that considers a variable thermal resistance per pipe $R'_k(t)$.

Figure 3-3 details the variation of the global thermal resistance with respect to the nominal pipe diameters for insulated and non-insulated pipes, for the characteristic terrain and initial soil temperature for each of the proposed climate zones detailed in section 2.1. These values will be also input parameters for the forthcoming problems, except for the operational cost optimization where it will vary over time as a function of the flow velocity.

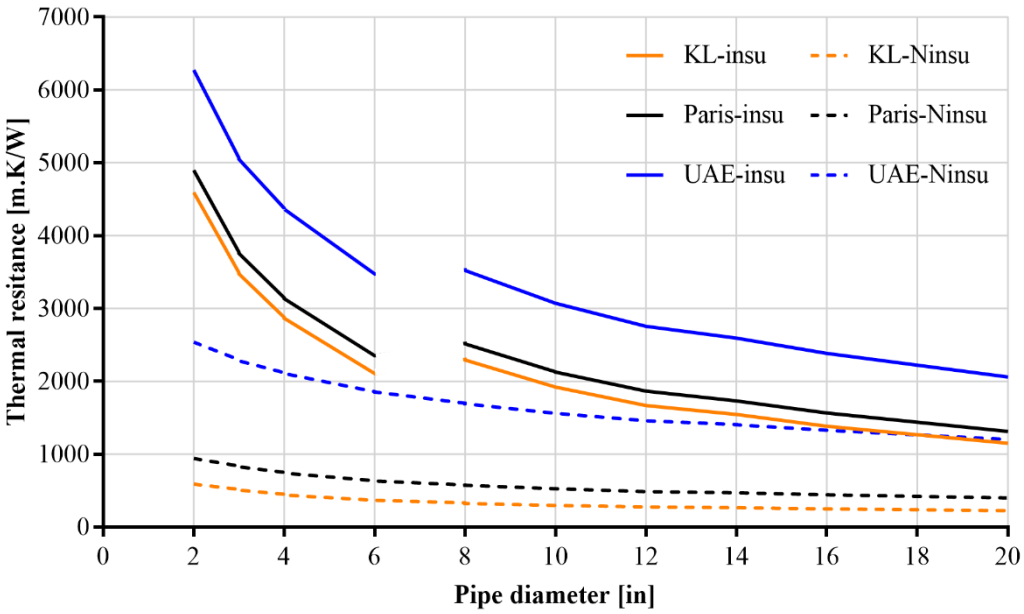

Figure 3-3.Variation of the total thermal resistance

We can evidence that for all the cases, as the pipe diameter size increases the value of the global thermal resistance decreases, presenting a major variation for insulated pipes. For the two kinds of pipes, the installation under the conditions of Kuala-Lumpur (KL) has the lowest thermal resistance. The discontinuity of *R'* for the insulated pipes corresponds to a change in the insulation thickness, which is one inch for the pipes with diameters smaller than 8 inches and 1.5 inches for the others. Furthermore, for big insulated pipe sizes (16" and 20") the resistance in KL is equivalent to the one computed for non-insulated pipes under the conditions of UAE. These values will have a major influence in the spatial distributions of temperature, as we will detail in the next subsection.

3.2.2 Steady-state simulation

In this section, we first detail the sensitivity analysis for the collocation points to be used in the steady-state simulations. Then we present the distribution of temperatures $\theta_k(x)$ obtained for the three external conditions presented in Section 2.1 and that will be used as initialization of the dynamic problem.

3.2.2.1 Collocation points for steady-state analysis

With all the elements of the distribution network already established, it is necessary to define the number of elements (nf) and points $(nj + 1)$ that will be used for the solution of the simulation and optimization problems. This sensitivity analysis is only valid for the Steady-state analysis. Sub-section 3.2.3.1 details the sensitivity analysis for the dynamic analyses.

For this purpose, several simulations of a steady-state problem were performed for an increasing number of collocation points. Figure 3-4 details the spatial distribution of the temperature over the left outward branch of the network (C_1 to C_{13} in Figure 2-1; the production site is located at $x = 0$), using non-insulated pipes with the external temperature of Kuala Lumpur (T_s $(t = 0)$) and consumers' demands $Q_{Cp}(t_{max})$. The solution of the steady-state model for each climate condition takes less than 0.5 seconds.

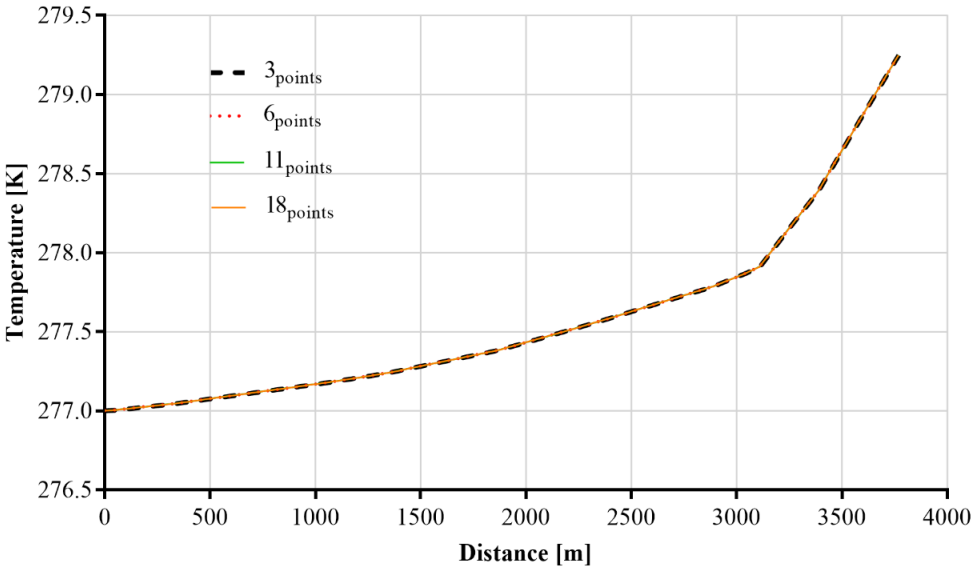

Figure 3-4. Comparison of the spatial distribution of temperature for different number of points

We use one finite element (nf) for the simulation with 3, 6 and 11 collocation points $(nj + 1)$, and 3 finite elements, with 6 collocation points each, for the simulation with 18 points.

We can evidence that for the four proposed arrangements of collocation points, it is possible to compute the same spatial distribution of temperature, showing the stability of the method. Then, using three collocation points, the next subsection details the results of the steady-state simulation.

3.2.2.2 Spatial distribution of temperature

We completed the steady-state simulation for the three climate zones (using $T_s\ (t = 0)$ as external temperature), soil conditions presented in section 2.1 and using insulated and non-insulated pipes. For each climate zone, the simulation was first performed for a system with insulated pipes, fixing the return temperature $\theta_{0_r,nf,nj}$ to compute the producer mass flow $\dot{m}_{0Cte}$. This latter is set as a parameter for the system with non-insulated pipes, where we compute the return temperature in order to compare the influence of the insulation under the same flow conditions. Table 3-2 details these results.

Table 3-2. External temperature and results for steady-state simulations

	Insulated pipes			**Non-insulated pipes**		
	KL	Paris	UAE	KL	Paris	UAE
T_s[K]	300.2	290.8	305.8	300.2	290.8	305.8
$\dot{m}_{0Cte}[kg/s]$	263.60	261.37	262.87	263.60	261.37	262.87
$\theta_{0_r,nf,nj}[K]$	287	287	287	287.7	287.2	287.1

For the insulated pipes, the system that reported the lowest thermal resistance (KL) demands more cold water from the provider to achieve the proposed return temperature using insulated pipes. On the other hand, although the UAE presents the biggest thermal resistance, this location represents also the hottest external temperatures, resulting in a bigger mass flow compared with the network installed in Paris. Moving to the systems with non-insulated pipes, the variation in the return temperature increases as the thermal resistance decreases.

As stated in section 3.1, the most important result of the steady-state simulation is the spatial distribution of temperature in the network $\theta_k(x)$. Figure 3-5 details these profiles for the mainline of the network using the two kinds of pipes, for the three cities. The production site is located at $x = 0$, the left side of the network (consumers 1 to 13) is represented on the negative side of the abscissas while the right side (consumers 14 to 20) on the positive one.

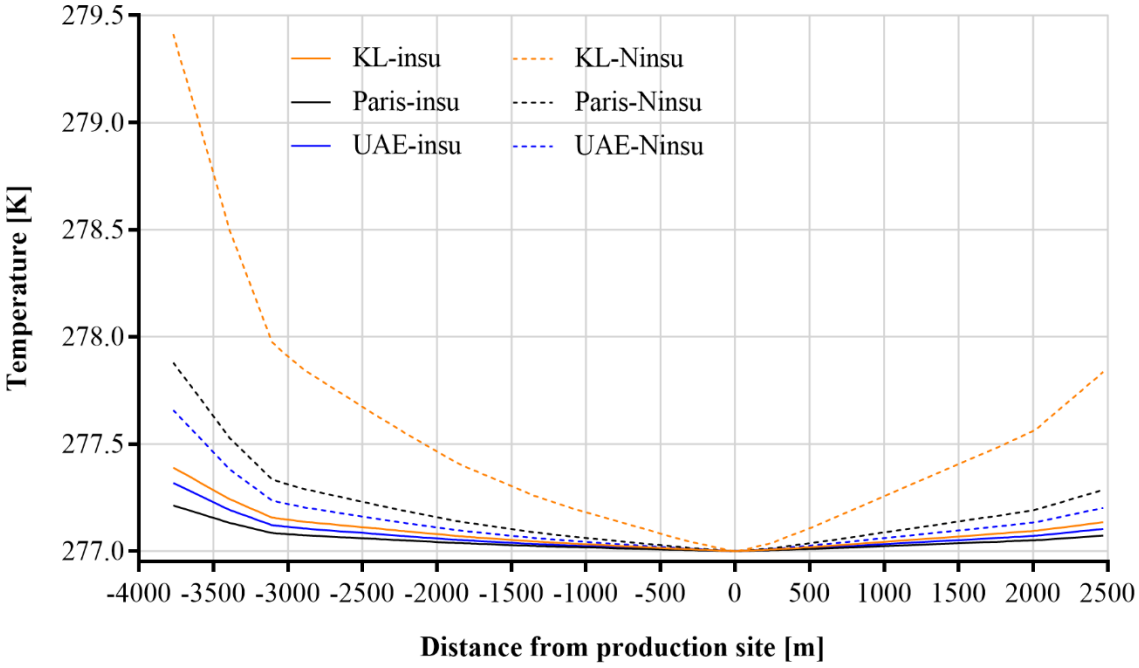

Figure 3-5. Spatial distribution of temperature in the outward path of the network

It is possible to observe that in all the cases the water in the pipes is increasing its temperature as it moves further from the production site. The results under the humid conditions in Kuala Lumpur presents the biggest temperature increments. Even if the variations in the spatial temperature are of the order of 2.5K or less (insulated pipes), its computation is important for the dynamic analysis, considering that these variations of temperature can increase during the day mainly if we have higher external temperatures and low mass flow in the pipes. Comparing the behaviour of the temperature for Paris and UAE using insulated and non-insulated pipes, it is possible to evidence that for insulated pipes the system in Paris presents the lowest temperature levels while for non-insulated pipes it is the UAE system. This variation is explained by the value of the convective heat transfer per unit length $\left(q_{c_0} = \frac{T_S - T_{0,1,0}}{R'}\right)$ of each system production site when changing the kind of piping, as detailed in Table 3-3. The system with insulated pipes in UAE presents major convective heat exchange compared with the system in Paris, while the contrary occurs when using non-insulated pipes. This highlights the fact that not only does the outside temperature play an important role in the heat losses, but also the nature of the soil and the moisture conditions that both determine the thermal conductivity of the soil.

Table 3-3. Convective heat transfer per unit length at the production sites

	Insulated pipes			**Non-insulated pipes**		
	KL	Paris	UAE	KL	Paris	UAE
$q_{c_0}[kW/m]$	0.0202	0.0105	0.0139	0.1022	0.0342	0.0239

The left side of the network presents a stiff change in the temperature level at 3117 meters that corresponds to the inlet of pipe 12, which feds consumers 12 and 13. There is a major reduction in the mass flow in this pipe (see Table 3-4) due to the change of the cooling demand levels. As seen in Table 2-2 consumer 11 presents a peak demand almost 3 times bigger than consumers 12 and 13 do together. Contrary, the right side of the network does not present this behaviour due to the high level of demand of client 20 that forces to pump an important mass through all this side of the network.

Table 3-4. Mass flow in main outward pipes for steady-state analysis

$\dot{m}_p[kg/s]$	KL	Paris	UAE
$\dot{m}_1$	141.36	140.17	140.97
$\dot{m}_2$	104.68	103.79	104.39
$\dot{m}_3$	89.02	88.27	88.78
$\dot{m}_4$	84.55	83.83	84.32
$\dot{m}_5$	67.10	66.53	66.92
$\dot{m}_6$	64.87	64.32	64.69
$\dot{m}_7$	44.73	44.36	44.61
$\dot{m}_8$	42.50	42.14	42.38
$\dot{m}_9$	36.91	36.59	36.80
$\dot{m}_{10}$	27.96	27.72	27.88
$\dot{m}_{11}$	24.16	23.95	24.09
$\dot{m}_{12}$	6.26	6.21	6.25
$\dot{m}_{13}$	4.03	3.99	4.02
$\dot{m}_{14}$	122.24	121.20	121.90
$\dot{m}_{15}$	88.69	87.94	88.44
$\dot{m}_{16}$	74.15	73.52	73.94
$\dot{m}_{17}$	65.65	65.09	65.47
$\dot{m}_{18}$	55.47	55.00	55.32
$\dot{m}_{19}$	35.34	35.04	35.24
$\dot{m}_{20}$	27.29	27.06	27.21

Following the same temperature level tendencies, Figure 3-6 details the spatial temperature profiles for the main return pipes. Here, the non-smooth changes correspond to the mixing process at the

return nodes where the different temperature levels arriving at the node ($T_{(p+1)_r}(L_{(p+1)_r})$ and $T_{out_{C_p}}(L_{out_{C_p}})$) result in a different level of temperature leaving it $\left(T_{(p)_r}\left(L_{(p)_r}\right)\right)$.

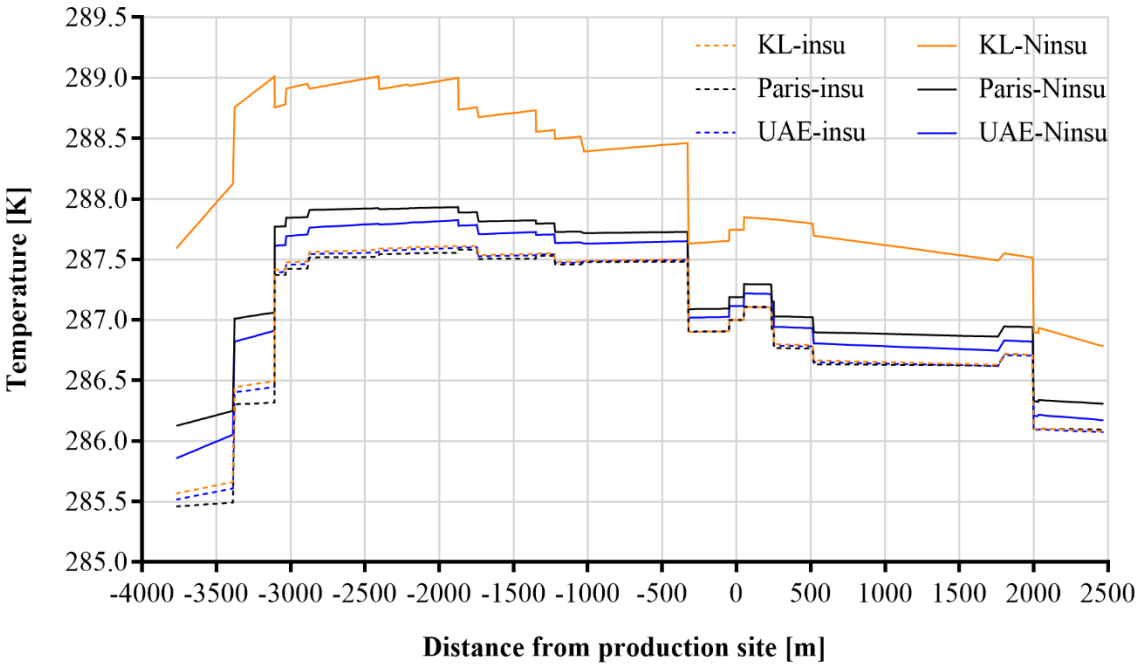

Figure 3-6. Spatial distribution of temperature in the return path of the network

The presented spatial temperature profiles are then used as initialization for the solution of the dynamic problems. Considering these results, the dynamic analysis of the system will be performed for the external conditions of KL, because they result in major variation of the temperature of the cooling fluid in the pipes.

3.2.3 Dynamic simulation analysis

As stated in Section 3.1, with the distribution of temperature $\theta_k(x)$ known, it is possible to perform the dynamic study of the system, that considers the variation in demand and external temperature presented in Section 2.1. Nevertheless, first, it is necessary to define the number of elements and points to be used on each domain for the discretization of the PDAE problem, to perform the simulation and optimization analyses.

3.2.3.1 Collocation points for dynamic analysis

Using the same procedure implemented for the steady-state analysis, we performed various dynamic simulations for different arrangements of finite elements (ne and nf) and collocation points ($ni+1$ and $nj+1$) on each domain (x and t). These dynamics simulations are performed for a time horizon of one day (24h). Figure 3-7 details the temperature profile for the return pipe $\left(T_{0_{r,e,i,nf,nj}}\right)$, for the external conditions of Kuala Lumpur using Non-insulated pipes (more detail on the behaviour of the

system is presented in the next subsection), for 5 different arrangements of finite elements and collocation points. The arrangements are detailed as follows:

- A: $ne = 12;\ (ni + 1) = 6;\ nf = 1; nj + 1 = 6$
- B: $ne = 12;\ (ni + 1) = 6;\ nf = 1; nj + 1 = 11$
- C: $ne = 24;\ (ni + 1) = 6;\ nf = 1; nj + 1 = 11$
- D: $ne = 24;\ (ni + 1) = 6;\ nf = 3; nj + 1 = 6$
- E: $ne = 48;\ (ni + 1) = 6;\ nf = 3; nj + 1 = 6$

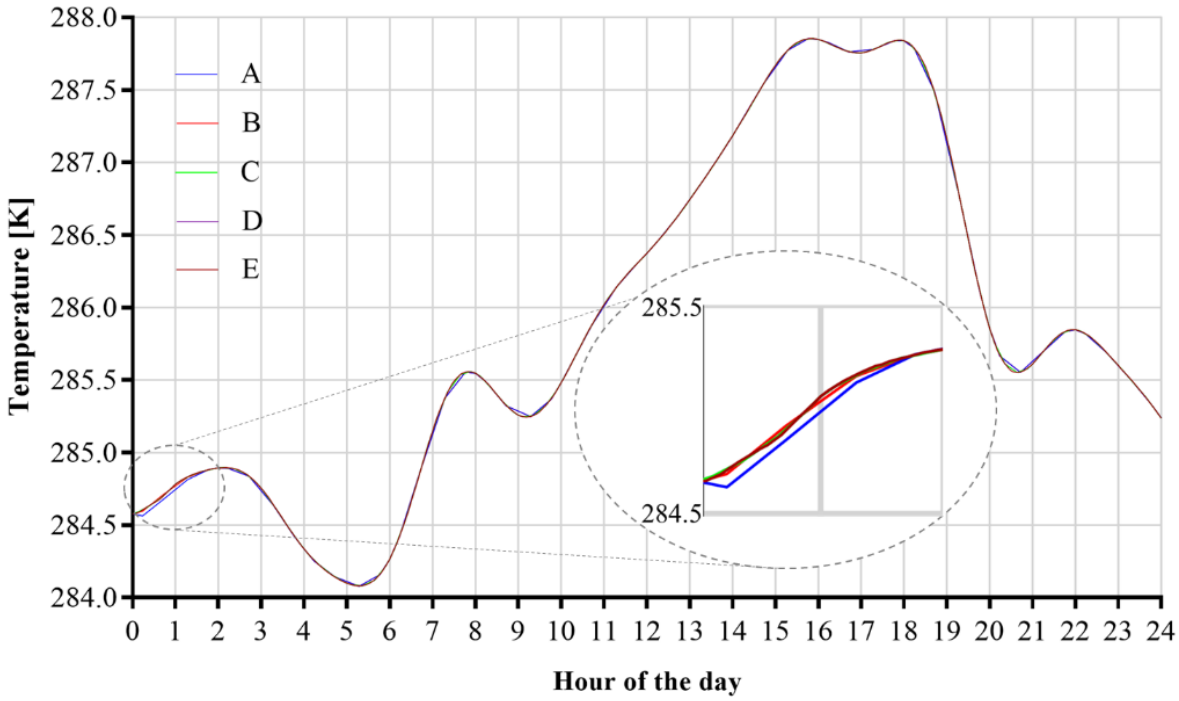

Figure 3-7. Return temperature profile for different arrangements of finite elements and collocation points

We can evidence that as the number of collocation points increases, the response of the system changes, and get stabilized for the configurations C, D and E. Furthermore, as we increase the number of total collocation points, the CPU time increases having 28, 37, 46, 58 and 99 seconds for each corresponding discretization arrangement. Considering the CPU time, and the response of the system for each arrangement we will use the discretization arrangement C for all the forthcoming dynamic analysis.

3.2.3.2 Dynamic response of the distribution system

As stated in equation (2-10) the producer mass flow is fixed to its computed steady-state value (Table 3-2) for the dynamic simulations. Figure 3-8 details the temperature profile at the outlet of consumers 1 and 11, for both insulated and non-insulated pipes. We chose to detail these consumers because of their high demand and to evidence the impact of the distance to the producer site. The CPU times

reported for the solution of the dynamic simulation problem were 56.7s for the system with insulated pipes and 46.8s for the network without insulation.

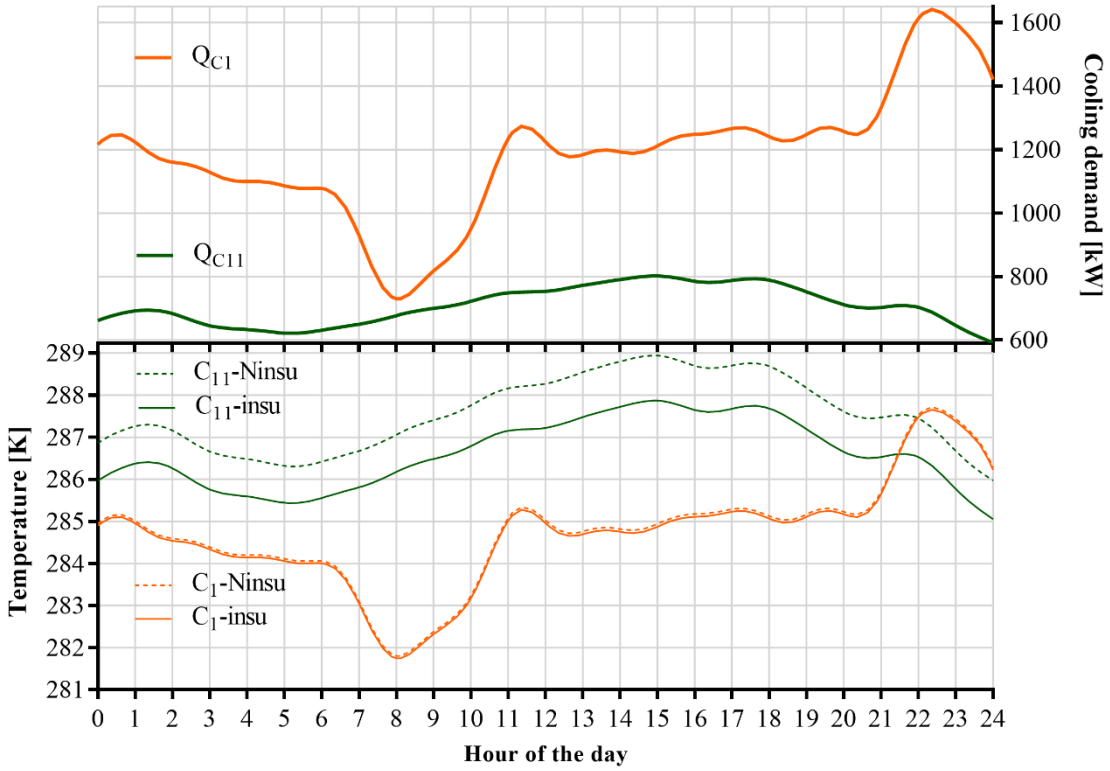

Figure 3-8. Outlet temperature in consumers 1 and 11 for constant flow policy under KL conditions

Using the constant flow policy, the outlet temperature of the consumers will vary over time following the path of the corresponding demand. The presented temperature profiles show that the influence of the insulation has more relevance as the fluid moves further from the production site, evidenced by the bigger differences in the temperature profiles for client C_{11} located at 3219m from the producer. Nevertheless, as stated in the steady-state analysis, the heat gains are related also to the level of demand of the consumers and consequently with the amount of chilled water flowing in the pipes. This is clearer if we do the same observation at the outlet pipes of consumers 13 and 20 (Figure 3-9). Each of them is the furthest consumer on each side of the network and present important differences in their levels of cooling demand.

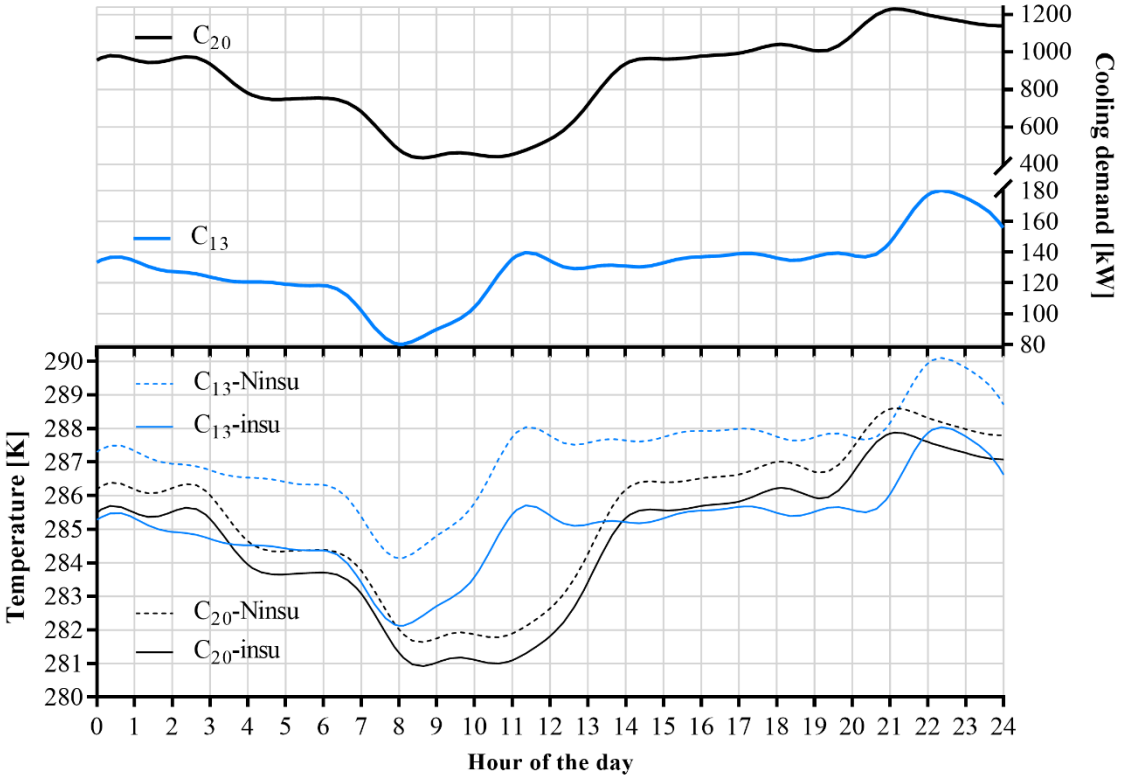

Figure 3-9. Outlet temperature in consumers 13 and 20 for constant flow policy under KL conditions

These results show the capacity of the method to accurately represent the dynamics of district cooling systems with low computational time, with potential application for the consumption forecast of these systems.

The presented variations in the outlet pipes of the users result in a non-uniform return temperature to the production site as shown in Figure 3-10. For both insulated and non-insulated pipes, the return temperature $\left(T_{0_r}\left(t, L_{0_r}\right)\right)$ is influenced by the total demand profile. These profiles exhibit a lag time compared to the profile of the total demand. This lag time represents the interval of time it takes to the fluid leaving each user to arrive at the production site. These variations in the return temperature represent a technical issue in the production site due to the need to stay close to the design temperature for the production of the cold utility [89]. Furthermore, the operation under this flow policy drives the system to low values of $\Delta T\left(T_{0_r}\left(t, L_{0_r}\right) - T_0(t, 0)\right)$ in the production site, as low as 6.28K (283.28K-277K), that affects the efficiency of the system.

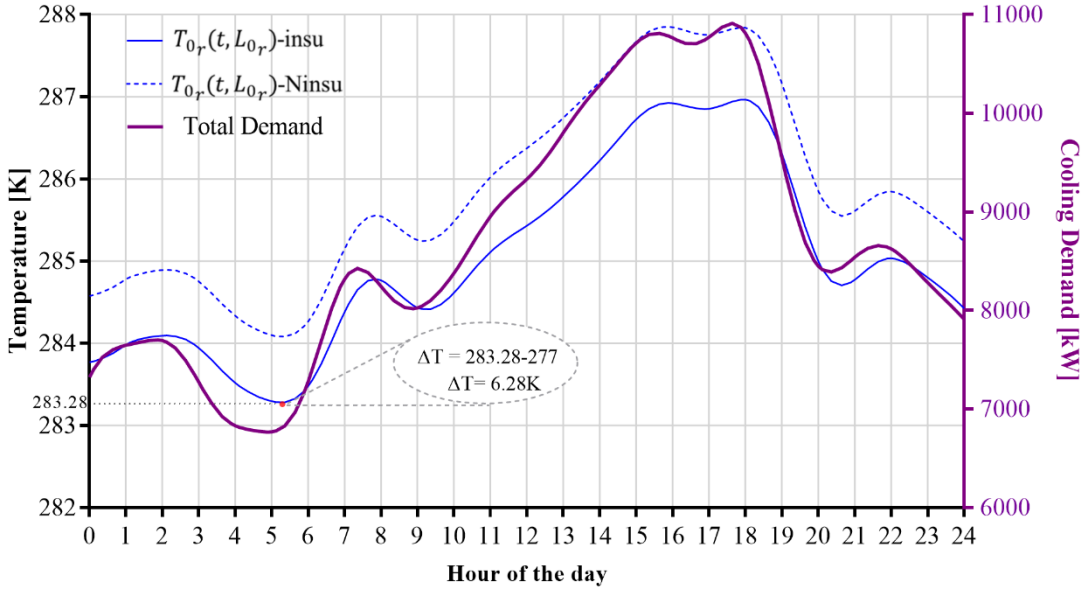

Figure 3-10. Return temperature under constant flow policy for KL conditions

The presented solution of the dynamic simulation problem will be used as the initial guess for the optimization problems, that will be formulated and detailed in the next section.

3.3 Conclusions of the simulation analysis

This chapter detailed the methodology of solution for the dynamic simulation of the proposed district cooling system. The procedure included the solution of steady-state simulations, that enabled us to compute the pipe diameters of the distribution network, and a proper initialization for the dynamic simulation problem.

The methodology was implemented to study the dynamic response of the system when operating under a constant flow policy, using insulated both and non-insulated pipes. This implementation resulted in reliable results with a low CPU time using a regular laptop computer.

The use of a constant flow policy resulted in variations in the temperatures of the pipes leaving the clients and consequently in the return network. These variations affect the efficiency of the production site and result also in economical penalties for the users. This latter because the users would have to invest in additional equipment to regulate the temperature leaving the substation before pumping it to the return network at a mora adequate temperature. Aiming to prevent this issue, the next chapter introduces an operational optimization that enables to operate the distribution system without major variations of temperature in the return network. This optimization will use the results of the presented dynamic simulation as initialization for its solution.

Chapter 4. Dynamic Optimization Analysis

As stated in 3.1, the solution of the dynamic simulation (Section 3.2), serves as initialization of the dynamic optimization problem, whose results are detailed here in Chapter 4. The analysis is made for two different objective functions. The first one, detailed in section 4.1, aims to control the temperature of the cooling utility leaving the consumers avoiding undesirable levels of temperature returning to the production site. The analysis considers the use of different manipulated variables. Including the level of temperature leaving the consumers as constraints, Section 4.2 details an operation cost objective function, that considers the cost of producing the cold utility and the electrical power demanded by a pump sending the chilled water to the network. In addition to the optimal operation profiles, this objective function computes the optimal diameters of the pipes to minimize the proposed cost function.

Chapter Contents

4.1 Objective function: Avoiding low ΔT syndrome

The efficiency of a district cooling is measured in terms of the difference between the temperature of the fluid leaving the production and the temperature of the fluid that returns to it (*ΔT)*. Generally, maintaining a high *ΔT* reduces the flow rates of the chilled water system and the costs of the distribution system due to the use of smaller pipe diameters. This results in savings in pumping energy costs and improves operating costs [24]. Typically *ΔT* in the production site for DCS is maintained around 8-12°C [25], [26]. When the *ΔT* is not properly controlled, the system might present an important issue known as "*low ΔT syndrome*" in DCS [24], that must be handled at the consumer location [25].

Frequently, the contract between the district cooling provider and the consumer dictates a minimum chilled water return temperature back from the consumer and a modulating valve (ΔT valve) is installed on the consumer return line that will close if the water returns colder than that stipulated temperature. While marginally effective, the ΔT control valve does not correct or cure the actual cause of low return water temperature. Another option to improve the performance is the inclusion of a heat pump at the buildings that would further increase the return temperature by discarding heat into the return line. Nevertheless, this option requires more equipment investment and do not solve the cause of the problem[80].

To optimize the *ΔT* and meet the consumer's demands, both the flow from the central plant and flow in the consumer's side must be varied [25]. These variations represent also savings in the pumping energy. It is possible to represent this complete dynamic flow policy of the system, as shown in Figure 4-1. This operating policy eliminates the use of the common pipe presented for the constant flow policy (Figure 2-5) and with this the mixing and an eventual reduction of the temperature in the return network.

The stated variations in temperature represent not only a technical issue but also an economic impact on the consumer. Indeed the consumer will be charged by 3% for each degree Celsius of the monthly average return temperature below the system design return temperature [24]. On the other hand, it is important to avoid high temperatures that might compromise the proper operation of the production site technology.

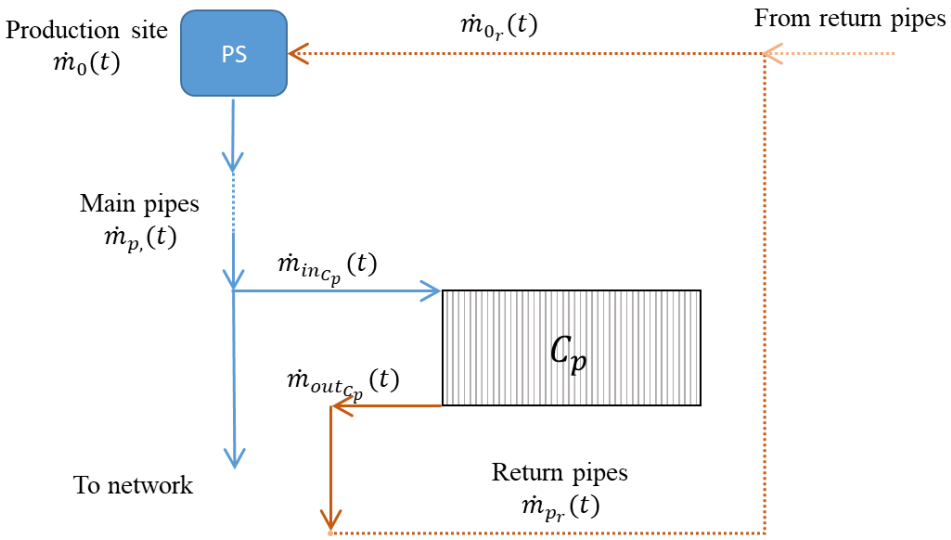

Figure 4-1. Dynamic flow policy diagram

Considering this, we define J as the quadratic error between the outlet temperature of the users and a set point. This objective function enables to simulate the current way the cooling networks are operated, where the provider imposes to each consumer a return temperature.

First, we analyse the system under a constant flow policy, and for this purpose, we perform the following optimization of the dynamic problem, for a design outlet temperature of 287K.

$$\min_{\substack{\dot{m}_{0Cte} \\ Var}} \sum_{p} \left(\int_0^{24} \left(T_{outC_p}(t) - 287 \right)^2 dt \right) \tag{4-1}$$

$$S.t. \text{ (2-1) to (2-11)}$$

Since a constant flow policy is implemented, equation(2-10) is embedded in the set of the model equations, as well as equation(2-11), which imposes that the ratios of the splitters are constant. Therefore, in this optimization, the only control variable is the value of the constant flow leaving the producer $\dot{m}_{0Cte}$. Var stands for all the other variables of the problem ($T(t,x), \dot{m}_k(,t), \ldots$) whose optimal paths minimize the difference between the consumers' outlet temperature and the proposed design temperature over time. The flow variables $\dot{m}_k(t)$ are treated as algebraic variables.

Then we perform the optimization of the dynamic problem (4-2) where none of the constant flow policy equations (2-10) and (2-11) are considered in the model. Then, the mass flow of the producer and the ratios of the splitters are time-dependent and will be the main control variables.

$$\min_{\substack{\dot{m}_{inC_p}(t)\\ Var}} \sum_p \left(\int_0^{24} \left(T_{outC_p}(t) - 287 \right)^2 dt \right) \quad (4\text{-}2)$$

$$S.t. \text{ (2-1) to (2-9)}$$

4.1.1 Dynamic optimization under constant flow policy

The DO problem stated in equation (4-1) (DO1) aims to evaluate the potential of the constant flow policy to maintain the system under the desired conditions of operation. For this problem, the only control variable is the constant flow of the production site.

In terms of CPU time, the solution of problem (4-1) implied 70s and 58s for insulated and non-insulated pipes respectively. For insulated pipes, the optimal producer mass flow is 228.36[kg/s] while for the non-insulated system it is 248.40[kg/s], which represents an increment of 8.7% in the quantity of chilled water produced for the non-insulated system. Table 4-1 compares the mass flow of the production site and those entering each client for dynamic simulation and DO1.

Table 4-1. Comparison of production and inlet clients mass flows

$\dot{m}_p[kg/s]$	Dynamic simulation	Dynamic Optimization	
	Insulated pipes	insulated pipes	Non-insulated pipes
$\dot{m}_0$	263.60	228.36	248.40
$\dot{m}_{inC_1}$	36.68	31.78	34.57
$\dot{m}_{inC_2}$	15.66	13.56	14.75
$\dot{m}_{inC_3}$	4.47	3.88	4.22
$\dot{m}_{inC_4}$	17.45	15.11	16.44
$\dot{m}_{inC_5}$	2.24	1.94	2.11
$\dot{m}_{inC_6}$	20.13	17.44	18.97
$\dot{m}_{inC_7}$	2.24	1.94	2.11
$\dot{m}_{inC_8}$	5.59	4.84	5.27
$\dot{m}_{inC_9}$	8.95	7.75	8.43
$\dot{m}_{inC_{10}}$	3.80	3.29	3.58
$\dot{m}_{inC_{11}}$	17.89	15.50	16.86
$\dot{m}_{inC_{12}}$	2.24	1.94	2.11
$\dot{m}_{inC_{13}}$	4.03	3.49	3.79
$\dot{m}_{inC_{14}}$	33.55	29.07	31.62
$\dot{m}_{inC_{15}}$	14.54	12.60	13.70
$\dot{m}_{inC_{16}}$	8.50	7.36	8.01
$\dot{m}_{inC_{17}}$	10.18	8.82	9.59

$\dot{m}_p[kg/s]$	Dynamic simulation	Dynamic Optimization	
	Insulated pipes	insulated pipes	Non-insulated pipes
$\dot{m}_{inC_{18}}$	20.13	17.44	18.97
$\dot{m}_{inC_{19}}$	8.05	6.98	7.59
$\dot{m}_{inC_{20}}$	27.29	23.64	25.71

Even using non-insulated pipes, via dynamic optimization the system operates using less amount of cooling utility than in the simulation results. Although this operation results in a higher minimum ΔT (7.25K) compared with the simulation results (6.28 K as seen in Figure 3-10), the return temperature still presents variations, as seen in Figure 4-2, which would compromise the operation of the central cooling plant [89].

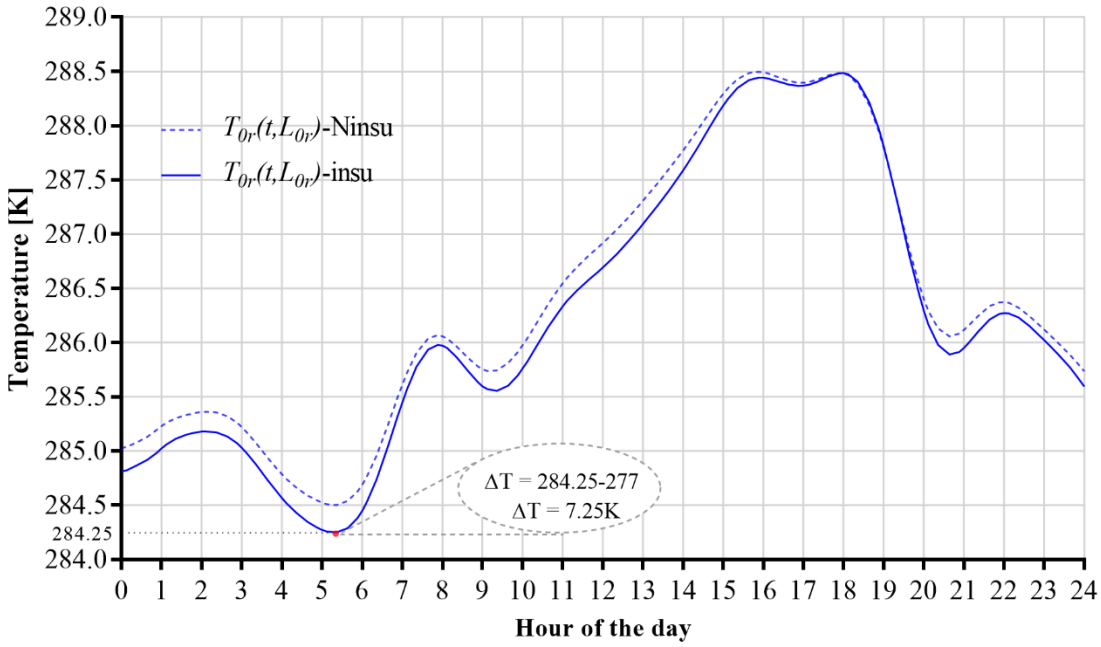

Figure 4-2. Return temperature profiles under for DO-1

As done for the simulation analysis, Figure 4-3 presents the behaviour of the consumers C_1 and C_{11}, for both insulated and non-insulated pipes in, evidencing a particular tendency of the outlet temperature of the consumers as they are located further from the production site.

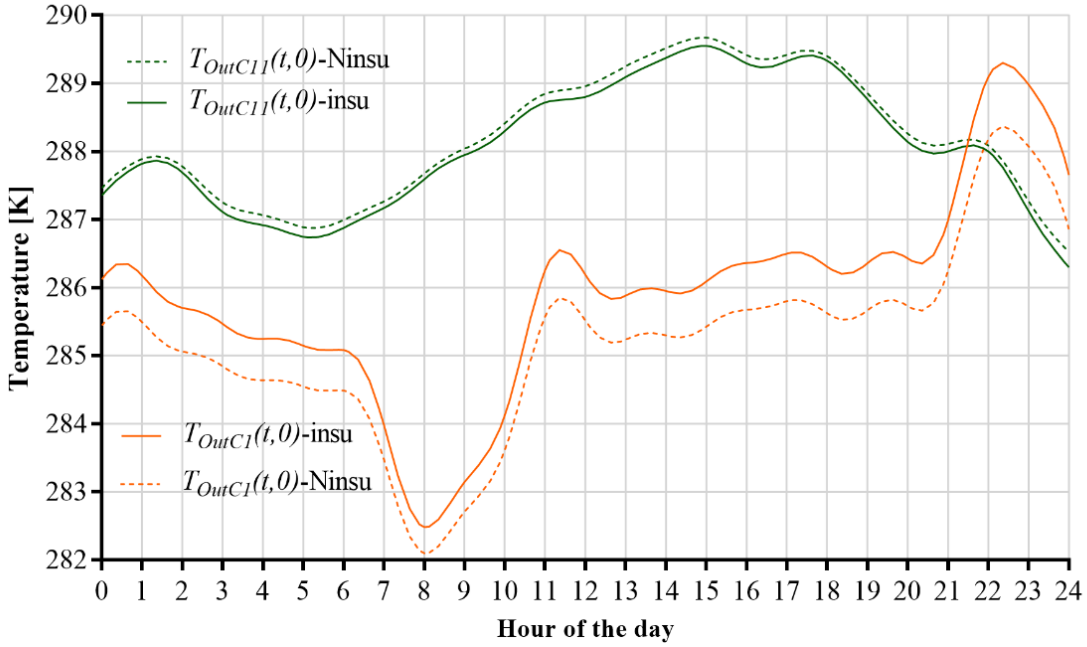

Figure 4-3. Outlet temperature profiles in consumers 1 and 11 for DO-1

At consumer C_{11} the outlet temperature level is higher when using non-insulated pipes. On the other hand, under the same conditions, consumer C_1 presents a lower level in the outlet temperature. This is due to the influence of the distance on the inlet temperature of each consumer, and the bigger mass flows in the non-insulated systems. Figure 4-4 details the inlet temperature profiles for consumers C_1 and C_{11}, located at 370 and 3219 meters from the producer respectively.

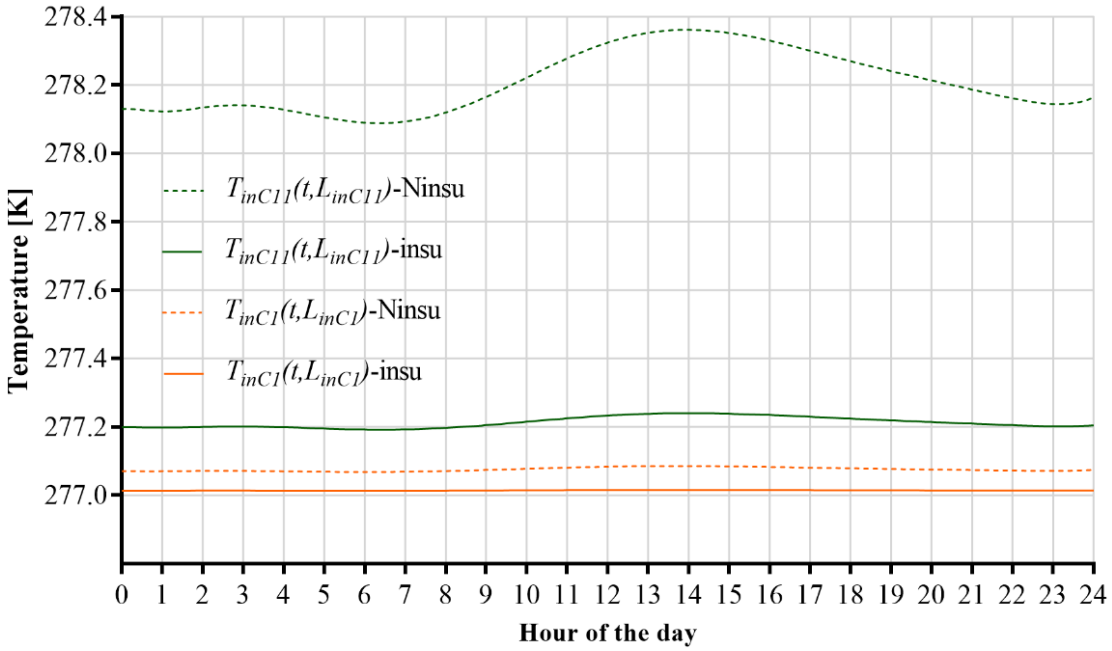

Figure 4-4. Inlet Temperature profile for selected consumers under constant flow

As mentioned in section 3.2, here in the dynamic analysis we can evidence the importance of computing the spatial thermal variation, and its influence in the operational conditions of the system. The difference in the values of the outlet temperature for C_1 when changing the kind of piping (insulated or non-insulated), ranges from 0.05 to 0.06 K, while for C_{11} this difference goes from 0.89 to 1.20 K. Therefore, C_1 is operating at almost the same level of temperature in the two cases, but due to the increment of the inlet mass flow to the consumer (31.78 [Kg/s] to 34.57[kg/s]), given its location from the production site, the outlet temperature results lower when using non-insulated pipes. This phenomenon was observed also in consumers C_2, C_3, C_4, C_{14}, C_{15} and C_{16}, as detailed in Figure 4-5 for consumers C_4 and C_{16} located at 1446m and 892m from the production site respectively.

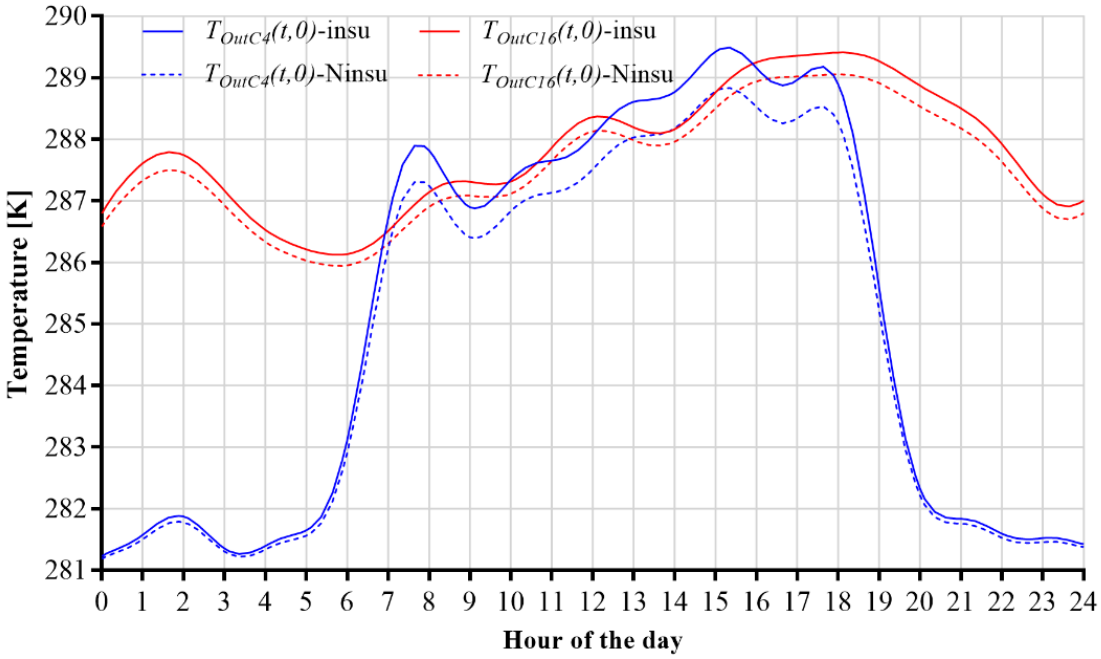

Figure 4-5. Return Temperatures for consumers C_4 and C_{16}

The persistent low ΔT syndrome shows that working at constant flow policy prevents the system from working under the desired parameters. Although the return temperature is warmer, its variation due to the demand profiles in the consumers precludes proper operation of the cooling network.

4.1.2 Dynamic optimization using variable mass flows

On the other hand, the implementation of a dynamic flow policy, as stated in the optimization problem presented in (4-2) (DO2), the system will operate with more uniform return temperatures, using insulated and non-insulated pipes as detailed in Figure 4-6.

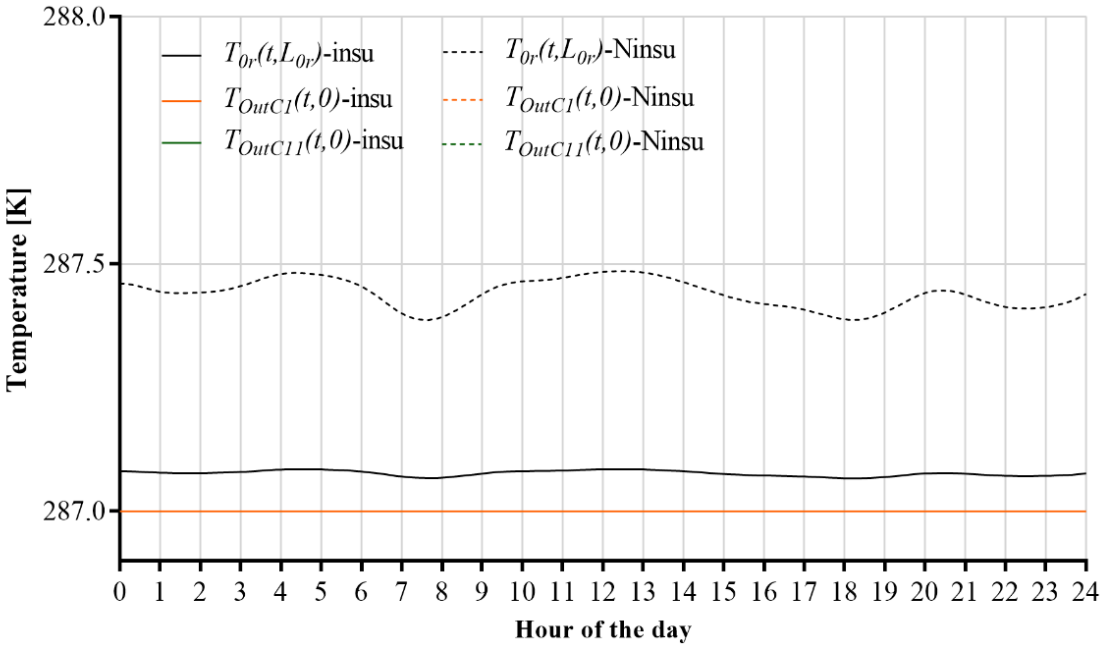

Figure 4-6. Temperature profiles for dynamic flow policy

Solving this problem took 517[s] and 334[s] for insulated and non-insulated pipes respectively. It is important to remark that this problem has a total of 2880 degrees of freedom (compared to only one for the problem (4-1)), which corresponds to the value of the 20 inlet mass flows in the 144 collocation points in time.

As expected, the return pipe of the insulated network presents a lower temperature than the non-insulated one. Nevertheless, for this latter, we increased the value of the upper bound of v_{max_k} by 0.3 m/s, because with the initial considered values of v_{max_k} and the consequent mass flows it was not possible to achieve the desired outlet temperature in all the consumers (8 to 13 and 20). This relaxation of bounds implied to trespass the original values of v_{max_k} in certain pipes as detailed in Figure 4-7. Although the velocity trespasses are small (the biggest is 0.24[m/s] for pipes 13 and 13_r) they should imply to change the corresponding pipe nominal diameters to implement a system without insulation. Indeed, contrary to Branan [83], the American Society of Heating, Refrigerating and Air-Conditioning Engineers (ASHRAE)[90], [91] does not report a maximum allowable velocity depending on the pipe nominal size, and indicates that in any case (application, size or material) the velocity in the pipes cannot exceed 4.6 m/s. As detailed in Figure 4-7, none of these pipes reports values higher than 2m/s. Then, although in these cases the original maximal velocities have trespassed, the computed solution leads to reliable operation.

This shows the lack of precision when using an approximation without heat losses to define the diameters of the pipes, and the interest of including the pipe diameter as a variable of optimization. This analysis will be detailed in the next section.

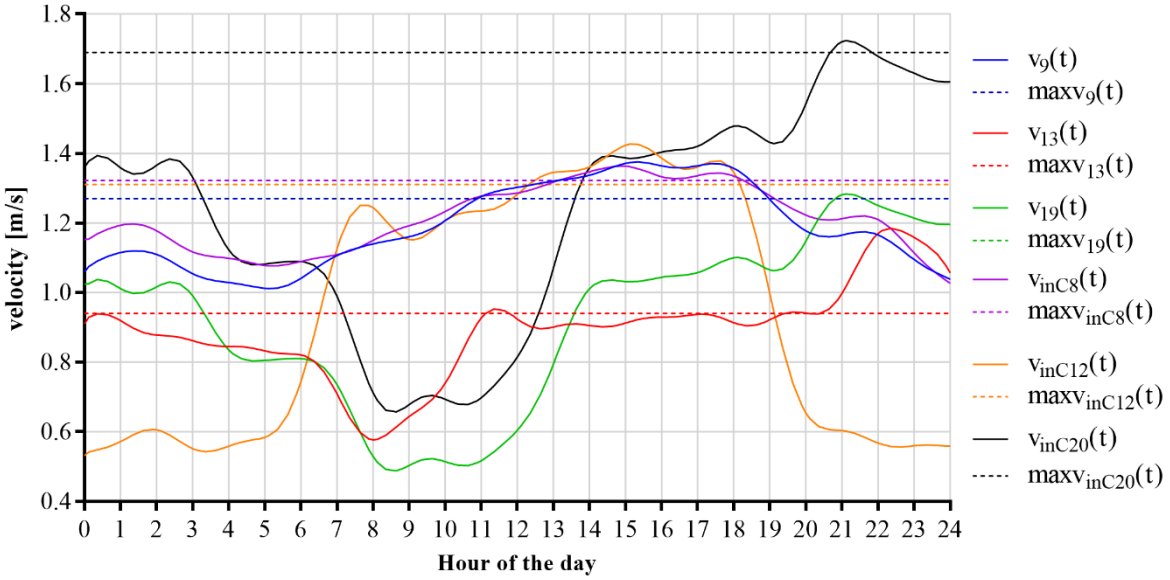

Figure 4-7. Velocity profiles of the pipes trespassing upper bounds

For the analysis of mass flows in DO2 solution, Figure 4-8 presents the optimal inlet mass flows for consumers C_1 and C_{11} as well as for the production site. The computed mass flows consider the heat gains along the pipes to accomplish the fluctuating demand of the consumers, reducing the variation of the outlet temperature on each consumer and with this, the uncontrolled deviation of the return temperature.

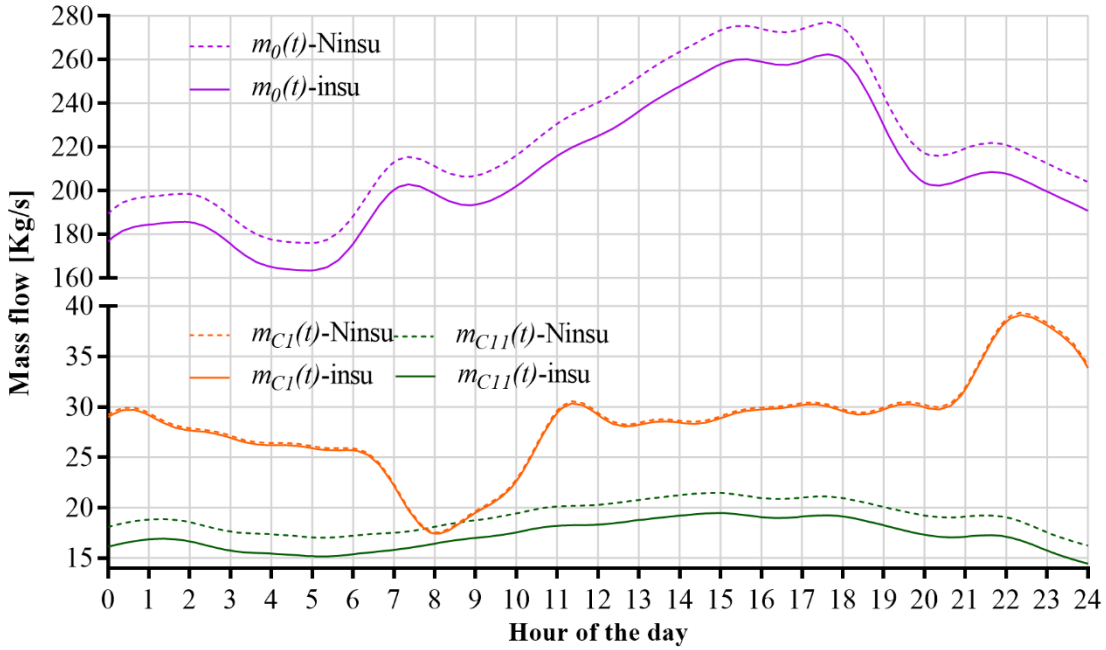

Figure 4-8. Optimal production and inlet mass flow for chosen consumers

The non-insulated system requires more cold water. However, due to the heat gains depending on the distance of the consumers from the production site, this difference is not proportional between all the users as seen when comparing the profiles of C_{11} (3219 m from production) and C_1 (370 m from production).

Furthermore, it is possible to compute the total production required per day using the presented pumping methodologies for the two kinds of piping as $\int_0^{24} \dot{m}_0(t)dt$. Indeed, comparing the energy produced does not give enough information to choose between the flow policies. We present these results in Table 4-2.

Table 4-2. Total chilled water production for the studied pumping methods

	DS	DO1-insu	DO1-Ninsu	DO2-insu	DO2-Ninsu
Total production [Ton]	22775	19734	21463	18141	19262
Energy in PS [MWh]	213.30	213.11	235.51	213.36	235.51

The use of insulation in the two flow policies leads to the same reduction in energy production (9.5%), whereas the insulation leads to a reduction of 8.06% in the production of cold water using the constant flow policy (DO1) and 5.8% using the dynamic flow policy (DO2). However, it is important to point out that the optimal dynamic flow policy (DO2), represents a reduction of 8.07% (insulated) and 10.25% (non-insulated) compared with the computed productions using an optimal constant flow (DO1). Even using non-insulated pipes in DO2, the production of water is lower than in DO1 with insulated pipes. Moreover, the system operates at the desired levels of temperature only if a complete dynamic policy is used.

To finish, Figure 4-9 compares the power of the production site (*Pw(t)*) for the two policies of flow for the two kinds of pipes with the total demand of the system.

From the presented profiles, it is possible to evidence that using the dynamic flow policy, at each instant the producer responds better to the total demand of the system while avoiding the low ΔT syndrome, allowing a more efficient operation at the production site. On the other hand, when operating with a constant flow policy, the power of the producer is affected by the variation of the temperature of return resulting in a delayed profile compared with the total demand. Furthermore, at each consumer, the demand is satisfied for the two policies but only using a dynamic flow policy is possible to operate under the desired level of temperature in the return network.

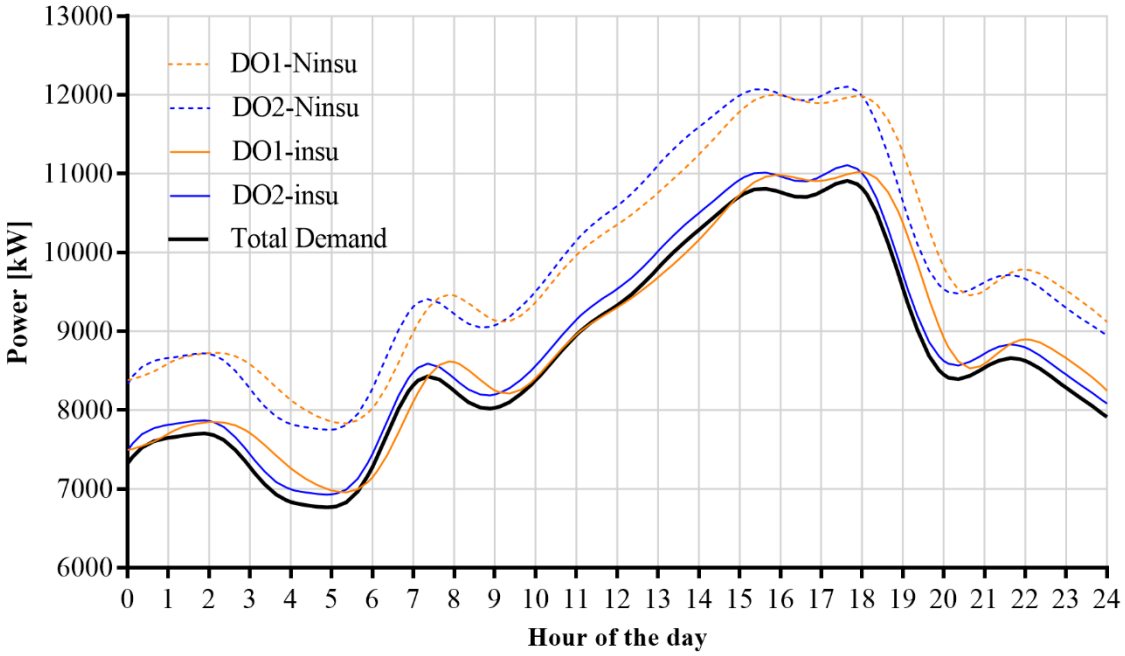

Figure 4-9. Production site power comparison

Although the computed dynamic policy results in proper operation of the distribution system, it is important to highlight that to implement the proposed methodology for the development of a forecasting operation tool, it is necessary to have access to proper predictions (or models) of the cooling demands of the consumers.

Considering the need for a better estimation of the pipe diameters of the cooling network and looking for a better evaluation of the operational cost of the system with insulated and non-insulated pipes, in the next section we detail an economic objective function. The problem will consider the cost of producing cold and the pumping cost for distribution systems with and without insulation. The system will operate under the same conditions of DO2. This will also show the ability of the methodology to be implemented in the design stages of cooling distributed systems.

4.2 Objective function: Operational cost

This section details the analysis of an operating cost objective function that considers the cost of producing the cold utility and the electrical power demanded by a pump sending the chilled water to the network. The analysis will include the diameter of the pipes as variables of decisions (continuous), affecting the behaviour of the pressure drops in the network and therefore the size of the pump that should be installed at the production site.

4.2.1 Formulation

We already can compute the power in the production site ($Pw(t)$). Nevertheless, to calculate the pump it is necessary to characterise the influence of the change of diameters in the flow regime in the pipes during the 24h time horizon. This requires defining a dynamic thermal resistance in the pipes ($R'_k\ (t)$). When the flow regime is defined, we introduce the calculation of the pressure drops in the systems that will allow computing the work of the pump that should be installed. Finally, we present the costs of electricity and chilled water to complete all the elements of the objective function.

4.2.1.1 Dynamic pipe resistance

The variation of the diameter has an influence on the value of the thermal resistance of the pipes that is a function of the flow regime as detailed in equations (1-2) to (1-7). On the other hand, the operational analyses presented in the previous sections were performed for a constant thermal resistance per pipe, computed for an average mass flow in the pipes computed after the solution of the model without heat loses as detailed in section 3.2. Then, in order to consider the influence of the flow regime in the economic analysis, we will compute the thermal resistance of each pipe over time $R'(t)$, based on the approximation presented in Section 1.3 ((1-2) to (1-7)) as:

$$R'_k(t) = \frac{1}{\pi D_{a_k} \overline{h_k}(t)} + \frac{\ln\left(\frac{2r_{b_k}}{D_{a_k}}\right)}{2\pi k_{ab}} + \frac{\ln\left(\frac{r_{c_k}}{r_{b_k}}\right)}{2\pi k_{bc}} + \frac{\ln\left(\frac{r_{d_k}}{r_{c_k}}\right)}{2\pi k_{cd}} + \frac{1}{Sk_s} \tag{4-3}$$

This, demands the redefinition of the average convective heat transfer $\bar{h}$, and the dimensionless relationships of Nusselt and Reynolds on each pipe as dynamic variables by:

$$\bar{h}_k(t) = \frac{\overline{Nu}_k(t) k_w}{D_{a_k}} \tag{4-4}$$

Assuming that the system operates always under a turbulent regime ($Re\_k\ (t) \geq 9000$) we can use the correlation of Dittus-Boelter (4-5) as:

$$\overline{Nu}_k(t) = 0.023(Re_k(t))^{\frac{4}{5}}(\mathrm{Pr}_k)^{0.4} \quad (4\text{-}5)$$

$$Re_k(t) = \frac{\rho_w v_k(t) \cdot D_{a_k}}{\mu_w} \quad (4\text{-}6)$$

As stated in section 2.2, it is important to limit the velocities of the flow inside the pipes in order to operate under common heuristic values. For this part of the study, we will relax the variable representing the internal diameter as continuous. Thus, in this section, we present the results with respect to the internal diameter instead of the nominal one. Considering that it is possible to represent the maximum allowable velocity (v_{max_k}) as a linear function of the internal diameter, for both the main and the lateral pipes. To do this, we consider the maximum velocity values reported by Branan[83] for nominal diameters (detailed in table 9-2) and the internal diameters for the corresponding nominal diameters reported in Annex A, as presented in Figure 4-10.

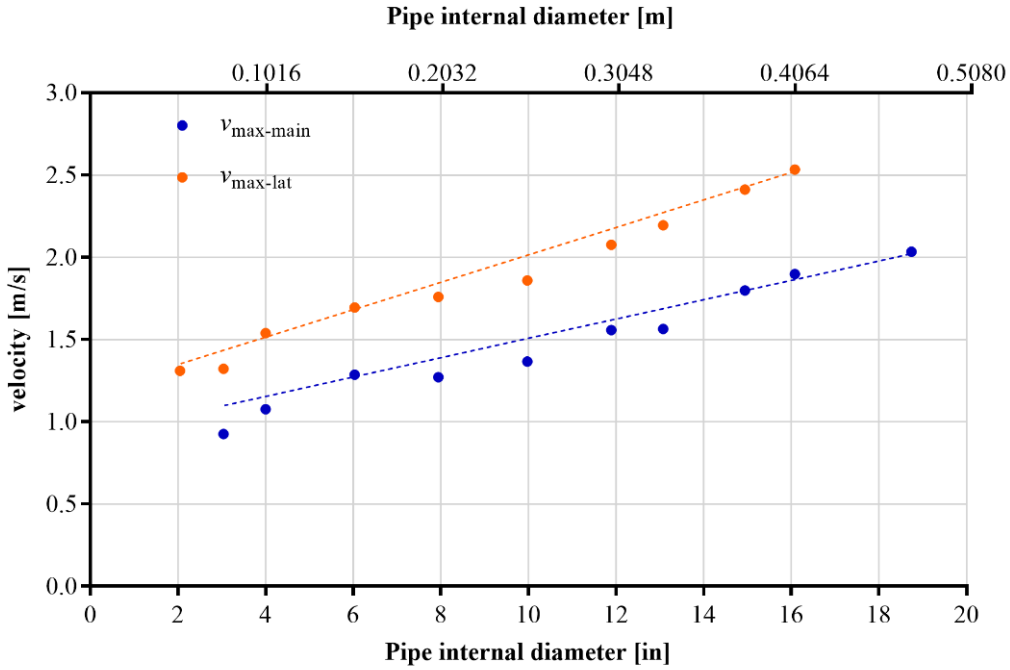

Figure 4-10. Definition of the maximum velocity per pipe diameter size

This will allow us to maintain the system under proper hydraulic conditions, for any internal diameter size.

Furthermore, it is necessary to define how the size of the corresponding layers covering the pipes will vary as the diameter changes. Revising the elements of equation (4-3) and moving outer in the diagram presented in Figure 1-9, we include the pipe wall thickness ($wall_k$) to have the external diameter of

the pipes $\left(r_{b_k} = \frac{D_{a_k}}{2} + wall_k\right)$. The wall thickness can be represented as a function of the internal diameter (D_{a_k}), based on the available data for PVC schedule 40 pipes [92] presented in Figure 4-11. These pipes ensure the operation to pressures as high as 8.2 bar for a nominal diameter of 24 inches, and higher pressure for smaller pipe diameters.

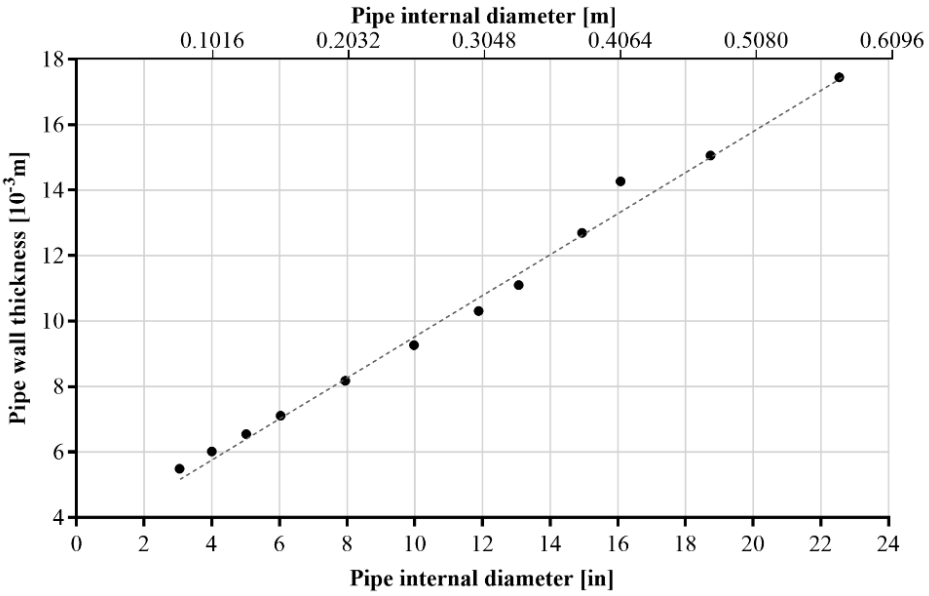

Figure 4-11. Variation of the pipe wall thickness respect to the internal diameter

Then, we have the layer of insulation $\left(r_{c_k} = r_{b_k} + insu_k\right)$ which is 1.5 inches for diameters greater than 8 inches and 1 inch for the other diameters, according to the North American Insulation Manufacturers Association [88]. In order to avoid numerical difficulties due to non-continuity of the insulation thickness, we use a sigmoid to represent continuous, even stiff, its variation, as shown in Figure 4-12.

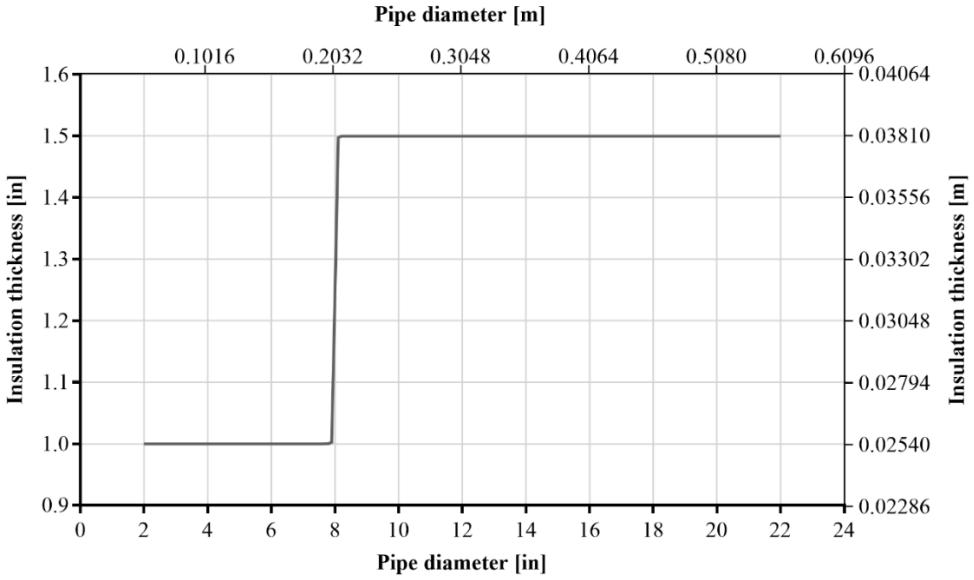

Figure 4-12: Variation of the insulation thickness as a function of the internal diameter

To finish, we have the casing that is assumed to have the same thickness of 3mm for all the pipes ($r_d = r_c + 0.003$). With the presented redefinition of the pipe characteristics and hydraulics, it is possible to compute the variation of the thermal resistance of the pipes by using equation (4-3).

4.2.1.2 Pressure drops and the work of the pump

To compute the work of the pump, it is necessary to know first the pressure drops due to friction in the pipes. This can be done as proposed by Mertz *et al.* [93] and Marty *et al.* [94] by using the Darcy - Weisbach equation, having on each pipe:

$$\Delta P_k(t) = \lambda_k(t) \cdot \frac{L_k}{D_{a_k}} \cdot \rho_w \cdot \frac{\left(v_k(t)\right)^2}{2} \tag{4-7}$$

Here, D_{a_k} represents the internal diameter of the pipe and $\lambda_k(t)$ is the coefficient of friction, which can be represented by the following Blasius correlation assuming smooth pipe and Reynolds number smaller than 100000:

$$\lambda_k(t) = [100.Re_k(t)]^{-0.25} \tag{4-8}$$

With this, we can compute the total pressure drop on each main branch (Left or Right) of the network. We assume that the total pressure is the sum of the linear ($\Delta P_k(t)$) and singular pressure, where the latter represents 30% of the total pressure drops as proposed by Mertz *et al.* [93] and Marty *et al.* [94] having:

$$\begin{aligned} \Delta PL(t) &= \frac{1}{0.7}\sum_{kL} \Delta P_{kL}(t), \quad kL = \{0,1,\dots,13,0_r,1_r,\dots,13_r,in_{13},out_{13}\} \\ \Delta PR(t) &= \frac{1}{0.7}\sum_{kR} \Delta P_{kR}(t), \quad kR = \{0,14,\dots,20,0_r,14_r,\dots,20_r,in_{20},out_{20}\} \end{aligned} \tag{4-9}$$

We consider the pressure drops of the two branches to compute the total mechanical work of pumping as:

$$W_{pump}(t) = \frac{1}{\rho_w}\left(\Delta PL(t) \cdot \dot{m}_1(t) + \Delta PR(t) \cdot \dot{m}_{14}(t)\right) \tag{4-10}$$

The configuration of the systems (Left branch is longer and serves more consumers) suggest that one of the branches will present less pressure drop. Then, on this latter is necessary to add a valve before the mixing node with the other branch in order to equilibrate the pressure of the two branches before returning to the production site.

Considering this, it is possible to compute the electrical power demanded by the pump as:

$$Pw_{pump}(t) = \frac{1}{\eta_{pump}} \cdot W_{pump}(t) \tag{4-11}$$

Here η_{pump} represents the total efficiency of the pump (which includes mechanical, transmission and motor efficiencies) and is assumed to a value of 70%.

For this analysis we consider that the system will operate using variable mass flows, and maintaining a constant temperature leaving the clients as in the solution of the problem DO2, considering that each consumer must respect a contractual outlet temperature. This latter condition is included as new constraints, while the internal diameters of the pipes, that were parameters in the previous problems, will be considered as decision variables. These latter will be bounded at a maximum value of 22.54 inches (0.57m) that corresponds to a nominal diameter of 24 inches based on the commercial availability of PVC pipes for district cooling purposes.

$$T_{outC_p}(t) = 287 \tag{4-12}$$

$$D_{a_k} \leq 0.57 \tag{4-13}$$

4.2.1.3 Objective function: Minimize the Operational cost.

The objective function considers the total cost of production and the cost of pumping the produced utility to the distribution system during the studied time horizon. We represent this cost function as:

$$\min_{\substack{D_{a_k} \\ Var}} C_{elec} \cdot \int_0^{24} Pw_{pump}(t)dt + C_{cold} \cdot \int_0^{24} Pw(t)dt \tag{4-14}$$

$$S.t. \text{ (2-1) to (2-9) and (4-3) to (4-13)}$$

Here C_{elec} represent the cost of electricity (0.153€/kWh, in France [95]) and C_{cold} represents the cost of producing cooling power. For this latter, we will compare two different values aiming to represent the cost of production using different technologies (for example mechanical compression vs Free cooling). These values are based on the data presented by the French federation of energy services and environment (FEDENE)[96] ($C_{cold1} = 0.1402$ €/kWh) and Turton[97] ($C_{cold2} = 0.01511$ €/kWh). Considering that the system is conceived to supply a given value of demand, and the fact that the system does not have an energy storage technology, the objective function aims to reduce the cost of

operation to provide the demand of the network. The first term of the objective function reduces the electrical consumption of the pump by optimizing the pressure drops. The second term is added to reduce the production of cold by optimizing its distribution to the consumers to reduce the heat gains of the cold water throughtout the distribution system. This objective function will allow us to obtain a compromise between the heat gains and the pressure drops for the computed internal diameters.

4.2.2 Initialization strategy

The solution of the problem DO2 will used initialization of the new optimization problem DO3 following the procedure detailed in Figure 4-13.

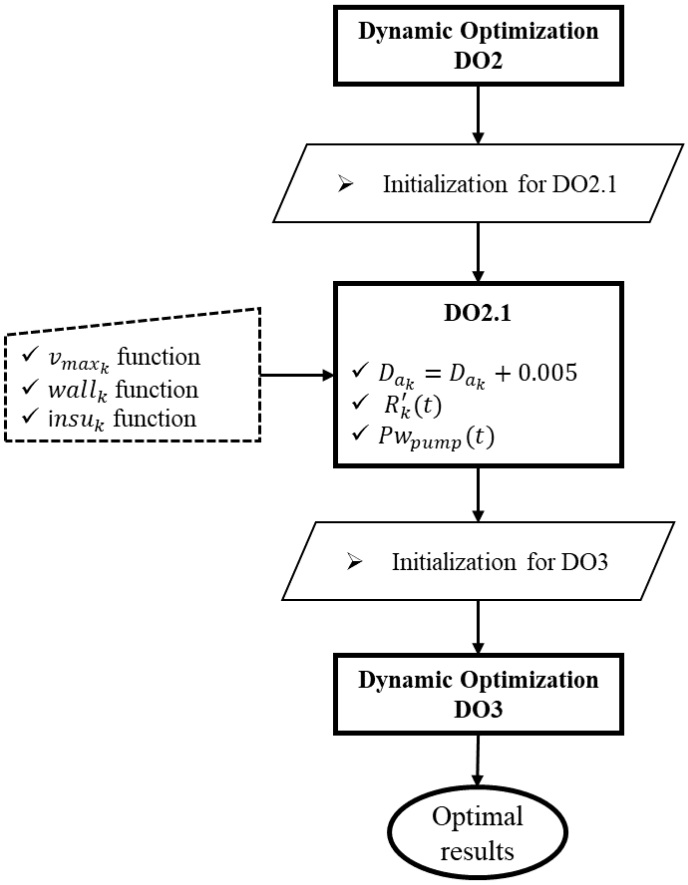

Figure 4-13. Procedure for the solution of the cost optimization

The solution of the optimization DO2 is used as initialization for the solution of an intermediate problem DO2.1. Here, the diameters are fixed but we include the value of the variables defined in equations (4-4) to (4-11) necessary to define the dynamic thermal resistance per pipe $R'_k(t)$, as well

as the new definitions of the maximum velocities, the pipe wall and the insulation thicknesses. This problem has the same objective function of avoiding the low ΔT syndrome as in DO2. The implementation of the dynamic thermal resistances will result in a dynamic profile of the mass flows and consequently of the flow velocities in the pipes. However, as seen in section 4.1 using fixed diameters, sometimes the upper bound of the velocity had to be raised to achieve the desired outlet temperature. So in order to avoid this kind of problem, the pipe diameters are 5 mm larger than the ones presented in section 3.2. Finally, the solution of this intermediate problem will then be used as initialization to solve the Dynamic optimization DO3. As we did for the previous optimization, we use CONOPT as non-linear solver.

4.2.3 Results and discussion

The results of this section include the evaluation of the dynamic thermal resistance for the two kinds of piping, the pressure drops profiles and the analysis of the computed pipe diameters for the proposed costs of production.

4.2.3.1 Evaluation of the new dynamic variables

Following the methodology described in Figure 4-13, we present first the evaluation of the thermal resistance of the pipes and the pressure drops in the intermediate problem DO2.1, used to initialize the definitive operational cost optimization problem. The solution of this problem took 320 seconds for the system using insulated pipes and 690 seconds for the non-insulated network.

Figure 4-14 details the profiles of the thermal resistance, $R'_k(t)$, for the production pipe and the furthest main pipes on each branch of the network with and without insulation. For each kind of piping, it is possible to evidence that the thermal resistance increases as the diameter of the pipes decrease following the same general tendency than the constant thermal resistances reported in section 3.2. As a reminder, the diameter of pipe 13 is the smallest and the diameter of pipe 0 is the biggest. When looking in detail the profiles of Figure 4-14 it is possible to evidence that the difference of diameter has a major impact in the level of the thermal resistance for the non-insulated pipes (in the upper part of this figure the scale is not the same as in the lower one). In the case of insulated pipes, the value of the thermal resistance depends strongly on the inclusion of the insulation layer, the relative variations due to the size of the pipe are less representative for these pipes than for the non-insulated ones. However, these variations present a similar behaviour as can be seen when comparing Figure 4-15 and Figure 4-16 for pipe 13.

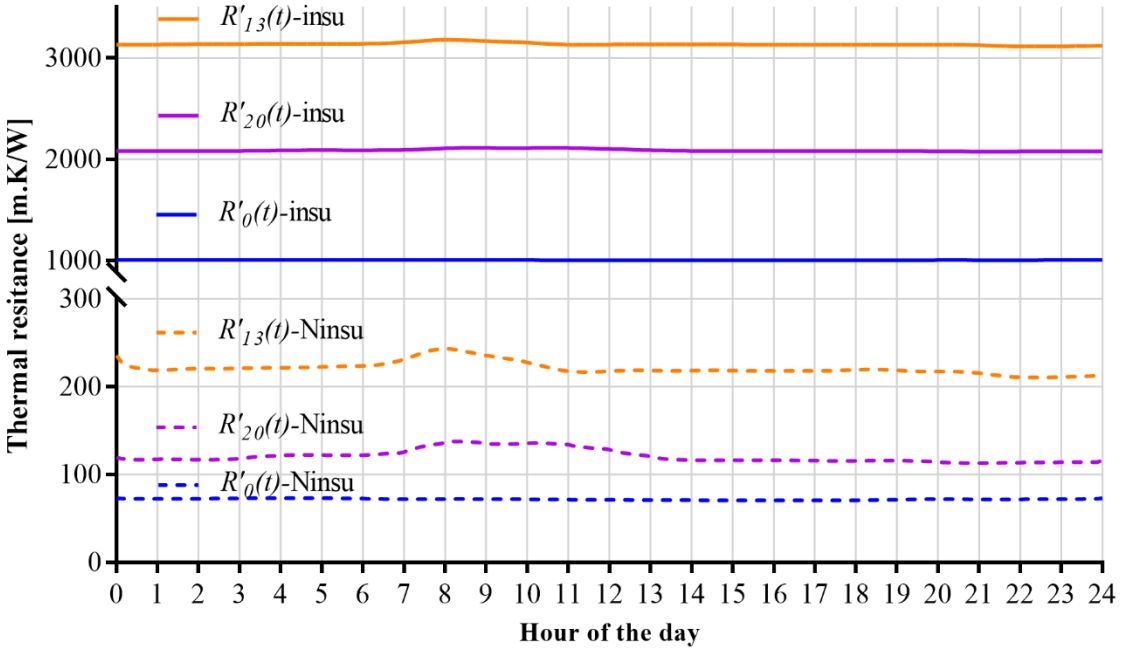

Figure 4-14. Dynamic resistance profile in selected pipes

These profiles provide a better understanding of the influence of the flow regime on the thermal resistance. The increment of the mass flow favours the heat transfer in the pipes, reducing the value of the thermal resistance, that follows the same path of $1/(m_{13}\ (t)\ )$ represented by the dotted green line.

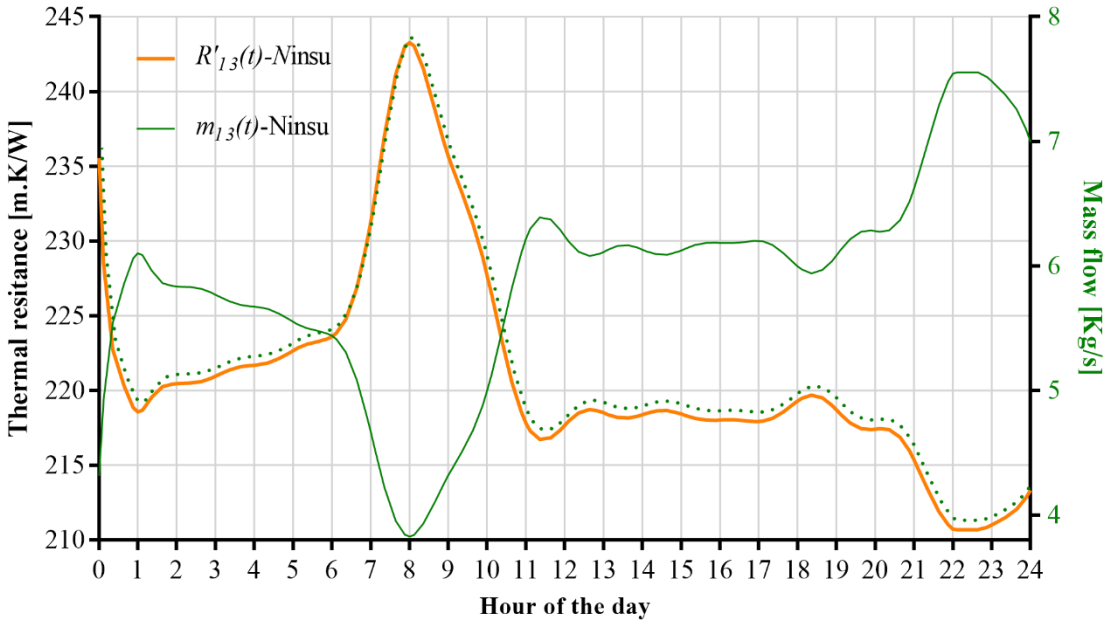

Figure 4-15. Dynamic thermal resistance and the influence of mass flow for non-insulated pipe 13

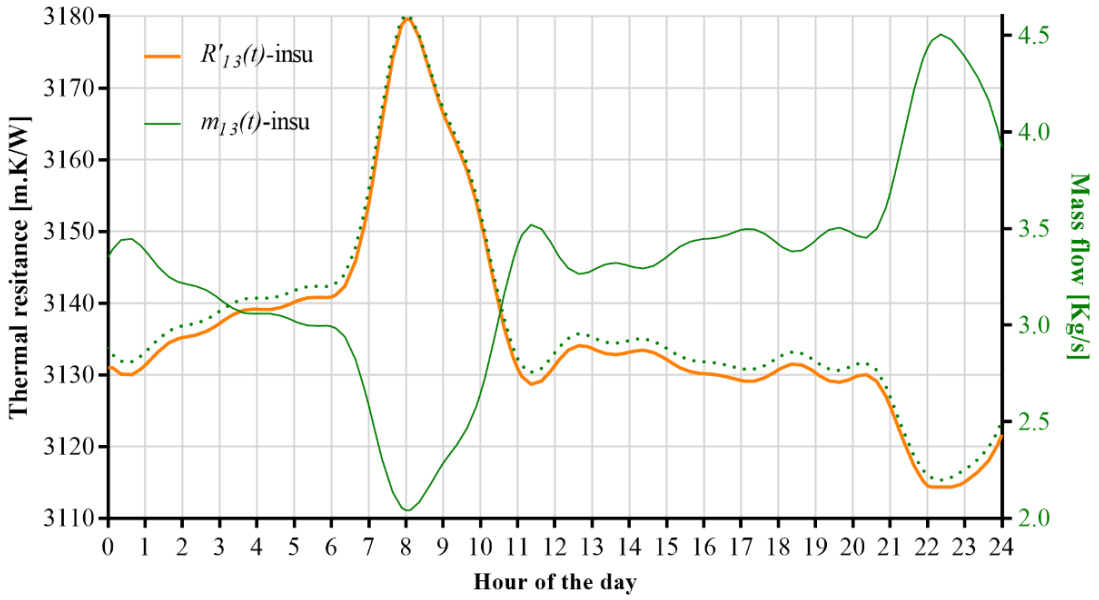

Figure 4-16. Dynamic thermal resistance and the influence of mass flow for insulated pipe 13

On the other hand, Figure 4-17 presents the variation of the total pressure drops per branch showing a major level of the pressure drops in the left branch using the two kinds of piping. These results confirm the fact that the longer branch serving more clients with a more important total demand should present bigger pressure drops.

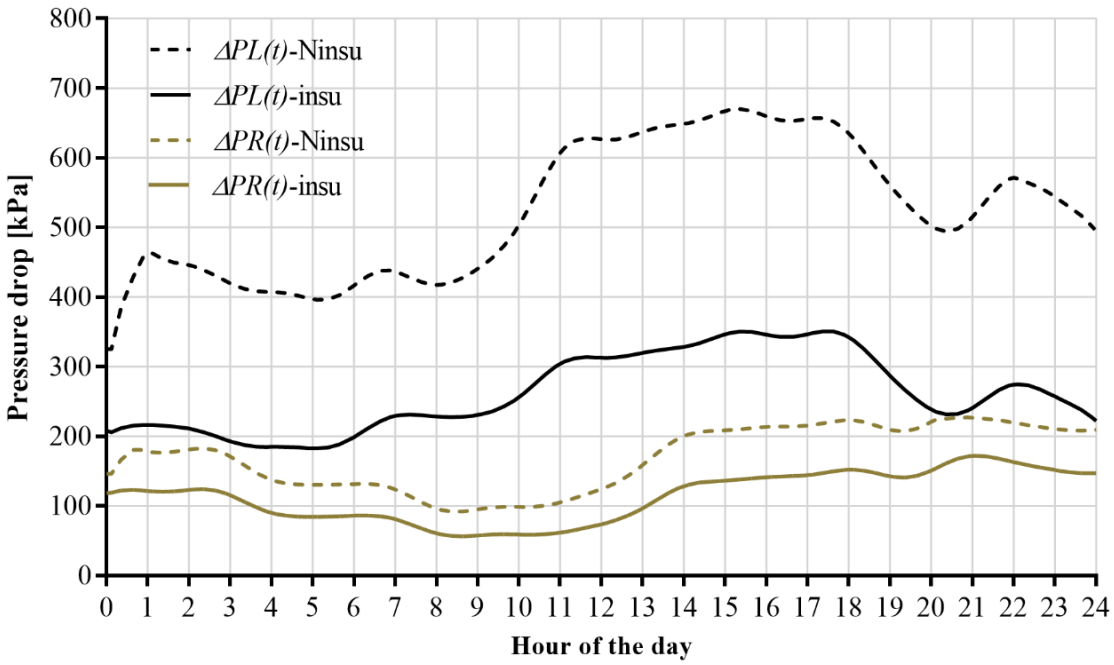

Figure 4-17. Total pressure drops per branch

4.2.3.2 Optimal diameters and minimum cost

Here we first present the value of the cost of operation for the intermediate problem DO2.1 in Table 4-3 as a base case to be compared with the computed optimal values detailed in Table 4-4.

Table 4-3. Evaluation of the Cost of operation for DO 2.1

	C_{cold1}		C_{cold2}	
	Insulated	Non-insulated	Insulated	Non-insulated
Pumping Energy consumption [kwh]	1460.522	3209.778	1460.522	3209.778
Cooling energy produced [MWh]	213.878	282.114	213.878	282.114
Cost [€]	30209.149	40043.4568	4644.068	6175.149

Table 4-4. Value of the objective function elements for DO3

	C_{cold1}		C_{cold2}	
	Insulated	Non-insulated	Insulated	Non-insulated
Pumping Energy consumption [kwh]	676.383	3324.121	134.191	505.613
Cooling energy produced [MWh]	214.173	280.183	215.657	289.919
Objective function value [€]	30130.508	39790.238	3279.110	4458.035

The major differences when optimizing the proposed cost of operation of the system can be evidenced in the value of the pump energy consumption, as detailed in Table 4-5, which presents the percentage differences of the cost for DO3 respect to DO2.1. The Optimization using the second cost of production results in more important cost reductions respect to the base case.

Table 4-5. Percentage differences for the cost DO3 with respect to DO2.1

	C_{cold1} (0.1402 € /kWh)		C_{cold2} (0.01511 € /kWh)	
	Insulated	Non-insulated	Insulated	Non-insulated
Pumping Energy consumption [kwh]	-53.69%	3.56%	-90.81%	-84.25%
Cooling energy produced [MWh]	0.14%	-0.68%	0.83%	2.77%
Objective function value [€]	-0.26%	-0.63%	-29.39%	-27.81%

Although for the optimization using non-insulated pipes and considering C_{cold1} the pumping energy consumption is 3.56% higher than in the base case (DO2.1), the final value of the objective function is lower. This can be explained by the weight of each term in the objective function when assuming the most expensive production of cooling. Then, a slight reduction in the cooling energy produced (-0.68%) with this cost results in a more important reduction in the value of the global cost, favouring in this way a major value of the pressure drops in the distribution system as detailed in Figure 4-18.

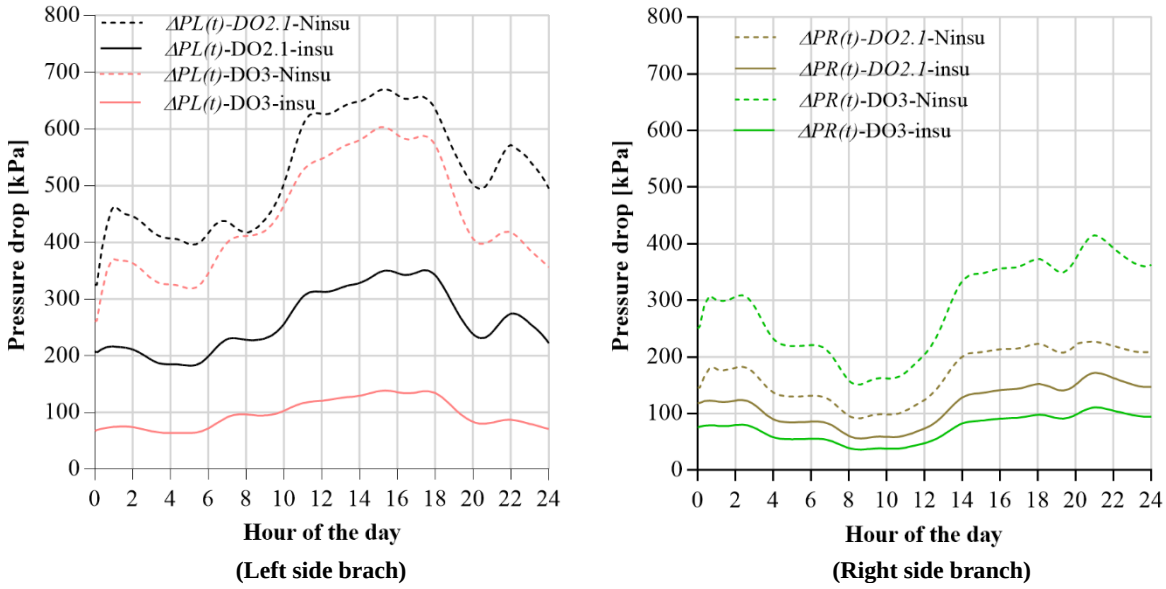

Figure 4-18. Pressure drops comparison between DO2 and DO3 using C_{cold1}

When comparing the profiles of the uninsulated pipes using C_{cold1} with those of the base case, we see that the computed pressure drops in the left side of the network are lower, while those in the right side are higher. Although the increments in the total pressure drops, the difference in the pressure drops between the branches are smaller. The reduction in the pump energy consumption for the insulated pipes and the resulting lower pressure drops using insulated pipes are caused by the increment of the diameter for these pipes as seen in Figure 4-19. This figure compares the diameters with and without insulation for the main pipes of the Outward (O) and return (R) paths.

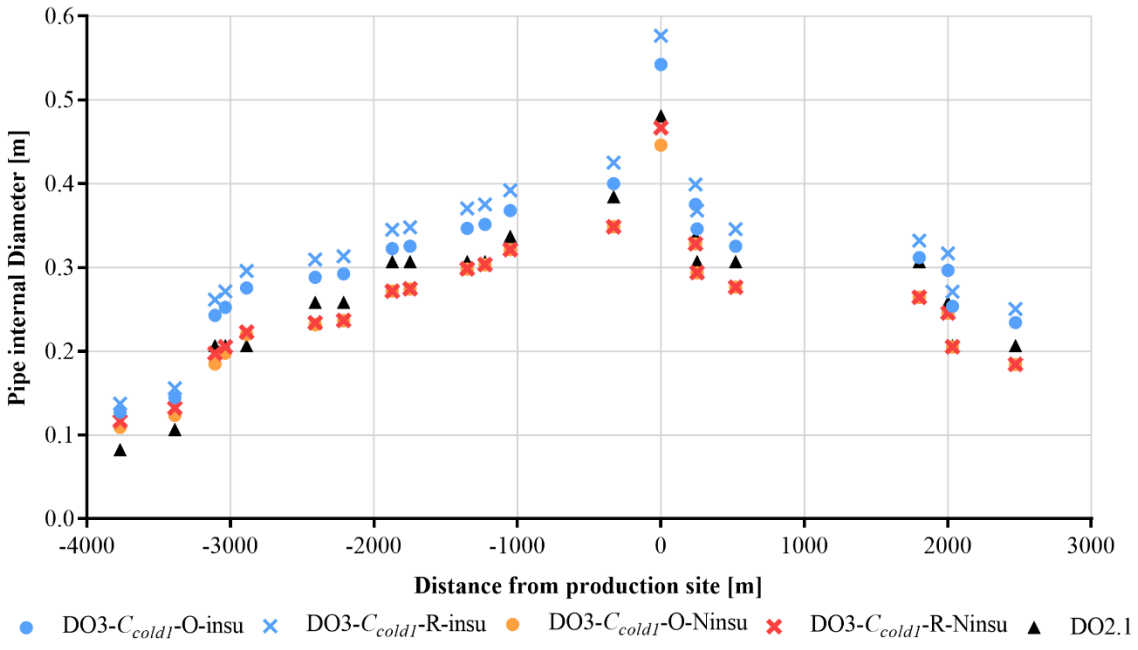

Figure 4-19. Optimal diameters for DO3 using C_{cold1}

The layer of insulation and consequent higher thermal resistance allows the increment of the diameters (more notorious in the return pipes) with a low impact on the levels of the temperature of the network. This can be seen comparing the return temperature profiles for C_{cold1} presented in Figure 4-20. The non-insulated case presents more variations at a higher level in the return temperature. However, in the two cases, the return temperature is still between 285K_- 289K (the recommended range for ΔT in the production site).

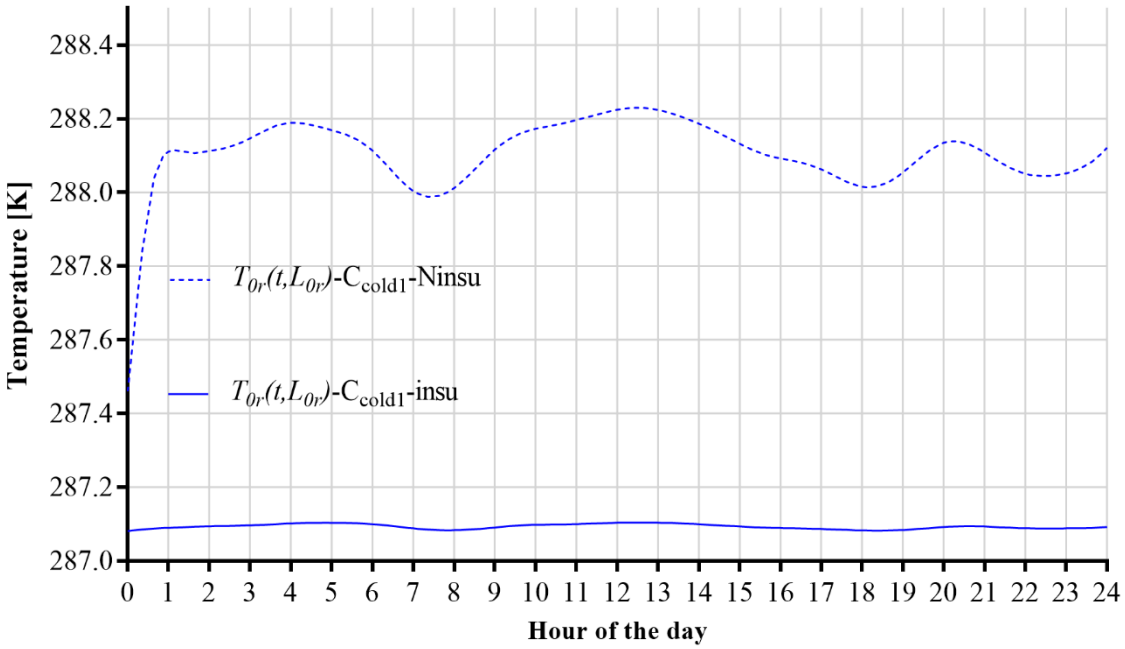

Figure 4-20. Return temperature profile for C_{cold1}

As presented in Table 4-5, when implementing DO 3 with C_{cold2}, the system operates with very lower pressure drops compared with all the other computed systems. The profiles of the pressure drops for each branch for the cost C_{cold2} are detailed in Figure 4-21, where all the pressure drops are below 80 kPa (the scale of this figure is ten times lower than in Figure 4-17 and Figure 4-18).

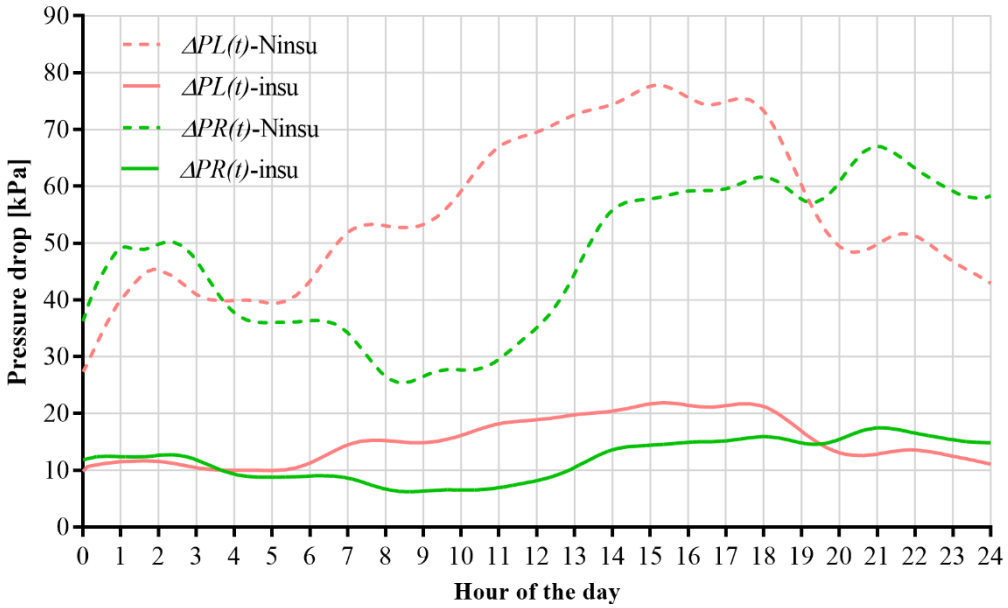

Figure 4-21. Pressure drops for DO3 using C_{cold2}

This reduction in the pressure drops is a consequence of the increment in the diameters of the pipes in the whole system, as detailed in Figure 4-22

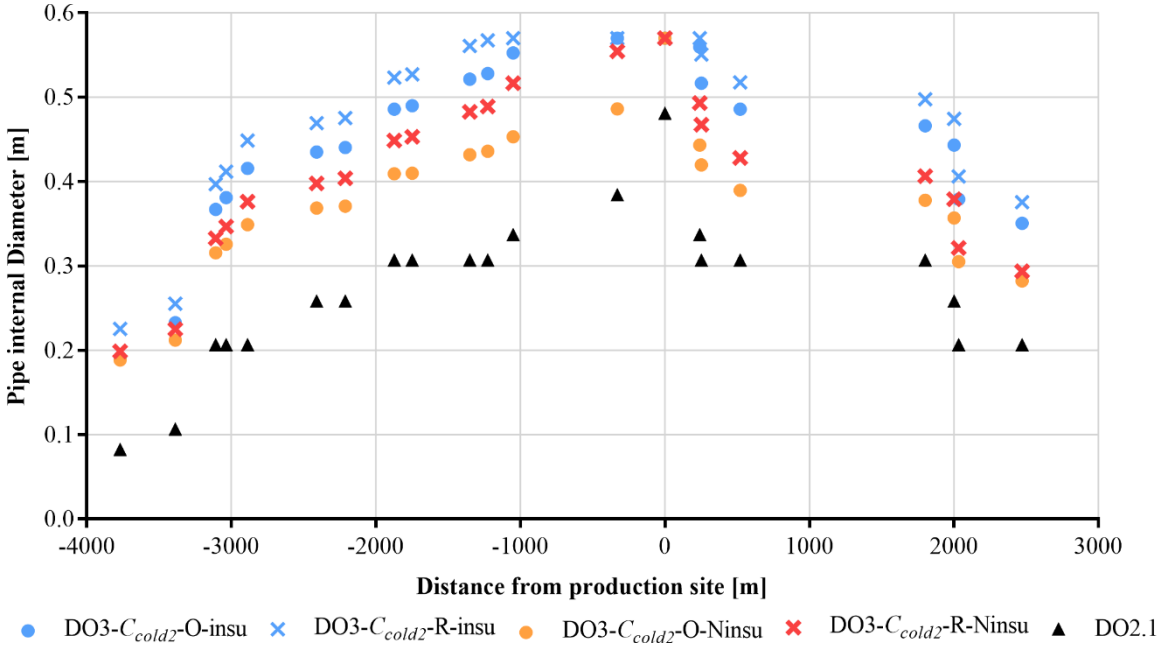

Figure 4-22. Optimal diameters for DO3 using C_{cold2}

Again, the diameters of the insulated pipes are larger, with more important variations than those computed for the cost C_{cold1}.

For the two costs of production of cold, the diameters for the return pipes are larger than the outward path pipes. This is linked to the fact that the water returning to the production site is warmer, reducing the heat exchange with the environment. This allows the increment of the diameters to reduce the pressure drops. Nevertheless, this results in strong variations in the temperature of return, mainly for non-insulated pipes as seen in Figure 4-20, which refers to the cost C_{cold1}, and Figure 4-23, which refers to the cost C_{cold2}. As in the case for the cost C_{cold1}, the return temperature for the cost C_{cold2} is still between the recommended range for ΔT in the production site.

Comparing the data of Table 4-4, the change to non-insulated piping for the cost C_{cold1} resulted in an increment of almost 4 times in the pumping energy consumption and 30.82% in the cooling energy produced resulting in a total increment of 32.06% in the value of the objective function with respect to the system with insulation. For C_{cold2} these increments are of 3.7 times, 34.43% and 35.95% respectively.

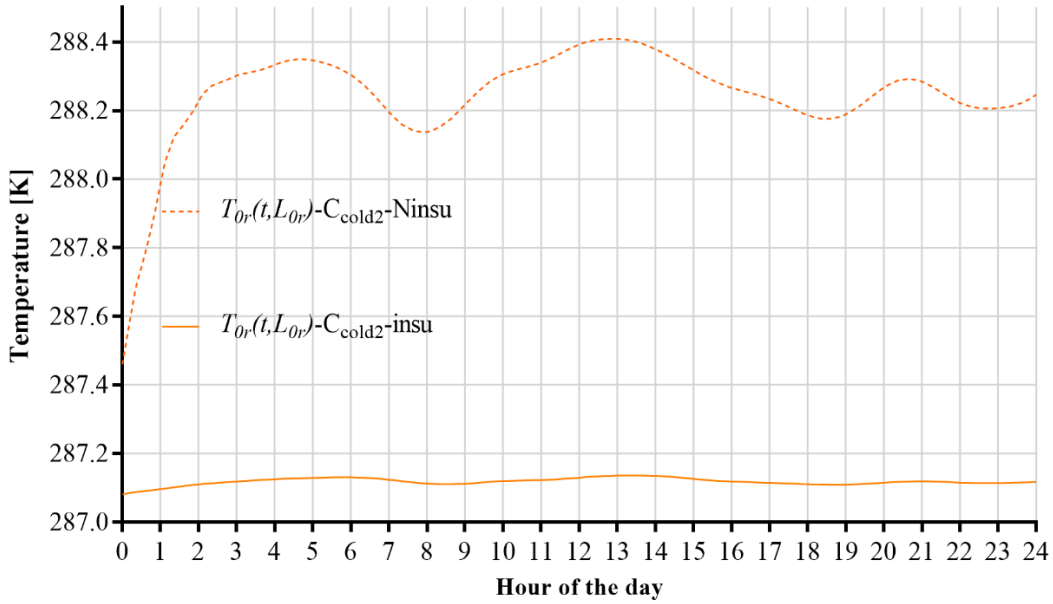

Figure 4-23. Return temperature profile for C_{cold2}

4.3 Conclusions of the Dynamic Optimization Analysis

The results presented in section 4.1 Show the potential of dynamic optimization as a tool to forecast the operation of this kind of systems, including perturbations in the demand and in the ambient temperature. The proposed methodology can be easily replicated for the dynamic analysis of district heating networks by changing the input data.

The objective function proposed in section 4.2 allowed evaluating the compromise between the pressure drops and the heat gains to find the best diameter depending mostly on the cost of production of the cold utility. Although the objective does not consider other economic factors such as the cost of the pipes and the insulation, the inclusion of the dynamic thermal resistance in the model and the evaluation of the piping system under different production costs offers a good basis to understand the phenomena that must be considered in the design of district cooling systems.

The solution of the presented problem can be considered as a good initialization for the optimization of a more detailed cost function, or even as a relaxed initialization for the solution of a MIDO (Mixed Integer Dynamic Optimization) problem in order to compute commercial nominal diameters.

CONCLUSION AND PERSPECTIVES

General Conclusion

The sector of district cooling systems in cities has been experimenting a vast development in the past years as a more efficient and eco-friendly option to cover the rapid growth in the levels of space cooling demand. This expansion asks for the development of new tools for the design and forecasting of the operation of these systems.

In this work, a literature review is included highlighting that most of the optimization applications for the study of district networks are based on steady-state models and most often deal with heat demand. However, it is important to point out that each kind of systems presents its own issues, related not only with the kind of utility produced (hot or cold) but also with its operation for improving the system efficiency. Moreover, the assumption of steady-state operation was an adequate approximation to develop numerical tools aiming to define the configuration, size and capacity of these systems (and their corresponding subsystems), but the incursion of renewables as a potential source of energy, the growing and diverse cooling demands in the cities and the fast development of these systems represent new challenges for their planning, design and operation. This underlines the importance of developing tools based on dynamic models, aiming to respond better to the new challenges in the operation and design of these systems. Dynamic studies of distributed systems have been devoted to the analysis of district heating systems, solving a one-dimensional heat transfer equation to evaluate the evolution of the temperature in the pipes but without considering the interactions between the network and the consumers. Considering this, we presented a methodology for the dynamic simulation and optimization of the distribution system in district cooling networks. The proposed methodology is illustrated with the analysis of a case study system with a diversity of demands, subject to variations in the environmental conditions over a time horizon of 24 hours. The work details the analysis for two objective functions (operation and cost), using insulated and non-insulated pipes.

The proposed case study is composed by a total of 20 consumers divided into 5 categories of buildings (office, residential, commercial, Leisure and services), that are served by a cooling network with a single production site. The distribution system includes an outward and a return network connecting 82 pipes and the consumers for a total length around 19 km. The dynamic model of the system includes the presented heat transfer equation (PDE), and the heat and mass balance in the interconnecting

nodes of the distributions system and at the consumers, as well as hydraulic constraints. The resulting arrangement is a Partial Dynamic Algebraic Equation (PDAE) system. This set of equations will be the constraints of the dynamic optimization problem where the objective function will take into account the integration of the desired criterion over the whole time domain. We propose to solve this dynamic optimization problem by a simultaneous approach based on the implementation of 2D-orthogonal collocation on finite elements (OCFE) for the solution of the model, totally discretizing it, in order to formulate an equivalent Non Linear Programming (NLP) problem.

The first challenge for the solution of dynamics problems is the implementation, of an appropriate initialization. For this, we presented a methodology based on the solution first, of two steady-state simulations, one adiabatic followed by one that considers the heat losses in the pipes. Then the solution of the fully dynamic simulation and finally the computation of the dynamic optimization. Here, each problem is initialized with the solution of its predecessor. All the problems were implemented in the environment of GAMS, using CONOPT as non-linear solver.

Following the presented strategy, we detailed the results of all the problems before the solution of the dynamic optimization problem. The main result of the steady-state model without heat losses is the diameter of the pipes, that will become parameters for all the simulation analyses and for the first optimizations (objective function: operation) and decision variables for the second optimization. Using the steady-state model, we computed the distribution of temperature (initial condition for the dynamic problem) in the pipes for three different locations (Kuala Lumpur, Paris and Ras Al Khaimah), with specific soil conditions and ambient temperatures. The dynamic analyses were performed for the location that reported the largest variations in the steady-state simulations, which was Kuala Lumpur. Using Dynamic simulation, we evaluated the response of the system when operating at the nominal values computed in steady-state. This operation resulted in a strong variation in the temperature returning to the production site, that included unappropriated low values. This issue is then solved via dynamic optimization

Finally, the dynamic optimization analysis details the results for two objective functions. The first one considers the importance of guaranteeing an appropriate temperature of the utility returning to the production site, to avoid a common technical issue in these systems known as low ΔT Syndrome. Then, keeping this optimal operation, the second objective function aims to minimize a cost function including the production of cold and the pumping. Furthermore, the model used in the second optimization problem included the diameter as a continuous variable and the computation of a dynamic thermal resistance per pipe.

The simultaneous strategy combined with the successive solution of simpler problems allowed a fast and reliable solution of the dynamic problems using a commercial laptop. The proposed case study allowed understanding the dynamic interactions between the consumers and the distribution network, and the optimization analyses resulted in:

- ✓ Optimal mass flow profiles of the production site and on the pipes serving each consumer, using both insulated and non-insulated pipes.
- ✓ Optimal diameters of the pipes considering the correlation between the pressure drops in the system and the heat losses for two costs of production of cold (representing two different technologies such as free cooling and vapour compression refrigeration cycle), using insulated and non-insulated pipes.

As a model-based tool, its application can be extended for the study of district heating systems by changing the input data (locations, demands and ambient temperature).

Perspectives

The potential applications that can be developed from the first version of this methodology are numerous. It can be used for the development of design and forecasting tools that could be eventually used by the providers of cooling services. Nevertheless, before these ambitious implementations, it is important to consider the improvements that can be done in order to develop a more reliable tool. These can include:

- ✓ The inclusion depth of the piping under the surface into the variables of the model,
- ✓ The computation of the pressure drops including the specific accessories in the system, and the eventual variations in the elevation depending on the location of the consumers,
- ✓ The evaluation of a more detailed cost function, considering the cost of piping, insulation and installation, to compute not only the optimal diameter but also the optimal insulation thickness,
- ✓ The study of larger time horizons (up to a year),
- ✓ Formulation of a mixed-integer dynamic optimization model (MIDO), to compute the optimal diameters using commercial pipe diameters.

Furthermore, it is expected to include in the model the interaction of the presented distribution system with a specific technology to produce the cold utility. Especially some technologies that use renewable resources, such as solar absorption chillers. In this case, the dynamic optimization would provide the temporal profile of cold production and enable to manage the storage of thermal energy (produced chilled water). Here, it is possible to propose MIDO formulations for the selection of the best technology according to the location, demand and costs of production. These models can be coupled with methods for the prediction of the demand in the users.

To finish, we consider that the proposed methodology could be a good starting point for applications aimed at the optimal control and real-time optimization of district energy systems (heating and cooling).

CONCLUSION ET PERSPECTIVES

Conclusion générale

Face à la recherche de solutions efficaces et plus respectueuses de la nature pour satisfaire le besoin croissant en froid, les réseaux de distribution de froid à l'échelle du quartier ont, récemment, été l'objet de nombreux développements. Il est alors nécessaire de développer des outils de dimensionnement et de pilotage de ces systèmes.

L'analyse bibliographique présentée dans ce travail montre que la plupart des travaux d'optimisation des réseaux portent sur le fonctionnement en régime permanent et, le plus souvent, sur des réseaux de chaleur. Cependant, il est important de souligner que chaque type de système présente des problèmes spécifiques, liés non seulement à la nature de l'utilité produite (chaud ou froid) mais également à sa gestion en vue d'en améliorer l'efficacité. L'hypothèse de régime permanent a permis de développer des outils numériques permettant de déterminer la configuration, le dimensionnement et la capacité de ces systèmes (et des sous-systèmes associés). Cependant, l'utilisation toujours plus importante d'énergie primaire renouvelable, la demande croissante toujours plus diversifiée de froid dans les villes et le développement rapide de ces systèmes lancent de nouveaux défis quant à leur planification, leur design et leur gestion. Cela met donc en évidence la nécessité de développer des outils prenant en compte la dynamique du système afin de mieux répondre aux défis relatifs à la gestion et au design de ces systèmes. Des travaux antérieurs ont porté sur l'étude dynamique des réseaux de distribution de chaleur : l'équation de la chaleur est résolue dans les canalisations en considérant une dimension d'espace et le temps, mais sans prendre en compte les interactions entre le réseau et les consommateurs. Dès lors, nous proposons ici une méthodologie pour la simulation et l'optimisation dynamique des réseaux de distribution de froid. La méthodologie proposée est illustrée par un exemple de réseau incluant une grande diversité de demandes, soumis à des variations des conditions ambiantes et cela, sur un horizon de temps de 24 heures. Nous analysons ici les résultats pour deux types de fonctions objectif (l'une de nature opérationnelle, l'autre relative au coût), en utilisant des canalisations isolés et non isolés.

L'exemple proposé comporte 20 consommateurs, répartis en 5 catégories de bâtiments (bureaux, résidentiel, commercial, loisir et service), alimentés par un réseau de froid ne comprenant qu'un unique site de production. Le système est constitué du réseau de distribution de froid à proprement parlé et du réseau de retour du fluide chaud au centre de production, soit dans notre cas, 82 tuyaux pour une longueur totale de 19km. Le modèle dynamique comprend l'équation de transfert de chaleur,

les bilans de matière et d'énergie ainsi que les contraintes hydrauliques. Ainsi formulé, le modèle comporte des équations différentielles partielles et des équations purement algébriques (PDAE). L'ensemble de ces équations seront considérées comme des contraintes du problème d'optimisation dont la fonction objectif intégrera les critères souhaités sur l'ensemble de l'horizon de temps considéré. Dans le cadre de cette stratégie de résolution globale (orientée-équations), nous mettons en œuvre une méthode de double collocation orthogonale sur éléments finis (OCFE) afin de discrétiser les contraintes différentielles et formuler un problème de programmation non linéaire (NLP) purement algébrique.

La résolution du problème d'optimisation dynamique exige une attention particulière quant à son initialisation. Pour cela nous proposons une stratégie en plusieurs étapes : nous résolvons tout d'abord le problème adiabatique en régime permanent. Puis, partant de cette solution, toujours en régime permanent, nous introduisons les pertes thermiques. La solution ainsi obtenue est utilisée comme conditions initiales d'une simulation dynamique du système soumis à des perturbations extérieures et tenant compte des demandes variables. Ce profil est alors utilisé comme initialisation du problème d'optimisation dynamique. Ces différents problèmes sont résolus dans l'environnement GAMS, en utilisant le solveur d'optimisation non linéaire en variables continues, CONOPT.

Nous présentons les résultats des différentes étapes intermédiaires de la stratégie d'initialisation du problème d'optimisation dynamique. La première étape de simulation en régime permanent permet de déterminer les diamètres des tuyaux, lesquels deviendront des paramètres des simulations suivantes, avant d'être eux-mêmes optimisés. Nous calculons également, en régime permanent, la distribution spatiale des températures pour trois environnement différents (Kuala Lumpur, Paris et Ras Al Khaimah) : températures ambiantes et natures du sol spécifiques. Les conditions ambiantes conduisant aux plus fortes variations spatiales (celles de Kuala Lumpur) font ensuite l'objet d'une analyse dynamique.

Enfin, nous présentons les résultats de l'optimisation dynamique pour deux fonctions objectif. La première porte sur la nécessité de garantir un écart minimal entre la température de production (température froide) et la température de retour de l'utilité à l'unité de production (température chaude) : « low ΔT syndrom ». Ensuite, en préservant cette condition de fonctionnement, la seconde fonction objectif vise à minimiser une fonction économique incluant le coût de production du froid et du pompage. Lors de la minimisation de cette seconde fonction objectif, les diamètres des tuyaux sont optimisés et la dynamique des résistances thermiques des tuyaux est prise en compte.

La stratégie de résolution globale, couplée à la stratégie d'initialisation progressive, permet une résolution rapide et robuste du problème d'optimisation dynamique en utilisant un ordinateur portable commercial. Le cas d'étude permet de comprendre les interactions dynamiques entre les consommateurs et le réseau. Les principaux résultats de l'optimisation dynamique sont :

Les profils des débits massiques dans chaque tuyau du réseau, qu'ils soient isolés ou pas.

Les diamètres des tuyaux calculés en tenant compte du nécessaire compromis entre les pertes de charges et les pertes thermiques, pour deux coût de production (correspondant à deux technologies différentes telles que le Free Cooling et une machine frigorifique à compression de vapeur), pour des tuyaux isolés ou pas.

La méthodologie développée est générale. L'outil proposé peut être paramétré de façon à optimiser des réseaux dans des conditions variées (localisation, profils de demande, température ambiante…).

Perspectives

L'outil proposé peut être utilisé pour l'optimisation du design et de la gestion des réseaux de distribution de froid. Ces premiers travaux ouvrent cependant un certain nombre de perspectives et certaines améliorations pourront être apportés :

- La prise en compte explicite (comme variable du modèle) de la profondeur d'enfouissement des tuyaux.
- Le calcul plus précis des pertes de charge, incluant les « pertes accidentelles » liées aux différents appareils et les éventuels changement d'altitude entre les différents organes du réseau.
- Le calcul plus détaillé de la fonction objectif économique, en tenant compte en particulier du coût d'investissement des tuyaux (en fonction du diamètre et de l'épaisseur de l'isolant) ainsi que du coût de leur installation.
- L'étude sur un horizon de temps plus grand (de l'ordre de l'année).
- La formulation d'un problème d'optimisation dynamique en variables mixtes (MIDO), pour tenir compte de la nature discrète des diamètres des tubes commerciaux.

De plus, une évolution importante consisterait à intégrer les modèles dynamiques des systèmes de production de froid, en particulier les systèmes utilisant une énergie primaire renouvelable, tel que les machines frigorifiques à absorption utilisant l'énergie solaire. Dès lors, l'optimisation dynamique permettrait de déterminer le profil temporel de la production de froid et de gérer le stockage de l'eau froide produite. Il serait alors envisageable de proposer une formulation en variables mixtes (MIDO) pour sélectionner la meilleure unité de production, au sens du coût, en fonction du lieu (conditions ambiantes) et de la demande. L'outil d'optimisation pourrait être couplé à un outil de prédiction de la demande.

Enfin, il nous semble que ces travaux sont un point de départ vers une approche type contrôle optimal ou vers une optimisation en ligne (temps réel) des systèmes énergétiques hybrides (chaud et froid).

Annex A. Dimensions of commercial PVC pipes Schedule 40

Table A 1 details the common dimensions for commercial pipes of PVC schedule 40. These dimensions were used to compute the thermal resistances of the pipes. This information is available in the online in the site of commercial providers[92].

Table A 1. Commercial diameters for PVC schedule 40 pipes

Nominal Diameter [in]	Internal diameter [in]	Internal diameter [m]	Wall thickness [in]	Wall thickness [m]	Maximum Pressure [PSI]	Maximum Pressure [bar]
3	3.0420	0.0773	0.2160	0.0055	260	17.93
3.5	3.5210	0.0894	0.2260	0.0057	240	16.55
4	3.9980	0.1015	0.2370	0.0060	220	15.17
5	5.0160	0.1274	0.2580	0.0066	190	13.10
6	6.0310	0.1532	0.2800	0.0071	180	12.41
8	7.9420	0.2017	0.3220	0.0082	160	11.03
10	9.9760	0.2534	0.3650	0.0093	140	9.65
12	11.8890	0.3020	0.4060	0.0103	130	8.96
14	13.0730	0.3321	0.4370	0.0111	130	8.96
16	14.9400	0.3795	0.5000	0.0127	130	8.96
18	16.8090	0.4269	0.5620	0.0143	130	8.96
20	18.7430	0.4761	0.5930	0.0151	120	8.27
24	22.5440	0.5726	0.6870	0.0174	120	8.27

References

[1] European Commission, “Strategy on Heating and Cooling.” 16-Feb-2016.

[2] Galindo Marina, Oger-Lacan Cyril, Gärs Uwe, and Aumaitre Vincent, *Efficient district heating and cooling markets in the EU: Case studies analysis, replicable key success factors and potential policy implications - EU Science Hub - European Commission*. Publications Office of the European Union, 2017.

[3] European Commission, *Overview of support activities and projects of the European Union on energy efficiency and renewable energy in the Heating and Cooling Sector*, 1 vols. Luxembourg, 2016.

[4] European Commission, “Communication from the Commission to the European Parliament, the Council, the European Economic and Social Committee and the Committee of the Regions, an Eu Strategy on Heating and Cooling.” .

[5] International Energy Agency, *Renewables for Heating and Cooling*, 2007th ed., vol. 1. Paris, France: IEA.

[6] G. Stryi-Hipp, *Renewable Heating and Cooling: Technologies and Applications*. Elsevier, 2015.

[7] United Nations Environment Programme, “District Energy in Cities: Unlocking the Potential of Energy Efficiency and Renewable Energy.” UNEP, 2015.

[8] “IEA District Heating and Cooling: The Technology.” [Online]. Available: http://www.iea-dhc.org/the-technology.html. [Accessed: 14-Dec-2017].

[9] “What is District Energy? | DISTRICT ENERGY INITIATIVE.” [Online]. Available: http://www.districtenergyinitiative.org/what-district-energy. [Accessed: 14-Dec-2017].

[10] A. Lake, B. Rezaie, and S. Beyerlein, “Review of district heating and cooling systems for a sustainable future,” *Renew. Sustain. Energy Rev.*, vol. 67, pp. 417–425, Jan. 2017.

[11] B. Rezaie and M. A. Rosen, “District heating and cooling: Review of technology and potential enhancements,” *Appl. Energy*, vol. 93, pp. 2–10, May 2012.

[12] “Why Cooling,” *Kigali Cooling Efficiency Program (K-CEP)*. [Online]. Available: https://www.k-cep.org/why-cooling/. [Accessed: 09-Apr-2019].

[13] CoolingEU, “Why cooling?,” *coolingEu*, 29-Nov-2016. [Online]. Available: https://coolingeu.eu/role-of-cooling/. [Accessed: 18-Dec-2017].

[14] S. Werner, “International review of district heating and cooling,” *Energy*, vol. 137, no. Supplement C, pp. 617–631, Oct. 2017.

[15] “Heating & Cooling - facts and figures,” *Euroheat & Power*, 19-Jun-2017. .

[16] M. Isaac and D. P. van Vuuren, “Modeling global residential sector energy demand for heating and air conditioning in the context of climate change,” *Energy Policy*, vol. 37, no. 2, pp. 507–521, Feb. 2009.

[17] OECD/IEA, “The Future of Cooling.” 2018.

[18] D. F. Dominković *et al.*, “Potential of district cooling in hot and humid climates,” *Appl. Energy*, vol. 208, pp. 49–61, Dec. 2017.

[19] V. Eveloy and D. S. Ayou, “Sustainable District Cooling Systems: Status, Challenges, and Future Opportunities, with Emphasis on Cooling-Dominated Regions,” *Energies*, vol. 12, no. 2, p. 235, Jan. 2019.

[20] “Home,” *Indigo Project*. [Online]. Available: http://www.indigo-project.eu/. [Accessed: 18-Dec-2017].

[21] “About - Rescue-project.eu.” [Online]. Available: http://www.rescue-project.eu/index.php?id=4. [Accessed: 18-Dec-2017].

[22] CoolingEU, “District cooling,” *coolingEu*, 12-Jan-2017. [Online]. Available: https://coolingeu.eu/district-cooling/. [Accessed: 18-Dec-2017].

[23] G. Sarraf, S.-P. Monette, T. E. Sayed, and W. Fayad, “Unlocking the potential of district cooling: The need for GCC governments to take action.” [Online]. Available: https://www.strategyand.pwc.com/reports/unlocking-potential-district-cooling-need. [Accessed: 25-Sep-2018].

[24] A. A. Olama, *District Cooling: Theory and Practice*, 1 edition. Boca Raton: CRC Press, 2016.
[25] G. Phetteplace *et al.*, *District Cooling Guide*. Atlanta, GA: ASHRAE, 2013.
[26] I. E. Agency, *District heating and cooling connection handbook*. Sittard: Netherlands Agency for Energy and the Environment, 2002.
[27] W. Gang, S. Wang, F. Xiao, and D. Gao, "District cooling systems: Technology integration, system optimization, challenges and opportunities for applications," *Renew. Sustain. Energy Rev.*, vol. 53, pp. 253–264, Jan. 2016.
[28] D. W. Wu and R. Z. Wang, "Combined cooling, heating and power: A review," *Prog. Energy Combust. Sci.*, vol. 32, no. 5, pp. 459–495, Sep. 2006.
[29] "The District Energy in Cities Initiative in India moves to the next phase | ICLEI South Asia." [Online]. Available: http://southasia.iclei.org/newsdetails/article/the-district-energy-in-cities-initiative-in-india-moves-to-the-next-phase.html. [Accessed: 25-Sep-2018].
[30] P. Dalin and A. Rubenhag, "Possibilities wih More District Cooling in Europe," Ecoheatcool and Euroheat & Power, Brussels, Belgium, Work Packcage 5, Dec. 2006.
[31] P. Dalin, J. Nilsson, and A. Rubenhag, "The European Cold Market," Ecoheatcool and Euroheat & Power, Brussels, Belgium, Work Packcage 2, Dec. 2006.
[32] U. Persson and S. Werner, "Quantifying the Heating and Cooling Demand in Europe," Halmstad University, Halmstad, sweden, Background Report 4, 2015.
[33] "Enquête 2018 sur les réseaux de chaleur et de froid-donnés 2017." FEDENE, Nov-2018.
[34] Capital Cooling, "District Cooling Showcases in Europe," REnewable Smart Cooling for Urban Europe, 2014.
[35] Capital Cooling, "Best practice examples of District Cooling systems," Renewable Smart Cooling for Urban Europe, 2014.
[36] M. D.- ONDI, "CLIMESPACE-The Organization," *Climespace GB*. [Online]. Available: https://www.climespace.fr/en/the-organisation/. [Accessed: 24-Sep-2018].
[37] M. D.- ONDI, "CLIMESPACE a Subsidiary of Engie, the world leader of district cooling," *Climespace GB*. [Online]. Available: https://www.climespace.fr/en/climespace-a-subsidiary-of-engie-the-world-leader-of-district-cooling-and-cold-distribution/. [Accessed: 24-Sep-2018].
[38] M. Sameti and F. Haghighat, "Optimization approaches in district heating and cooling thermal network," *Energy Build.*, vol. 140, no. Supplement C, pp. 121–130, Apr. 2017.
[39] J. Allegrini, K. Orehounig, G. Mavromatidis, F. Ruesch, V. Dorer, and R. Evins, "A review of modelling approaches and tools for the simulation of district-scale energy systems," *Renew. Sustain. Energy Rev.*, vol. 52, pp. 1391–1404, Dec. 2015.
[40] T. Oppelt, T. Urbaneck, U. Gross, and B. Platzer, "Dynamic thermo-hydraulic model of district cooling networks," *Appl. Therm. Eng.*, vol. 102, pp. 336–345, Jun. 2016.
[41] I. Ben Hassine and U. Eicker, "Impact of load structure variation and solar thermal energy integration on an existing district heating network," *Appl. Therm. Eng.*, vol. 50, no. 2, pp. 1437–1446, Feb. 2013.
[42] J. Duquette, A. Rowe, and P. Wild, "Thermal performance of a steady state physical pipe model for simulating district heating grids with variable flow," *Appl. Energy*, vol. 178, no. C, pp. 383–393, 2016.
[43] S. Zhou, M. Tian, Y. Zhao, and M. Guo, "Dynamic modeling of thermal conditions for hot-water district-heating networks," *J. Hydrodyn. Ser B*, vol. 26, no. 4, pp. 531–537, Sep. 2014.
[44] B. van der Heijde *et al.*, "Dynamic equation-based thermo-hydraulic pipe model for district heating and cooling systems," *Energy Convers. Manag.*, vol. 151, no. Supplement C, pp. 158–169, Nov. 2017.
[45] G. Schweiger, P.-O. Larsson, F. Magnusson, P. Lauenburg, and S. Velut, "District heating and cooling systems – Framework for Modelica-based simulation and dynamic optimization," *Energy*, vol. 137, no. Supplement C, pp. 566–578, Oct. 2017.
[46] T. L. Bergman and F. P. Incropera, *Fundamentals of Heat and Mass Transfer*. John Wiley & Sons, 2011.

[47] R. H. S. Winterton, “Where did the Dittus and Boelter equation come from?,” *Int. J. Heat Mass Transf.*, vol. 41, no. 4, pp. 809–810, Feb. 1998.
[48] L. T. Biegler and I. E. Grossmann, “Retrospective on optimization,” *Comput. Chem. Eng.*, vol. 28, no. 8, pp. 1169–1192, Jul. 2004.
[49] B. Talebi, P. A. Mirzaei, A. Bastani, and F. Haghighat, “A Review of District Heating Systems: Modeling and Optimization,” *Front. Built Environ.*, vol. 2, 2016.
[50] T. T. Chow, A. L. S. Chan, and C. L. Song, “Building-mix optimization in district cooling system implementation,” *Appl. Energy*, vol. 77, no. 1, pp. 1–13, Jan. 2004.
[51] N. Deng *et al.*, “A MINLP model of optimal scheduling for a district heating and cooling system: A case study of an energy station in Tianjin,” *Energy*, vol. 141, pp. 1750–1763, Dec. 2017.
[52] J. Söderman, “Optimisation of structure and operation of district cooling networks in urban regions,” *Appl. Therm. Eng.*, vol. 27, no. 16, pp. 2665–2676, Nov. 2007.
[53] T. Mertz, S. Serra, A. Henon, and J.-M. Reneaume, “A MINLP optimization of the configuration and the design of a district heating network: Academic study cases,” *Energy*.
[54] F. Marty, S. Serra, S. Sochard, and J.-M. Reneaume, “Simultaneous optimization of the district heating network topology and the Organic Rankine Cycle sizing of a geothermal plant,” *Energy*, vol. 159, pp. 1060–1074, Sep. 2018.
[55] R. Khir and M. Haouari, “Optimization models for a single-plant District Cooling System,” *Eur. J. Oper. Res.*, vol. 247, no. 2, pp. 648–658, Dec. 2015.
[56] K. M. Powell and T. F. Edgar, “Modeling and control of a solar thermal power plant with thermal energy storage,” *Chem. Eng. Sci.*, vol. 71, pp. 138–145, Mar. 2012.
[57] K. M. Powell, J. D. Hedengren, and T. F. Edgar, “Dynamic optimization of a hybrid solar thermal and fossil fuel system,” *Sol. Energy*, vol. 108, pp. 210–218, Oct. 2014.
[58] “APMonitor Optimization Suite.” [Online]. Available: http://apmonitor.com/. [Accessed: 02-Oct-2018].
[59] A. C. Chiang, *Elements of Dynamic Optimization*. McGraw-Hill, 1992.
[60] T. Todorova, “Introduction to Dynamic Optimization: The Calculus of Variations,” in *Problems Book to Accompany Mathematics for Economists*, John Wiley & Sons, 2010.
[61] E. Nagypál, “Dynamic Optimization user’s guide.” Stanford University, 1998.
[62] M. Kelly, “An Introduction to Trajectory Optimization: How to Do Your Own Direct Collocation,” *SIAM Rev.*, vol. 59, no. 4, pp. 849–904, Jan. 2017.
[63] B. A. Finlayson, L. T. Biegler, and I. E. Grossmann, “Mathematics in Chemical Engineering,” in *Ullmann’s Encyclopedia of Industrial Chemistry*, Wiley-VCH Verlag GmbH & Co. KGaA, 2000.
[64] L. T. Biegler, “An overview of simultaneous strategies for dynamic optimization,” *Chem. Eng. Process. Process Intensif.*, vol. 46, no. 11, pp. 1043–1053, Nov. 2007.
[65] J. M. Longuski, J. J. Guzmán, and J. E. Prussing, *Optimal Control with Aerospace Applications*. New York: Springer-Verlag, 2014.
[66] L. T. Biegler, “Nonlinear programming strategies for dynamic chemical process optimization,” *Theor. Found. Chem. Eng.*, vol. 48, no. 5, pp. 541–554, Oct. 2014.
[67] L. T. Biegler, “Advanced optimization strategies for integrated dynamic process operations,” *Comput. Chem. Eng.*, vol. 114, pp. 3–13, Jun. 2018.
[68] M. Gerdts, *Optimal Control of ODEs and DAEs*. Walter de Gruyter, 2012.
[69] G. F. Carey and B. A. Finlayson, “Orthogonal collocation on finite elements,” *Chem. Eng. Sci.*, vol. 30, no. 5–6, pp. 587–596, May 1975.
[70] U. Ascher and L. Petzold, *Computer Methods for Ordinary Differential Equations and Differential Algebraic Equations*, vol. 61. 1998.
[71] Finlayson, Ed., *The method of weighted residuals and variational principles, with application in fluid mechanics, heat and mass transfer, Volume 87*. New York: Academic Press, 1972.
[72] E. Ebrahimzadeh, M. N. Shahrak, and B. Bazooyar, “Simulation of transient gas flow using the orthogonal collocation method,” *Chem. Eng. Res. Des.*, vol. 90, no. 11, pp. 1701–1710, Nov. 2012.

[73] H. Binous, S. Kaddeche, and A. Bellagi, “Solution of six chemical engineering problems using the Chebyshev orthogonal collocation technique,” *Comput. Appl. Eng. Educ.*, vol. 25, no. 4, pp. 594–607, Jul. 2017.
[74] B. A. Finlayson, “Orthogonal Collocation in Chemical Reaction Engineering,” *Catal. Rev.*, vol. 10, no. 1, pp. 69–138, Jan. 1974.
[75] L. T. Biegler, *Nonlinear Programming: Concepts, Algorithms, and Applications to Chemical Processes*. SIAM-Society for Industrial and Applied Mathematics, 2010.
[76] J. D. Hedengren, R. A. Shishavan, K. M. Powell, and T. F. Edgar, “Nonlinear modeling, estimation and predictive control in APMonitor,” *Comput. Chem. Eng.*, vol. 70, pp. 133–148, Nov. 2014.
[77] L. T. Jacobsen, B. J. Spivey, and J. D. Hedengren, “Model predictive control with a rigorous model of a Solid Oxide Fuel Cell,” in *2013 American Control Conference*, 2013, pp. 3741–3746.
[78] A. K. Mittal, I. A. Ganaie, V. K. Kukreja, N. Parumasur, and P. Singh, “Solution of diffusion–dispersion models using a computationally efficient technique of orthogonal collocation on finite elements with cubic Hermite as basis,” *Comput. Chem. Eng.*, vol. 58, pp. 203–210, Nov. 2013.
[79] E. Esche, H. Arellano-Garcia, G. Wozny, and L. T. Biegler, “Optimal Operation of a Membrane Reactor Network,” in *Computer Aided Chemical Engineering*, vol. 31, I. A. Karimi and R. Srinivasan, Eds. Elsevier, 2012, pp. 1321–1325.
[80] S. Tredinnick and G. Phetteplace, “8 - District cooling, current status and future trends,” in *Advanced District Heating and Cooling (DHC) Systems*, R. Wiltshire, Ed. Oxford: Woodhead Publishing, 2016, pp. 167–188.
[81] “Comprehensive Energy Solutions,” *Araner*. [Online]. Available: https://www.araner.com/. [Accessed: 19-Oct-2018].
[82] “Weather Forecast & Reports - Long Range & Local,” *Weather Underground*. [Online]. Available: /. [Accessed: 07-Dec-2018].
[83] C. R. Branan, “1 - Fluid Flow,” in *Rules of Thumb for Chemical Engineers (Fourth Edition)*, Burlington: Gulf Professional Publishing, 2005, pp. 2–28.
[84] J. V. Villadsen and W. E. Stewart, “Solution of boundary-value problems by orthogonal collocation,” *Chem. Eng. Sci.*, vol. 22, no. 11, pp. 1483–1501, Nov. 1967.
[85] C. Canuto, M. Y. Hussaini, A. Quarteroni, and T. A. Zang, “Spectral Approximation,” in *Spectral Methods in Fluid Dynamics*, C. Canuto, M. Y. Hussaini, A. Quarteroni, and T. A. Zang, Eds. Berlin, Heidelberg: Springer Berlin Heidelberg, 1988, pp. 31–75.
[86] H. Surjanhata, “On orthogonal collocation solutions of partial differential equations,” Ph.D. Thesis, New Jersey Institute of Technology, 1993.
[87] S. M. Safdarnejad, J. D. Hedengren, N. R. Lewis, and E. L. Haseltine, “Initialization strategies for optimization of dynamic systems,” *Comput. Chem. Eng.*, vol. 78, no. Supplement C, pp. 39–50, Jul. 2015.
[88] North American Insulation Manufacturers Association (NAIMA), *Guide to Insulating Chilled Water Systems with Mineral Fibe Pipe Insulation*, First Edition. Alexandria, VA 22314: North American Insulation Manufacturers Association (NAIMA), 2015.
[89] A. Lo, “Optimizing the cost and energy performance of district cooling system with the low delta-T syndrome,” phd, Cardiff University, 2014.
[90] R. and A.-C. E. American Society of Heating, *2013 ASHRAE handbook: fundamentals.* 2013.
[91] L. B. Hyman, G. Phetteplace, and S. Tredinnick, “District Heating and Cooling,” in *Ashrae Handbook 2016: HVAC Systems and Equipment: SI Edition*, ASHRAE, 2016.
[92] “PVC Pipe Dimensions 1/8" through 24",” 17-Sep-2013. [Online]. Available: https://www.pvcfittingsonline.com/resource-center/pvc-pipe-dimensions-18-through-24/. [Accessed: 30-Jun-2019].
[93] T. Mertz, S. Serra, A. Henon, and J.-M. Reneaume, “A MINLP optimization of the configuration and the design of a district heating network: Academic study cases,” *Energy*, vol. 117, pp. 450–464, Dec. 2016.
[94] F. Marty, S. Serra, S. Sochard, and J.-M. Reneaume, “Exergy Analysis and Optimization of a Combined Heat and Power Geothermal Plant,” *Energies*, vol. 12, no. 6, p. 1175, Jan. 2019.

[95] “Prix du kWh d’électricité en 2019 EDF, Engie, Direct Energie.” [Online]. Available: https://www.fournisseurs-electricite.com/guides/prix/kwh-electricite. [Accessed: 02-Jul-2019].
[96] “Enquête nationale sur les réseaux de chaleur et de froid : Edition 2017,” Syndicat National du chauffage urbain et de la climatisation urbaine (SNCU), Paris, France, Sep. 2017.
[97] R. Turton, J. A. Shaeiwitz, D. Bhattacharyya, and W. B. Whiting, *Analysis, synthesis, and design of chemical processes*, 5th ed. Prentice Hall, 2018.